RAI 03.07.02-29, Revision 1

QUESTION:

RAI from Section 3.7 Audit, October 2010

For SSE ground motions, 10 CFR Part 50, Appendix S requires that SSCs will remain functional and within applicable stress, strain, and deformation limits and the evaluation must take into account soil-structure interaction (SSI) effects. Criterion III, "Design Control," of Appendix B to 10 CFR Part 50 states, in part, that "measures shall also be established for the selection and review for suitability of application of materials, parts, equipment, and processes that are essential to the safety related functions of the structures, systems and components." Additionally, Criterion III states in part that, "the design control measures shall provide for verifying or checking the adequacy of design,..." SRP Review guideline 3.8.1.II.4.F specifies that computer programs used in the design and analysis should be described and validated.

During the STP audit of Section 3.7, the verification and validation (V&V) documents of computer programs SASSI2000, SAP2000, and SHAKE2000 used in the seismic analysis of Category I structures were reviewed. The following issues were identified regarding these V&V documents:

SASSI2000 Version 3.0:

The SSI analysis performed with SASSI2000 is used to obtain the maximum accelerations, acceleration response spectra, and dynamic soil pressures that are used for seismic evaluation and design of the RB, CB, UHS Basin, RSW Pump House, and other seismic Category I structures. The dynamic forces, moments, and stresses are also calculated from the SASSI2000 analysis but are not used as design basis.

The V&V of three SASSI codes were reviewed. These codes are S&L SASSI2000-v3.0, SGH SASSI2000-v3.0 and SGH SASSI2000-v3.0-SGH. All three program V&V documentations do not adequately address all the program features that are used to calculate and obtain maximum accelerations, acceleration response spectra, and dynamic soil pressures. In particular, the scope of the test problems does not address the adequacy of the following program features that may be used in STP applications:

- General direction of load application in the model
- General orientation of elements in the model
- Accuracy of triangular elements (solid, shell and plane-strain) that may be used
- Acceptable aspect ratio of rectangular elements (solid, shell and plane-strain) to obtain accurate results, as used in the models
- Required mesh refinement to output out-of-plane responses in shell element
- Accuracy of the subtraction method for calculating foundation impedance

In addition, potential numerical instabilities with the use of high Poisson's ratio for modeling the saturated soil behavior in SASSI2000 may be of concern, as the Poisson's ratio approaches 0.5. As a result, the SASSI2000-v3.0 limitations with respect to capping the Poisson's ratio to avoid possible stability problems should be validated and stated.

Significant differences in the out-of-plane acceleration response of thick versus thin shell element models have also been observed in the analysis results with the thick shell model producing lower responses. This also needs to be further evaluated for SASSI2000-v3.0 as to the adequacy and limitations of the specific shell element type.

Without further demonstration that encompasses validation of the program features discussed above for STP applications, the staff cannot make a determination in the SER that the programs used in the seismic analysis will not adversely affect the SSI analysis result and meet the applicable regulations. As such, the applicant is requested to further demonstrate acceptability of SASSI2000 with additional test problems addressing the issues discussed above.

SAP2000 Version 10.1 and 14.1:

SAP2000 is used to calculate forces, moments and stresses for design of the site-specific seismic Category I structures such as UHS Basin, RSW Pump House, and RSW tunnel. The forces and moments are calculated by integrating stresses across design sections. It also appears that the thick shell element is used for modeling and design of slabs. Mesh sensitivity studies are also performed using time-history modal superposition method of fixed-base structure to assess the adequacy of the structural mesh refinement for calculation of accelerations and acceleration response spectra. To that extent, the SAP2000 V&V does not provide adequate validations for the following items:

- Accuracy of forces and moments calculated from section cuts in shell models
- Accuracy of thick shell element for calculating out-of-plane dynamic responses
- Accuracy of time-history modal analysis of fixed-base structures modeled using shell elements

As such, the applicant is requested to supplement the SAP2000 V&V with additional test problems to address the items discussed above. The staff needs this information to be able to conclude in the SER that the use of SAP2000 in STP applications will not adversely affect calculation of seismic forces and moments and the evaluation of SSI effects for Category I structures.

SHAKE2000 Version 3.5:

SHAKE2000 is used to calculate SSE-based foundation motions for SSI analysis of UHS Basin, RSW Pump House, and other Seismic Category I structures. The SHAKE2000 V&V has only tested soil models with up to 8 soil layers while the STP profile is a deep soil site that is modeled using large number of soil layers.

As such, the applicant is requested to further demonstrate acceptability of SHAKE2000 with additional test problems that check the use of large number of soil layers to encompass STP soil site. The staff needs this information to be able to conclude that the SSE-based foundation motion determined using SHAKE2000 computer program is adequate for STP application and meets the requirement of Appendix S to 10 CFR Part 50.

REVISED RESPONSE:

The original response to this RAI was submitted with STPNOC letter U7-C-STP-NRC-110009, dated January 18, 2011. This revision provides the following based on discussions with the NRC on February 2nd and 3rd, 2011.

- Provides figures for some of the test problems in the original response
- Provides additional SASSI2000 test problems with thick shell elements having two-way slab action
- Provides validation for the SAP2000 spectra generation provided in Figures 03.07.02-25.10 and 03.07.02-25.11 of RAI 03.07.02-25, Revision 1 which is being submitted concurrently with this response.

The revisions are indicated by revision bars in the margin.

SASSI2000 Version 3.0:

The SASSI2000 Version 3.0 was procured from Isatis (agent for the Regents of the University of California). The program was installed at S&L computer system and named S&L SASSI2000-v3.0. Similarly, the program installed by SGH at their Boston office is named SGH SASSI2000-v3.0. These programs have been verified and validated (V&V) and the V&V documents for S&L SASSI2000-v3.0 and SGH SASSI2000-v3.0 are available in S&L office and SGH office, respectively.

All STP 3&4 soil-structure interaction (SSI) and structure-soil-structure interaction (SSSI) analyses have been performed using SGH SASSI2000-v3.0 and/or S&L SASSI2000-v3.0 except for the SSI analysis of the Ultimate Heat Sink (UHS)/Reactor Service Water (RSW) Pump House using a more refined mesh (i.e. model with 23.5 Hz passing frequency in the horizontal direction) as described in the response to RAI 03.07.02-24, Supplement 2, submitted with STPNOC letter U7-C-STP-NRC-100268, dated December 14, 2010, where the program SGH SASSI2000-v3.0-SGH was used. When the UHS/RSW Pump House SSI model was refined to accommodate higher passing frequency, the refined model exceeded the size capability of SGH SASSI2000-v3.0. The SGH SASSI2000-v3.0-SGH is a modified version of the SGH SASSI2000-v3.0 which allows handling of larger file sizes and reduces run time by using a more efficient solver. The validation of SGH SASSI2000-v3.0-SGH was performed by comparing the SSI analysis results for the UHS/RSW Pump House with the original SSI model (i.e. model with 15.6 Hz passing frequency in the horizontal direction) that were obtained using SGH

SASSI2000-v.3 and SGH SASSI2000-v3.0-SGH. The results from the two programs matched within 2%. Furthermore, SGH SASSI2000-v3.0 and S&L SASSI2000-v3.0 are identical. Therefore, for ease of discussion, in the remainder of this response they will be referred to as "SASSI2000".

Prior to addressing the individual items noted in this RAI, the following should be noted in regards to the SSI and SSSI analyses for the STP 3&4 project:

- In all SSI and SSSI analyses, load applications are only in the global directions.
- In all SSI and SSSI analyses, elements are oriented along the global planes
- With the exception of a few transition elements for the refined model of the UHS/RSW Pump House, all shell elements in the SSI and SSSI analyses are rectangular elements. With the exception of a few transition elements of the 2D SSSI analyses, all plane-strain elements are rectangular elements. No triangular solid elements have been used in any of the SSI and SSSI analyses.
- With the exception of the original SSI model for UHS/RSW Pump House with maximum aspect ratio of 5.25, for all the remaining SSI and SSSI models including the refined model for the UHS/RSW Pump House, the maximum aspect ratio for the shell, solid and plain-strain elements is less than 5.
- All shell elements in the SSI analyses for spectra generation are thick shell elements.
- All shell elements in the SAP2000 models used for design of the structures are thick shell elements
- None of the designs are based on the element stresses from the SSI and/or SSSI analyses.

There are twenty five (25) existing problems, which have been used in V&V of various features of S&L SASSI2000-v3.0. The matrix of these 25 problems with the options validated by each problem is available in Table 5.1 of Calculation SVVR03.7.316-3.0 and was included as Table 1 in the program release memorandum. Similarly, there are 26 existing problems used in V&V of various features of SGH SASSI2000-v3.0. The matrix of these 26 problems with options validated by each problem is available in Table 1 of SGH document SAS-V3-0 Rev. 0.

The following provides the response to NRC Staff questions on specific program features. Please note that the V&V documentation of the computer programs are proprietary documents. Thus, only limited details are provided for the additional test problems described in this response. Full details and documentation for these test problems are available for inspection at S&L and SGH offices.

- **General direction of load application in the model**

  As noted earlier, in all STP 3&4 SSI and SSSI analyses the load applications are only along the global coordinates. Both S&L and SGH V&V documentation for SASSI2000 already have several problems with load applications along the global coordinates. Thus no additional test problems are performed.

- **General orientation of elements in the model**

  As noted earlier, in all STP 3&4 SSI and SSSI analyses the elements are oriented along the global planes. Both S&L and SGH V&V documentation for SASSI2000 already have several problems with load applications along the global coordinates. Thus no additional test problems are performed.

- **Accuracy of triangular elements (solid, shell and plane-strain) to obtain accurate results, as used in the models**

  Triangular elements have not been used in the STP 3&4 SSI analyses performed by S&L SASSI2000-v3.0. However, the existing S&L validation problems include triangular solid elements. These problems have been validated for obtaining the transfer functions and acceleration responses in the models.

  The SSI analyses performed for STP using the SGH SASSI2000-v3.0 use rectangular elements, except for the refined mesh SSI analysis of the UHS/RSW Pump House as described in the response to RAI 03.07.02-24, Supplement 2, submitted with STPNOC letter U7-C-STP-NRC-100268, dated December 14, 2010, and 2-D model for SSSI analysis of UHS/RSW Pump House, RSW Piping Tunnel, DGFOSV 1B, DGFOSV 1C and RB as described in the response to RAI 03.07.02-24, Supplement 1, Revision 1, submitted with NINA letter U7-C-NRC-NINA-110042, dated March 7, 2011, where at isolated locations triangular elements are used for mesh transition. No stress results are calculated or used from the triangular elements. A review of the V&V documentation found that triangular elements were used in some problems but validation of the dynamic properties of triangular elements was not specifically addressed. The following additional validation problems have been included to further validate the accuracy of solid, shell, and plane-strain triangular elements.

  Validation problem for thick shell in-plane:

  A 6 in. long, 1 in. tall and 0.01 in. thick massless cantilever shear wall model aligned in the Y-Z plane with total mass of 0.2 lb-s^2/in^2 distributed as mass elements along the top of the wall is used. The wall has interaction nodes at the base and is connected to rigid soil. The nodes at the top of the wall are restrained in the vertical direction in order to model a pure shear case. The rectangular element finite element model consists of 150 (5 x 30) 3-D thick shell elements and the triangular element finite element model consists of 300 3-D thick shell elements as shown in Figure 03.07.02-29.1. Element and material properties are shown in Figure 03.07.02-29.1. The material damping is 4%.

  In this model, the soil is assigned to behave rigidly. The shear wave velocity equal to 20,000 in./sec and compression wave velocity equal to 40,000 in./sec. The soil density is 0.130 lb/$in.^3$ and damping ratio is 0%.

The seismic time history analysis is performed in the horizontal Y-direction (in-plane of the wall) for vertically propagating shear waves. The input motion is applied at the surface.

Table 03.07.02-29.1 shows the natural frequency comparison and Table 03.07.02-29.2 shows comparison for peak response spectra. Figure 03.07.02-29.2 through Figure 03.07.02-29.4: show comparisons of response spectra using the rectangular element model and the triangular element model. As can be seen from these comparisons, there is good agreement between the results from the triangular element model and the rectangular element model.

Validation problem for thick-shell out-of-plane:

The cantilever shear wall model is developed for two cases: 10 ft x 5 ft x 6 in. thick and 10 ft x 5 ft x 4 ft thick consisting of 50 (5 x 10) rectangular shell elements or 100 triangular elements. Model geometry and element and material properties are shown in Figure 03.07.02-29.5. Material damping is 4%.

The soil properties are assigned to behave rigidly. The shear wave velocity equal to 20,000 ft/sec and compression wave velocity equal to 40,000 ft/sec. The soil density is 0.130 kcf and damping ratio is 0%.

The seismic time history analysis is performed in the horizontal X-direction (out-of-plane of the wall) for vertically propagating shear waves. The input motion is applied at the surface.

Table 03.07.02-29.3 shows the natural frequency comparison and Table 03.07.02-29.4 shows comparison for peak response spectra. Figures 03.07.02-29.6 through 03.07.02-29.9 show comparisons of response spectra using the rectangular element model and the triangular element model. As can be seen from these comparisons, there is good agreement between the results from the triangular element model and the rectangular element model.

Validation problem for thick-shell axial:

The cantilever shear wall model is developed for a 10 ft x 5 ft x 4 ft structure consisting of 50 (5 x 10) rectangular shell elements or 100 triangular elements. Model geometry and element and material properties are shown in Figure 03.07.02-29.10. The shell elements are massless, mass elements are placed at the top of the wall, and material damping is 4%.

The soil properties are assigned to behave rigidly. The shear wave velocity equal to 20,000 ft/sec and compression wave velocity equal to 40,000 ft/sec. The soil density is 0.130 kcf and damping ratio is 0%.

The seismic time history analysis is performed in the vertical Z-direction for vertically propagating compression waves. The input motion is applied at the surface.

Table 03.07.02-29.5 shows the natural frequency comparison and Table 03.07.02-29.6 shows comparison for peak response spectra. Figures 03.07.02-29.11 and 03.07.02-29.12 show comparisons of response spectra using the rectangular element model and the triangular element model. As can be seen from these comparisons, there is good agreement between the results from the triangular element model and the rectangular element model.

Validation problem for plane-strain in-plane:

The cantilever shear wall model is developed for a 20 ft x 4 ft x 1 ft thick wall consisting of 5 2-D plane strain rectangular shell elements or 10 triangular elements modeled inside an excavated area. Model geometry is shown in Figure 03.07.02-29.13. Material damping is 4%.

The soil properties are assigned to behave rigidly. The shear wave velocity equal to 20,000 ft/sec and compression wave velocity equal to 40,000 ft/sec. The soil density is 0.130 kcf and damping ratio is 0%.

The seismic time history analysis is performed in the horizontal X-direction for vertically propagating shear waves. The input motion is applied at the surface.

Table 03.07.02-29.7 shows the natural frequency comparison and Table 03.07.02-29.8 shows comparison for peak response spectra. Figure 03.07.02-29.14 shows comparison of response spectra using the rectangular element model and the triangular element model. As can be seen from these comparisons, there is good agreement between the results from the triangular element model and the rectangular element model.

Validation problem for plane-strain axial:

The cantilever shear wall model is developed for a 20 ft x 4 ft x 1 ft thick wall consisting of 5 2-D plane strain rectangular shell elements or 10 triangular elements. Model geometry is shown in Figure 03.07.02-29.13. Additional elements, 1 through 5, are included in the model, but are inactive since structural nodes connected to these elements are fixed. Material damping is 4%.

The soil properties are assigned to behave rigidly. The shear wave velocity equal to 20,000 ft/sec and compression wave velocity equal to 40,000 ft/sec. The soil density is 0.130 kcf and damping ratio is 0%.

The seismic time history analysis is performed in the vertical Z-direction for vertically propagating compression waves. The input motion is applied at the surface.

Table 03.07.02-29.9 shows the natural frequency comparison and Table 03.07.02-29.10 shows comparison for peak response spectra. Figure 03.07.02-29.15 shows comparison of response spectra using the rectangular element model and the triangular element model. As can be seen from these comparisons, there is good agreement between the results from the triangular element model and the rectangular element model.

- **Acceptable aspect ratio of rectangular elements (solid, shell and plane-strain) to obtain accurate results, as used in the models**

Both S&L and SGH V&V documentation for SASSI2000 have been expanded to include additional problems for aspect ratio of rectangular elements. Provided below are the details of the test problems and results added to the V&V documentation of S&L SASSI2000-v3.0 followed by details of the SGH test problems.

A parametric study with aspect ratios of 1:1, 1:2, 1:3, 1:4 and 1:5 (models with solid elements, thick shell elements, thin shell elements and plane-strain elements) has been performed by S&L and is being added in the V&V documents. A similar parametric study with aspect ratios of 1:1, 1:2, 1:3, 1:4, 1:5 and 1:10 has been performed by SGH. The results show that rectangular elements with aspect ratio up to 1:5 provide results within 5% accuracy with respect to elements with aspect ratio of 1:1. For STP SSI analyses the aspect ratio of rectangular elements is well within 1:5 except for a few elements with aspect ration of 5.25 which are used in the original SSI model for UHS/RSW Pump House. The following summarizes the details of each validation problem:

Validation Problem with Thin Shell Elements (S&L)

A 100 ft width, 80 ft long, and 4 ft thick concrete foundation supporting a 80 ft long, 1000 ft tall and 4 ft thick concrete wall at the middle strip of the foundation is used for the study. Five models are constructed, which have rectangular elements with aspect ratios of 1:1, 1:2, 1:3, 1:4 and 1:5. In the models, the foundation and excavated soil volume are modeled by solid elements and the concrete wall is modeled by thin plate/shell elements. The input motions are specified at the ground surface, in the global axes (two horizontal X, Y and vertical Z directions). The results compared are; (a) maximum accelerations, (b) forces/moments and (c) In-structure response spectra at various elevations.

Figure 03.07.02-29.16 shows the structural models for element aspect ratios of 1:1 and 1:2. For other aspect ratios, the models are similar with elements modified for the desired aspect ratios.

Table 03.07.02-29.11 shows the results of comparisons of maximum accelerations for various aspect ratios. The maximum difference between the accelerations is 4.0%, for model with aspect ratio of 1:5 (as compared to the aspect ratio of 1:1).

Table 03.07.02-29.12 shows the results of comparisons of maximum forces/moments for various aspect ratios. The maximum difference between the maximum forces/moments is 1.0%, for model with aspect ratio of 1:5 (as compared to the aspect ratio of 1:1).

Figures 03.07.02-29.17 through 03.07.02-29.19 show some typical comparisons of 5% damped in-structure response spectra. The comparisons show that the in-structure response spectra compare well for aspect ratios up to 1:5.

Based on above results it is concluded that the thin shell elements can be used with aspect ratios up to 1:5.

Validation Problem with Thick Shell Elements (S&L)

Models similar to above (thin plate element models) with 3-D thick plate/shell elements are analyzed and results compared.

Figure 03.07.02-29.20 shows the structural models for element aspect ratios of 1:1 and 1:2. For other aspect ratios, the models are similar with elements modified for the desired aspect ratios.

Table 03.07.02-29.13 shows the results of comparisons of maximum accelerations for various aspect ratios. The maximum difference between the accelerations is 4.2%, for model with aspect ratio of 1:5 (as compared to the aspect ratio of 1:1).

Table 03.07.02-29.14 shows the results of comparisons of maximum forces/moments for various aspect ratios. The maximum difference between the maximum forces/moments is 2.1%, for model with aspect ratio of 1:5 (as compared to the aspect ratio of 1:1).

Figures 03.07.02-29.21 through 03.07.02-29.23 show the comparisons of some typical 5% damped in-structure response spectra. The comparisons show that the in-structure response spectra compare well for aspect ratios up to 1:5.

Based on above results it is concluded that the 3-D thick plate elements can be used with aspect ratios up to 1:5.

Validation Problem with Solid Elements (S&L)

Models similar to above with 3-D solids are analyzed and results compared.

Figures 03.07.02-29.24 and 03.07.02-29.25 show the structural models for element aspect ratios of 1:1 and 1:2 respectively. For other aspect ratios, the models are similar with elements modified for the desired aspect ratios.

Table 03.07.02-29.15 shows the results of comparisons of maximum accelerations for various aspect ratios. The maximum difference between the accelerations is 3.5%, for model with aspect ratio of 1:5 (as compared to the aspect ratio of 1:1).

Table 03.07.02-29.16 shows the results of comparisons of maximum forces for various aspect ratios. The maximum difference between the maximum forces is 2.9%, for model with aspect ratio of 1:5 (as compared to the aspect ratio of 1:1).

Figures 03.07.02-29.26 through 03.07.02-29.28 show the comparisons of some typical 5% damped in-structure response spectra. The comparisons show that the in-structure response spectra compare well for aspect ratios up to 1:5.

Based on above results it is concluded that the 3-D solid elements can be used with aspect ratios up to 1:5.

Validation Problem with Plane Strain Elements (S&L)

A unit width (1 ft) of 4 ft thick, 100 ft width concrete foundation supporting 10 ft thick wall (1 ft width) at the middle strip of foundation is analyzed. Five models are constructed, which have rectangular elements with aspect ratios of 1:1, 1:2, 1:3, 1:4 and 1:5. The input motions are specified in horizontal and vertical directions. The results compared are; (a) maximum accelerations, (b) In-structure response spectra at various elevations and (c) Maximum shear and axial forces.

Figures 03.07.02-29.29 and 03.07.02-29.30 show the structural models for element aspect ratios of 1:1 and 1:2 respectively. For other aspect ratios, the models are similar with elements modified for the desired aspect ratios.

Table 03.07.02-29.17 shows the results of comparisons of maximum accelerations for various aspect ratios. The maximum difference between the accelerations is 7.8% (less than 10%), for model with aspect ratio of 1:5 (as compared to the aspect ratio of 1:1).

Table 03.07.02-29.18 shows the results of comparisons of maximum forces for various aspect ratios. The maximum difference between the maximum forces is 5.9% (less than 10%), for model with aspect ratio of 1:5 (as compared to the aspect ratio of 1:1).

Figures 03.07.02-29.31 and 03.07.02-29.32 show the comparisons of some typical 5% damped in-structure response spectra. The comparisons show that the in-structure response spectra compare well for aspect ratios up to 1:5.

Based on above results it is concluded that the plane strain plate elements can be used with aspect ratios up to 1:5.

Validation Problem with Thick Shell having Two-way Slab Action

The SSI model consists of a reinforced concrete box-structure with plan dimension of 54 ft x 36 ft and height of 48 ft (the aspect ratio of length to width is 1.5 and aspect ratio of height to width is 1.33, thus the walls and slabs have two-way slab action). The structure has four walls each 4 ft thick, roof slab 4 ft thick and base mat 6 ft thick. The grade elevation is 12 ft above the base mat element. All elements are modeled by rectangular thick shell. Figures 03.07.02-29.33 and 03.07.02-29.34 show the model for element aspect ratios of 1:1. Figure 03.07.02-29.33 shows the isometric view and Figure 03.07.02-34 shows the base mat. Figures 03.07.02-29.35 and 03.07.02-29.36 show the model for element aspect ratios of 1:5. Figure 03.07.02-29.35 shows the isometric view and Figure 03.07.02-36 shows the base mat. As shown in Figure 03.07.02-29.35 and 03.07.02-29.36, the width of the model (width of roof slab, 36 ft wide walls and the width of the base mat are divided in 1.2 ft wide elements to provide an aspect ratio of 1:5. The node numbers are also shown, in these figures, where the 5% damped in-structure response spectra for various aspect ratios models are compared. The locations of these nodes are at about the center of the walls, center of roof slab and the center of the base mat. For other desired aspect ratios (1:2, 1:3 and 1:4) the width of the structure are divided similarly. Since the number of interaction nodes in each model is different, the point radius in Module POINT of SASSI2000 is calculated based on average of dx and dy (horizontal distances between the adjacent interaction nodes) multiplied by 0.90.

The shear wave velocity of soil is 1000 ft/sec, which provides minimum passing frequency of 33Hz in the SSI model. 33Hz cutoff frequency is used in the analyses. The input motions are specified at the ground surface, in the global axes (two horizontal X, Y and vertical Z directions). The SSI analyses are performed using direct method. The results compared are; (a) In-structure response spectra at various elevations and (b) maximum accelerations and (c) forces/moments at the walls section cuts above the base mat.

(a) In-structure Response Spectra Comparisons

Figures 03.07.02-29.37 through 03.07.02-29.40 show the comparisons of X direction 5% damped in-structure response spectra due to the X direction excitation, for various aspect ratios models, at various locations of the structure. The comparisons show that the response spectra compare well for aspect ratios up to 1:5.

Figures 03.07.02-29.41 through 03.07.02-29.44 show the comparisons of Y direction 5% damped in-structure response spectra due to the Y direction excitation, for various aspect ratio models. The comparisons show that the response spectra compare well for aspect ratios up to 1:5.

Figures 03.07.02-29.45 through 03.07.02-29.48 show the comparisons of Z direction 5% damped in-structure response spectra, due to the Z direction excitation, for various aspect ratios models. The comparisons show that the response spectra compare well for aspect

ratios up to 1:5, for all locations except at the top of roof slab (Figure 03.07.02-29.48). At the top of the structure, the peak of the response spectra for models with the aspect ratios 1:2 to 1:5 are 7% - 9% higher than the 1:1 aspect ratio model. This exceedance is within 10% and also conservative compared to the 1:1 aspect ratio model.

(b) Comparisons of Maximum Accelerations

Table 03.07.02-29.28 shows the results of comparisons of maximum accelerations for various aspect ratios, at various locations of the structure. The comparisons show that the maximum accelerations compare well for aspect ratios up to 1:5.The maximum difference between the accelerations is 4.5% (less than 10%), for model with aspect ratio of 1:5 (as compared to the aspect ratio of 1:1).

(c) Comparisons of Forces / Moments at the Walls Section Cuts above the Base Mat

Table 03.07.02-29.29 shows the results of comparisons of maximum forces and moments calculated at the wall sections above the base mat. The comparisons show that the forces/moments compare well for aspect ratios up to 1:5, except for the out of plane bending moment in 36 ft long walls, due to Y-direction excitation. For this case, the bending moments for the aspect ratios of 1:2 to 1:5, are higher (maximum 10.2% higher).

Validation Problem with Thick Shell Elements (SGH)

Two structures are used to study the effect of element aspect ratio:

- A 10 ft wide by 1.0 ft thick cantilever beam
- A 20 ft tall by 1.0 ft thick shear wall

For each structure, five models using rectangular 3-D thick plate/shell structural elements with aspect ratios of 1:1, 2:1, 4:1, 5:1, and 10:1 are used. The height of the cantilever in each model varies with aspect ratio of the elements used, with the total height equal to 100 ft multiplied by the aspect ratio of the elements in the model. The length of the shear wall in each model also varies with the aspect ratio of the elements used, with length equal to 50 ft multiplied by the aspect ratio of the element. Both structures are modeled on rigid soil. The models are subjected to harmonic and seismic loadings. The models are shown in Figures 03.07.02-29.49 through 03.07.02-29.53.

For harmonic loadings a force is applied to nodes at the top of the model corresponding to vertical (z) force applied to the cantilever model, horizontal out-of-plane force applied to the cantilever model, and horizontal in-plane (Y) force applied to the shear wall model. The harmonic force loading analyses are used to calculate element stresses and model stiffness which are compared to calculated theoretical values.

For seismic excitations, concentrated inertias are placed at the top of the model, and material damping is 4.0%. Seismic excitation is applied at the ground surface model

corresponding to vertical (z) excitation applied to the cantilever model, horizontal out-of-plane excitation applied to the cantilever model, and horizontal in-plane (Y) excitation applied to the shear wall model. The nodal acceleration transfer functions are compared to theoretical calculated natural frequencies.

Table 03.07.02-29.19 shows the results of the comparisons of element stresses SASSI2000 with various aspect ratios output from SASS2000 from to theoretical values. The maximum difference between the element stresses calculated with SASSI2000 and theoretical values is 2.5%.

Table 03.07.02-29.20 shows the results of the comparisons of structural stiffnesses with various aspect ratios calculated using output from SASSI2000 to theoretical values. The maximum difference between the structural stiffnesses calculated using output from SASSI2000 and theoretical values is 3.0%.

Table 03.07.02-29.21 shows the results of the comparisons of the first natural frequency of each structure with various aspect ratios output from SASSI2000 to theoretical values. The maximum difference between the first natural structural frequency calculated using output from SASSI2000 and theoretical values is 1.3%.

Based on above results it is concluded that the 3-D thick plate/shell elements can be used with aspect ratios up to 10:1.

Validation Problem with 3-D Solid Elements (SGH)

Models similar to above with 3-D solid structural elements used to model the cantilever and shear wall. The models are shown in Figures 03.07.02-29.54 through 03.07.02-29.59.

Table 03.07.02-29.22 shows the results of the comparisons of element stresses SASSI2000 with various aspect ratios output from SASS2000 from to theoretical values. The maximum difference between the element stresses calculated with SASSI2000 and theoretical values is 0.0%.

Table 03.07.02-29.23 shows the results of the comparisons of structural stiffnesses with various aspect ratios calculated using output from SASSI2000 to theoretical values. The maximum difference between the structural stiffnesses calculated using output from SASSI2000 and theoretical values is 2.9%.

Table 03.07.02-29.24 shows the results of the comparisons of the first natural frequency of each structure with various aspect ratios output from SASSI2000 to theoretical values. The maximum difference between the first natural structural frequency calculated using output from SASSI2000 and theoretical values is 3.0%.

Based on above results it is concluded that the 3-D solid elements can be used with aspect ratios up to 10:1.

Validation Problem with 2-D Plane Strain Elements (SGH)

Models similar to the validation of the thick shell elements (SGH) are used for validation of 2D plane strain elements. The models are excavated, and the 2D plane strain elements are placed within the excavation but not connected to the excavation sides, and the models are not loaded in the out-of-plane direction because out-of-plane motion is incompatible with 2D analyses. The models are shown in Figures 03.07.02-29.60 through 03.07.02-29.67.

Table 03.07.02-29.25 shows the results of the comparisons of element stresses SASSI2000 with various aspect ratios output from SASS2000 from to theoretical values. The maximum difference between the element stresses calculated with SASSI2000 and theoretical values is 0.0%.

Table 03.07.02-29.26 shows the results of the comparisons of structural stiffnesses with various aspect ratios calculated using output from SASSI2000 to theoretical values. The maximum difference between the structural stiffnesses calculated using output from SASSI2000 and theoretical values is 3.1%.

Table 03.07.02-29.27 shows the results of the comparisons of the first natural frequency of each structure with various aspect ratios output from SASSI2000 to theoretical values. The maximum difference between the first natural structural frequency calculated using output from SASSI2000 and theoretical values is 3.6%.

Based on above results it is concluded that the 2-D plane strain elements can be used with aspect ratios up to 10:1.

Validation Problem with Thick Shell having Two-way Slab Action (SGH)

A concrete box structure 36 ft wide (along Y axis), 54 ft long (along X axis), and 54 ft high (Z axis) with 12 ft of embedment having exterior walls 4 ft thick, a 4 ft thick roof slab, and a 6 ft thick base mat is analyzed. Five models are constructed having rectangular elements with aspect ratios of 1:1, 1:2, 1:3, 1:4, and 1:5 for the base mat, roof, and short walls and 1:1 ratio on the long walls in all cases. The analyses used a constant 1:1 spacing for interaction nodes and excavation elements. The seismic input motions are specified in horizontal and vertical directions. Results compared are; (a) in-structure acceleration response spectra (ISRS) at center of roof slab, center of base slab, center of one short wall, and center of one long wall; and (b) wall section forces for the base of a long wall and a short wall.

The 1:1 and 1:5 models are shown in Figures 03.07.02-29.68 and 03.07.02-29.69 respectively and the excavation elements are shown in Figure 03.07.02-29.70. Other

aspect ratio models are constructed similarly but node and element numberings vary between models.

Figures 03.07.02-29.71 to 03.07.02-29.82 show ISRS comparing the analyses with various element aspect ratios. All spectra compare very well for ratios 1:1 up to 1:5.

Tables 03.07.02-29.30 to 03.07.02-29.31 show comparison of section forces at the base of the structure. The results show less than 5% difference between section forces calculated using 1:1 element ratios to those calculated using other aspect ratios up to 1:5.

Based on the above results it is concluded that the thick shell elements can be used for element demands and response spectra generation with aspect ratios up to 1:5. The example problem demonstrates this result specifically for seismic analysis of 2-way slabs structures.

- **Required mesh refinement to output out-of-plane responses in shell elements**

  The required mesh refinement to output out-of-plane responses in shell elements is not considered part of V&V process. Mesh refinements for out-of-plane responses depends on structural configuration and boundary conditions, hence is problem dependent. The user, who is experienced in finite element modeling, uses refined model for getting accurate final responses. Per NRC Staff request a mesh refinement study was performed for the SSI analysis of UHS/RSW Pump House and the design of UHS/RSW Pump House and in-structure response spectra cover the results obtained from the refined analysis. For more detailed information, see the response to RAI 03.07.02-24, Supplement 2, submitted with STPNOC letter U7-C-STP-NRC-100268, dated December 14, 2010.

- **Accuracy of subtraction method for calculating foundation impedance**

  Accuracy of subtraction method for calculating foundation impedance is covered in a number of existing V&V problems (as shown in Table 5.1 of Calculation S&L SVVR03.7.316-3.0, there are nine problems validating accuracy of subtraction method. There is also a problem, which compares results from subtraction method and direct method. Similarly, there are V&V problems demonstrating the accuracy of subtraction method, in the V&V document for SGH SASSI2000 v-3.

- **Limitations with respect to capping the Poisson's ratio to avoid possible stability problems should be validated and stated**

  The limitation with respect to capping the Poisson's ratio to avoid possible stability problems is not considered a part of the V&V process. The significance of the limitation with respect to capping the Poisson's ratio to avoid stability problems in SASS2000 is problem dependent, i.e. depending on the soil properties. In general Poisson's ratio is capped in the range of 0.47 to 0.49 for determining the compression wave velocity for

soil layers below groundwater level. The issue of numerical stability is part of the program user responsibilities. For STP 3&4 this issue has been studied in detail as described in the response to RAI 03.07.01-25, Supplement 1, submitted with STPNOC letter U7-C-STP-NRC-100253, dated November 29, 2010.

- **Adequacy and limitations of the specific shell element type (i.e. thin or thick shell elements)**

  For shell elements, two thickness formulations are available, thin or thick, with the difference being in the consideration of transverse shear deformations as noted below:

  - Thick shell formulation includes the effects of transverse shear deformation
  - Thin shell formulation neglects transverse shear deformation

  For situations where shear deformations are rather negligible and, therefore, use of thin shell elements may be justified, use of thick shell elements will not introduce any inaccuracy and the results using thick shell elements will be nearly identical (yet more accurate) to those using thin shell elements. For more information, see the response to RAI 03.07.02-25 submitted with STONOC letter U7-C-STP-NRC-100268, dated December 14, 2010.

  The adequacy and limitations of the specific shell element type (i.e. thin or thick shell elements) is not considered part of the V&V process, because selection of appropriate shell element type is problem dependent and thus these issues are part of the program user responsibilities.

Update of SASSI 2000 V&V Reports

To further clarify/expand the V&V documentation, the SASSI2000 V&V Reports (both S&L and SGH) are updated as follows:

- Purpose and scope of the V&V document is updated and expanded to clearly specify how V&V of SASSI2000 program is performed.
- Purpose of each test problem is expanded to clearly state which options are being validated.
- Conclusion of each test problem is expanded to clearly specify what options are considered validated.
- The summary and conclusion section of the document is expanded to show in detail features of the program that are validated along with identification of the supporting test problem.

SAP2000 Version 10.1 and 14.1:

The following provides the response to NRC staff questions on specific SAP2000 program features:

- **Accuracy of forces and moments calculated from section cuts in shell models**

  Please note that this SAP2000 program feature has not yet been used for the STP 3 & 4 project. However, as requested by the NRC staff the following additional test problem has been added to the SAP2000 V&V documentation.

  A 300" long x 24" wide x 12" deep beam fixed on one end and simply supported on the other which supports a mid-span load of 60 kips along with an axial load of 60 kips axial load is modeled and the accuracy of the forces and moments from various section cuts are compared against the values determined by manual calculations. The SAP2000 finite element (FE) model consists of a 6 by 24 mesh with thick shell elements. The transverse load is 60 kips total at center and the axial load is 60 kips total at x=300". The finite element model is shown in Figure 03.07.02-29.83.

  The model has the following boundary conditions.

  - $\delta x = \delta z = \theta y = 0$ @ x = 0"
  - $\delta x = 0$ @ x = 300"

  Comparison of shears and moments for 12 inches wide (half of the beam width) section at 5 locations are provided in Table 03.07.02-29.32. This comparison shows good agreement between the results from manual calculations and the SAP2000 section cuts with a maximum difference of 2%.

- **Accuracy of thick shell element for calculating out-of-plane dynamic responses**

  The following additional test problem has been added to the SAP2000 V&V documentation.

  A 300" x 400", 9" thick concrete plate supported on all 4 sides ($\delta x = \delta y = \delta z = 0$) is subjected to a concentrated harmonic load at the center. The finite element model is shown in Figure 03.07.02-29.84. The maximum amplitude of the load is 1000 lbs, and the sine loading history consists of 5 cycles with period of 0.05 sec. The total analysis time is 1 sec. The problem was solved in SAP2000 using the modal time history analysis method (5 modes) and the results were compared against those from a similar ANSYS model. Table 03.07.02-29.33 provides a comparison of the results for modal frequencies, plate center displacement and support reactions. As can be seen from these comparisons, there is good agreement between the results from SAP2000 and ANSYS with a maximum difference of 8.6%.

- **Accuracy of time-history modal analysis of fixed-base structures modeled using shell elements**

  The following additional test problem has been added to the SAP2000 V&V documentation.

  The problem consists of a 720" tall 200" x 300" tube (shell elements) with fixed base. The thickness of the shell element is 12". The finite element model is shown in Figure 03.07.02-29.85. The tube is subjected to a 22 second long horizontal ground acceleration (parallel to the short side) history used in the STP 3&4 project. Modal time history analysis is to be used. All modes up to mass participation of 90% are included (28 modes). The results from SAP2000 analysis are compared to the results from ANSYS analysis. Tables 03.07.02-29.34 and 03.07.02-29.35 provide comparisons for modal frequencies, displacements, and support reactions. As can be seen from these comparisons, there is good agreement between the results from SAP2000 and ANSYS with a maximum difference of 8.1%.

- **Validation of response spectra provided in Figures 03.07.02-25.10 and 03.07.02-25.11 of RAI 03.07.02-25, Revision 1, submitted concurrently with this response**

  The spectra in Figure 03.07.02-25.10 and 03.07.02-25.11 were generated using the SAP2000 program for a 49 ft x 78 ft slab panel (similar to the STP Pump House roof slab panel), fixed on all four edges as shown in Figure 03.07.02-29.86. The model was analyzed for slab thicknesses of six inches and six feet, using both thin and thick shell formulations. Time history analyses of these slab models were performed by subjecting the models in the transverse direction with the vertical STP site-specific SSE base motion.

  In order to verify these spectra, the SAP2000 analysis noted above was repeated using the validated and verified ANSYS program. To generate the response spectra at the center of the slab, the resulting joint acceleration time histories from the ANSYS analysis were then used in Sargent and Lundy validated and verified RSG program.

  Comparison of the response spectra at the center of the six inch slab for thin shell elements is shown in Figure 03.07.02-29.87. As can be seen at about 2.7 hz, the acceleration from SAP2000 is about 15% higher than that from ANSYS.

  Comparison of the response spectra at the center of the six inch slab for thick shell elements is shown in Figure 03.07.02-29.88. As can be seen at about 2.7 hz, the acceleration from SAP2000 is about 15% higher than that from ANSYS.

  Comparison of the response spectra at the center of the six foot slab for thin shell elements is shown in Figure 03.07.02-29.89. As can be seen at about 28 hz, the acceleration from SAP2000 is about 5% lower than that from ANSYS.

Comparison of the response spectra at the center of the six foot slab for thick shell elements is shown in Figure 03.07.02-29.90. As can be seen at about 29.6 hz, the acceleration from SAP2000 is about 5% lower than that from ANSYS.

Examination of Figures 03.07.02-29.87 through 03.07.02-29.90 shows that the shapes of the spectra and the peak locations are very close between SAP2000 and ANSYS analyses.

The differences between the spectra generated by SAP2000 and ANSYS can be attributed to the following factors:

- Difference in formulation of both thin and thick shell elements.
- Difference in dynamic solution (integration) strategies.
- Difference in inherent software compiler numerical precision

In view of the comparison described above, SAP2000 is found to be satisfactory in combining the capability of shell element dynamic analysis and response spectrum generation.

SHAKE2000 Version 3.5

The theory and analysis technique used in SHAKE2000 Version 3.5 is essentially same as original SHAKE, "A computer Program for Earthquake Response Analysis of Horizontally Layered Sites"; by Schnabel, P.B; Lysmer, J; and Seed, H.B Report No. 72-12, Earthquake Engineering Research Center, College of Engineering, University of California, Berkeley, December 1972.

The program is based on the continuous solution to wave equation adopted for use with transient motions through Fast Fourier Transform algorithm. The nonlinearity of the shear modulus and damping is accounted for by the use of equivalent linear soil properties using an iterative procedure to obtain values for modulus and damping compatible with effective strains in each layer. In the SHAKE2000 program, the maximum number of soil layer limitation of 200 for analysis of a soil profile is a program dimension assignment, and any anomaly caused by use of large number of soil layers can be detected by a qualified SSI analyst.

As requested by the NRC Staff, V&V documentation of the SHAKE2000 program has been expanded to include six (6) additional test problems with 116 soil layers to demonstrate acceptability of the SHAKE2000 program when using large number of soil layers. All STP 3&4 SHAKE2000 analyses have been performed using 100 or fewer soil layers. These 6 problems cover both in-profile (within) and Outcrop input-output options of the program. The analyses and results from these six problems demonstrate that the program is validated for large number of layers up to 116 layers.

Validation Problem 1

This validation problem is used to validate the iterated strain compatible shear modulus and damping and accelerations for various soil layers, for input motion defined at the base of the model. The soil profile property for validation problem 1 is same as 8-layer problem used in the original V&V. Total depth of the soil profile is 116 ft. The soil profile is divided in 116 layers. The input motion is specified at the base of the soil profile and iterated strain compatible shear modulus and damping ratios and maximum accelerations of soil layers obtained from the 116 layer and 8 layer models are compared. The maximum difference between shear modulus values is less than 0.5% (see Table 03.07.02-29.36). The maximum difference between damping values is less than 2.3% (see Table 03.07.02-29.36). The maximum difference between acceleration values is less than 0.8% (see Table 03.07.02-29.37). Thus, the option to calculate the iterated strain compatible shear modulus and damping values, and accelerations for various soil layers due to seismic input at the base of the soil profile, for large number of soil layers, up to 116 layers is validated.

Validation Problem 2

This validation problem is used to validate the iterated strain dependent shear modulus and damping and accelerations for various soil layers, for input motion defined at the ground surface. This problem is the same as validation problem 1, except that the input is specified as outcrop at the ground surface. Iterated strain compatible shear modulus and damping ratios and maximum accelerations of soil layers obtained from the 116 layer and 8 layer models are compared. The maximum difference between shear modulus values is less than 0.3% (see Table 03.07.02-29.38). The maximum difference between damping values is less than 0.8% (see Table 03.07.02-29.38). The maximum difference between acceleration values is less than 3.3% (see Table 03.07.02-29.39). Thus the option to calculate the iterated strain compatible shear modulus and damping values, and accelerations for various soil layers due to seismic input defined at the ground surface, for large number of soil layers, up to 116 layers is validated.

Validation Problem 3

This validation problem is used to validate outcrop option of the program for within (in-profile) motion applied at the base of the soil profile and determining outcrop motion at the ground surface. The 116 layers problem is used with seismic input motion at the base of the model and in-profile motion (response spectra) and outcrop motion at 1 foot below the ground surface are obtained. The input motion is applied at the base as in-profile. For this problem, the in-profile and outcrop motion at 1 ft below the ground surface are compared. It is a technical fact that the in-profile and outcrop motion at the top layer (ground surface) is the same. The in-profile and outcrop motion are selected at 1 foot below the ground surface, since in SHAKE2000, the motion at the ground surface is always defined as outcrop. The selected 1 foot below the ground surface is used and is acceptable for comparison, because the frequency of the first layer is well above 50 Hz (much higher than

the frequency content of input motion). For such a case the in-profile and outcrop motions at 1 foot depth should be the same. Figure 03.07.02-29.91 shows the comparison between the in-profile and outcrop 5% damped spectra at 1 foot below the ground surface. The two spectra are same (lay over on each other). Thus the option of the program for in-profile motion applied at the base of the soil profile and resulting outcrop motion at the ground surface is validated for large number of soil layers, up to 116 layers.

Validation Problem 4

This validation problem is used to validate outcrop option of the program for outcrop motion applied at the base of the soil profile and determining outcrop motion at the ground surface. The 116 layers problem is used with seismic outcrop input motion at the base of the model and in-profile motion (response spectra) and outcrop motion at 1 foot below the ground surface are obtained. For this problem, the in-profile and outcrop motion at 1 foot below the ground surface are compared. It is a technical fact that the in-profile and outcrop motion at the top layer (ground surface) are the same. The in-profile and outcrop motion are selected at 1 foot below the ground surface, since in SHAKE2000, the motion at the ground surface is always defined as outcrop. The selected 1 foot below the ground surface is used and is acceptable for comparison, because the frequency of the first layer is well above 50 Hz (much higher than the frequency content of input motion). For such a case the in-profile and outcrop motions at 1 foot depth should be same. Figure 03.07.02-29.92 shows the comparison between the in-profile and outcrop 5% damped spectra at 1 foot below the ground surface. The two spectra are same (lay over on each other). Thus the option of the program for outcrop motion applied at the base of the soil profile and resulting outcrop motion at the ground surface is validated for large number of soil layers, up to 116 layers.

Validation Problem 5

This validation problem is used to validate outcrop option of the program for outcrop motion applied at the ground surface and determining the outcrop motion at a certain depth of the soil profile. The 116 layer problem, with very stiff soil modulus is analyzed with outcrop input at the ground surface. The stiffness of the soil profile is such that the soil column has a frequency greater than 50 Hz. The input motion is the STP 3&4 site-specific SSE motion, which has highest frequency of 33 Hz. The in-profile motion and outcrop motion at 42 feet below the ground surface are obtained. For this problem, the in-profile and out-crop motion at a location below the ground surface should be same.
Figure 03.07.02-29.93 shows the comparison between the in-profile and outcrop 5% damped spectra at 42 feet below the ground surface. The two spectra are the same (lay over on each other). Thus the option to obtain outcrop motion at certain depth of the soil profile with outcrop input motion applied at the ground is validated for large number of soil layers, up to 116 layers.

Validation Problem 6

This validation problem is used to validate outcrop motion applied at a depth of the soil profile and determining outcrop motion at the ground surface. The 116 layer problem, with very stiff soil modulus is analyzed with outcrop motion input 42 feet below the ground surface. The stiffness of the soil profile is such that the soil column has a frequency greater than 50 Hz. The input motion is the STP 3&4 site-specific SSE motion, which has highest frequency of 33 Hz. In-profile and outcrop motion at 1 foot below the ground surface are obtained. For this problem, the in-profile and outcrop motion at 1 foot below the ground surface should be same. Figure 03.07.02-29.94 shows the comparison between the in-profile and outcrop 5% damped spectra at 1 foot below the ground surface. The two spectra are the same (lay over on each other). Thus the option to obtain outcrop motion at the ground surface with outcrop input motion applied at a depth of the soil profile is validated for large number of soil layers, up to 116 layers.

COLA will be revised as shown in Enclosures 1 as a result of this response.

Table 03.07.02-29.1: Natural Frequency for Thick Shell Element Model with In-Plane Load

Element Model	Natural Frequency (Hz)		
	SASSI	Hand Calculation	Difference
Rectangular	2.88	2.96	2.70%
Triangle	2.88	2.96	2.70%

Table 03.07.02-29.2: Peak of Response Spectra for Thick Shell Element Model with In-Plane Load

Node	Acceleration (g)		
	Rectangular El. Model	Triangular El. Model	Difference
158	3.90	3.79	2.84%
171	3.03	3.09	-1.73%
184	3.90	3.75	3.92%

Table 03.07.02-29.3: First Mode Natural Frequencies for Thick Shell Element Model with Out-of-Plane Load

Element Model/ Node	Natural Frequency (Hz)				
	Rectangular El. Model	Triangular El. Model	Difference	Thin Plate Hand Calculation	Difference
10'x5'x6" - 31	0.27	0.27	0.00%	0.27	0%
10'x5'x4'- 31	1.98	2.00	-1.01%	2.16	8%
10'x5'x6" - 61	0.27	0.27	0.00%	0.27	0%
10'x5'x4'- 61	1.98	2.00	-1.01%	2.16	8%

Table 03.07.02-29.4: Peak of Response Spectra for Thick Shell Element Model with Out-of-Plane Load

Model/Node	Acceleration (g)		
	Rectangular El. Model	Triangular El. Model	Difference
10'x5'x6" - 31	1.93	2.00	-3.63%
10'x5'x4'- 31	2.10	2.15	-2.38%
10'x5'x6" - 61	1.86	1.77	4.84%
10'x5'x4'- 61	5.47	5.52	-0.91%

Table 03.07.02-29.5: First Mode Natural Frequencies for Thick Shell Element Model with Vertical Axial Load

Element Model/ Node	Natural Frequency (Hz)				
	Rectangular El. Model	Triangular El. Model	Difference	Thin Plate Hand Calculation	Maximum. Difference
10'x5'x4'- 31	8.11	8.13	-0.25%	8.12	0.12%
10'x5'x4'- 61	8.13	8.15	-0.25%	8.12	0.37%

Table 03.07.02-29.6: Peak of Response Spectra for Thick Shell Element Model with Vertical Axial Load

Model/Node	Acceleration (g)		
	Rectangular El. Model	Triangular El. Model	Difference
10'x5'x4'- 31	1.22	1.20	1.84%
10'x5'x4'- 61	2.28	2.24	1.65%

Table 03.07.02-29.7: First Mode Natural Frequencies for 2-D Plane Strain Element Model with In-Plane Load

Node	Natural Frequency (Hz)				
	Rectangular El. Model	Triangular El. Model	Difference	Hand Calculation	Difference
52	7.10	7.10	0.00%	7.04	-0.85%

Table 03.07.02-29.8: Peak of Response Spectra 2-D Plane Strain Element Model with In-Plane Load

Node	Acceleration (g)		
	Rectangular El. Model	Triangular El. Model	Difference
52	2.49	2.49	0.00%

Table 03.07.02-29.9: First Mode Natural Frequencies 2-D Plane Strain Element Model with Vertical Axial Load

Node	Natural Frequency (Hz)				
	Rectangular El. Model	Triangular El. Model	Difference	Hand Calculation	Difference
52	11.47	11.47	0.00%	11.48	0.09%

Table 03.07.02-29.10: Peak of Response Spectra 2-D Plane Strain Element Model with Vertical Axial Load

Node	Acceleration (g)		
	Rectangular El. Model	Triangular El. Model	Difference
52	1.89	1.89	0.00%

Table 03.07.02-29.11

Comparison of Maximum Acceleration (g) – Thin Shell Model									
Aspect Ratio	X Responses Due to X Direction Input Motion			Y Responses Due to Y Direction Input Motion			Z Responses Due to Z Direction Input Motion		
	Bottom of Wall	Middle of Wall	Top of Wall	Bottom of Wall	Middle of Wall	Top of Wall	Bottom of Wall	Middle of Wall	Top of Wall
1:1	0.1462	0.3110	0.6320	0.1356	0.2133	0.3056	0.1343	0.1426	0.1460
1:2	0.1462	0.3117	0.6381	0.1364	0.2178	0.3127	0.1348	0.1436	0.1471
1:3	0.1463	0.3110	0.6375	0.1366	0.2193	0.3149	0.1348	0.1437	0.1472
1:4	0.1462	0.3106	0.6372	0.1367	0.2201	0.3163	0.1349	0.1438	0.1473
1:5	0.1462	0.3105	0.6369	0.1367	0.2206	0.3173	0.1349	0.1439	0.1474
Maximum Difference (%)									
	0.07	0.4	1.0	0.8	3.4	4.0	0.4	0.9	1.0

Table 03.07.02-29.12

Comparison of Maximum Forces/Moment – Thin Shell Model			
Aspect Ratio	X –Dir. Input Motion Induced Bending Moment (ft-kips/ft)	Y-Dir. Input Motion Induced Total In-Plane Shear Force (kips)	Z-Dir. Input Motion Induced Total Axial Force (kips)
1:1	595.8	1017.3	648.2
1:2	596.3	1019.3	653.9
1:3	596.3	1021.7	654.2
1:4	596.3	1025.3	654.9
1:5	596.3	1027.7	655.3
Maximum Difference (%)	0.1	1.0	1.1

Table 03.07.02-29.13

Maximum Acceleration (g) – Thick Shell Model									
Aspect Ratio	X Responses Due to X Direction Input Motion			Y Responses Due to Y Direction Input Motion			Z Responses Due to Z Direction Input Motion		
	Bottom of Wall	Mid-Height of Wall	Top of Wall	Bottom of Wall	Mid-Height of Wall	Top of Wall	Bottom of Wall	Mid-Height of Wall	Top of Wall
1:1	0.1461	0.3168	0.6449	0.1357	0.2132	0.3058	0.1343	0.1426	0.1460
1:2	0.1462	0.3192	0.6500	0.1364	0.2186	0.3139	0.1348	0.1436	0.1471
1:3	0.1462	0.3194	0.6506	0.1366	0.2200	0.3162	0.1348	0.1437	0.1472
1:4	0.1462	0.3194	0.6507	0.1367	0.2208	0.3179	0.1349	0.1438	0.1473
1:5	0.1462	0.3195	0.6508	0.1368	0.2212	0.3189	0.1349	0.1439	0.1474
Maximum Difference (%)									
	0.07	0.9	0.9	0.8	3.8	4.2	0.4	0.9	1.0

Table 03.07.02-29.14

Comparison of Maximum Forces/Moment – Thick Shell Model			
Aspect Ratio	X –Dir. Input Motion Induced Bending Moment (ft-kips/ft)	Y-Dir. Input Motion Induced Total In-Plane Shear Force (kips)	Z-Dir. Input Motion Induced Total Axial Force (kips)
1:1	594.2	1013.3	644.3
1:2	594.1	1012.7	653.9
1:3	594.1	1017.5	655.9
1:4	594.1	1021.1	657.4
1:5	594.1	1023.4	658.1
Maximum Difference (%)	0.0	1.0	2.1

Table 03.07.02-29.15

Comparison of Maximum Acceleration (g) – 8-Node Solid Element Model									
Aspect Ratio	X Response Due to X Direction Input Motion			Y Response Due to Y Direction Input Motion			Z Response Due to Z Direction Input Motion		
	Bottom of Wall	Mid-Height of Wall	Top of Wall	Bottom of Wall	Mid-Height of Wall	Top of Wall	Bottom of Wall	Mid-Height of Wall	Top of Wall
1:1	0.1455	0.3179	0.6573	0.1359	0.2150	0.3084	0.1349	0.1432	0.1466
1:2	0.1455	0.3179	0.6578	0.1365	0.2195	0.3158	0.1351	0.1435	0.1469
1:3	0.1455	0.3183	0.6583	0.1366	0.2204	0.3173	0.1351	0.1436	0.1470
1:4	0.1455	0.3182	0.6584	0.1367	0.2208	0.3179	0.1351	0.1436	0.1470
1:5	0.1455	0.3180	0.6581	0.1368	0.2214	0.3192	0.1351	0.1437	0.1471
Maximum Difference (%)	< 1%	< 1%	< 1%	< 1%	2.9%	3.5%	< 1%	< 1%	< 1%

Table 03.07.02-29.16

Comparison of Wall Section Forces (kips) – 8-Node Solid Element Model			
Aspect Ratio	X Direction Input Motion Induced Total Shear Force V_{zx} (kips)	Y Direction Input Motion Induced Total Shear Force V_{zy} (kips)	Z Direction Input Motion Induced Total Axial Force P_z (kips)
1:1	953.3	1007.4	660.5
1:2	950.7	1027.8	662.1
1:3	951.0	1032.2	662.2
1:4	950.7	1034.2	662.3
1:5	951.0	1037.1	662.8
Maximum Difference (%)	< 1%	2.9%	< 1%

Table 03.07.02-29.17

Maximum Zero Period Accelerations (ZPA)						
Case	X-Dir Model			Z-Dir Model		
	Bottom of Wall (Node 21) - a_x (g)	Middle of Wall (Node 35) - a_x (g)	Top of Wall (Node 45) - a_x (g)	Bottom of Wall (Node 21) - a_z (g)	Middle of Wall (Node 35) - a_z (g)	Top of Wall (Node 45) - a_z (g)
1 (Aspect Ratio 1:1)	0.1501	0.2965	0.6442	0.1370	0.1396	0.1405
2 (Aspect Ratio 1:2)	0.1526	0.3039	0.6557	0.1374	0.1403	0.1412
3 (Aspect Ratio 1:3)	0.1533	0.3135	0.6594	0.1375	0.1404	0.1413
4 (Aspect Ratio 1:4)	0.1534	0.3176	0.6605	0.1375	0.1405	0.1414
5 (Aspect Ratio 1:5)	0.1535	0.3197	0.6609	0.1375	0.1405	0.1414
Maximum Difference	2.3%	7.8%	2.6%	0.4%	0.6%	0.6%

Table 03.07.02-29.18

Maximum Forces at the Bottom Wall Section		
Case	**X-Dir Model**	**Z-Dir Model**
	Shear Force Vx (kip)	**Axial Force Pz (kip)**
1 (Aspect Ratio 1:1)	39.130	19.869
2 (Aspect Ratio 1:2)	39.547	19.963
3 (Aspect Ratio 1:3)	40.724	19.981
4 (Aspect Ratio 1:4)	41.232	19.991
5 (Aspect Ratio 1:5)	41.458	19.995
Maximum Difference	5.9%	0.6%

Table 03.07.02-29.19

Maximum Element Stresses - Thick Plate/Shell Model							
			Aspect Ratio				
			1:1	2:1	4:1	5:1	10:1
Cantilever Subjected to Harmonic Axial Vertical (Z) Force	Vertical Stress at Bottom of Cantilever (kip/ft)	SASSI2000	0.100	0.100	0.100	0.100	0.100
		Theoretical	0.100	0.100	0.100	0.100	0.100
		Percent Difference	0.0%	0.0%	0.0%	0.0%	0.0%
	Horizontal Stress at Bottom of Cantilever (kip/ft)	SASSI2000	0.017	0.017	0.017	0.017	0.017
		Theoretical	0.017	0.017	0.017	0.017	0.017
		Percent Difference	0.0%	0.0%	0.0%	0.0%	0.0%
Cantilever Subjected to Harmonic Out-of-Plane Horizontal (Y) Force	Shear Stress at Bottom of Cantilever (kip/ft)	SASSI2000	0.100	0.100	0.100	0.100	0.100
		Theoretical	0.100	0.100	0.100	0.100	0.100
		Percent Difference	0.0%	0.0%	0.0%	0.0%	0.0%
	Bending Stress at Bottom of Cantilever (kip-ft/ft)	SASSI2000	9.502	19.005	38.009	47.512	95.025
		Theoretical	9.500	19.000	38.000	47.500	95.000
		Percent Difference	0.0%	0.0%	0.0%	0.0%	0.0%
Shear Wall Subjected to Harmonic In-Plane Horizontal (X) Force	Shear Stress at Bottom of Wall (kip/ft)	SASSI2000	0.0200	0.0098	0.0049	0.0039	0.0020
		Theoretical	0.0200	0.0100	0.0050	0.0040	0.0020
		Percent Difference	0.0%	-2.0%	-2.0%	-2.5%	0.0%
Maximum Percent Difference			0.0%	2.0%	2.0%	2.5%	0.0%

Table 03.07.02-29.20

Structural Stiffnesses - Thick Plate/Shell Model							
			Aspect Ratio				
			1:1	2:1	4:1	5:1	10:1
Cantilever Subjected to Harmonic Axial Vertical (Z) Force	Structural Stiffness at Top of Cantilever (kip/ft)	SASSI2000	3.218	1.609	0.805	0.644	0.322
		Theoretical	3.125	1.563	0.781	0.625	0.313
		Percent Difference	3.0%	3.0%	3.0%	3.0%	3.0%
Cantilever Subjected to Harmonic Out-of-Plane Horizontal (Y) Force	Structural Stiffness at Top of Cantilever (kip/ft)	SASSI2000	10.053	1.256	0.157	0.080	0.010
		Theoretical	10.000	1.250	0.156	0.080	0.010
		Percent Difference	0.5%	0.5%	0.5%	0.5%	0.5%
Shear Wall Subjected to Harmonic In-Plane Horizontal (X) Force	Structural Stiffness at Top of Wall (kip/ft)	SASSI2000	1.0755	2.1473	4.2863	5.3533	10.6952
		Theoretical	1.0684	2.1368	4.2735	5.3419	10.6838
		Percent Difference	0.7%	0.5%	0.3%	0.2%	0.1%
Maximum Percent Difference			3.0%	3.0%	3.0%	3.0%	3.0%

Table 03.07.02-29.21

First Natural Frequency - Thick Plate/Shell Model							
			Aspect Ratio				
			1:1	2:1	4:1	5:1	10:1
Cantilever Subjected to Harmonic Axial Vertical (Z) Force	First Natural Frequency at Top of Cantilever (Hz)	SASSI2000	16.162	11.426	8.081	7.227	5.103
		Theoretical	15.959	11.285	7.979	7.137	5.047
		Percent Difference	1.3%	1.3%	1.3%	1.3%	1.1%
Cantilever Subjected to Harmonic Out-of-Plane Horizontal (Y) Force	First Natural Frequency (Hz)	SASSI2000	28.564	10.107	3.564	2.563	0.903
		Theoretical	28.548	10.093	3.568	2.553	0.903
		Percent Difference	0.1%	0.1%	-0.1%	0.4%	0.1%
Shear Wall Subjected to Harmonic In-Plane Horizontal (X) Force	First Natural Frequency (Hz)	SASSI2000	9.351	9.351	9.326	9.326	9.326
		Theoretical	9.331	9.331	9.331	9.331	9.331
		Percent Difference	0.2%	0.2%	-0.1%	-0.1%	-0.1%
Maximum Percent Difference			1.3%	1.3%	1.3%	1.3%	1.1%

Table 03.07.02-29.22

Maximum Element Stresses - 3-D Solid Model							
			Aspect Ratio				
			1:1	2:1	4:1	5:1	10:1
Cantilever Subjected to Harmonic Axial Vertical (Z) Force	Vertical Stress at Bottom of Cantilever (kip/ft^2)	SASSI2000	0.010	0.010	0.010	0.010	0.010
		Theoretical	0.010	0.010	0.010	0.010	0.010
		Percent Difference	0.0%	0.0%	0.0%	0.0%	0.0%
Cantilever Subjected to Harmonic Out-of-Plane Horizontal (Y) Force	Shear Stress at Bottom of Cantilever (kip/ft^2)	SASSI2000	0.010	0.010	0.010	0.010	0.010
		Theoretical	0.010	0.010	0.010	0.010	0.010
		Percent Difference	0.0%	0.0%	0.0%	0.0%	0.0%
Shear Wall Subjected to Harmonic In-Plane Horizontal (X) Force	Shear Stress at Bottom of Wall (kip/ft^2)	SASSI2000	0.004	0.002	0.001	0.001	0.000
		Theoretical	0.004	0.002	0.001	0.001	0.000
		Percent Difference	0.0%	0.0%	0.0%	0.0%	0.0%
Maximum Percent Difference			0.0%	0.0%	0.0%	0.0%	0.0%

Table 03.07.02-29.23

Structural Stiffnesses - 3-D Solid Model							
			Aspect Ratio				
			1:1	2:1	4:1	5:1	10:1
Cantilever Subjected to Harmonic Axial Vertical (Z) Force	Structural Stiffness at Top of Cantilever (kip/ft)	SASSI2000	400.8	200.4	100.2	80.19	40.08
		Theoretical	400.0	200.0	100.0	80.00	40.00
		Percent Difference	0.2%	0.2%	0.2%	0.2%	0.2%
Cantilever Subjected to Harmonic Out-of-Plane Horizontal (Y) Force	Structural Stiffness at Top of Cantilever (kip/ft)	SASSI2000	9709	1236	155.8	79.87	10.01
		Theoretical	10000	1250	156.3	80.00	10.00
		Percent Difference	-2.9%	-1.1%	-0.3%	-0.2%	0.1%
Shear Wall Subjected to Harmonic In-Plane Horizontal (X) Force	Structural Stiffness at Top of Wall (kip/ft)	SASSI2000	5.342	10.6838	21.3675	26.7094	53.4188
		Theoretical	5.342	10.6838	21.3675	26.7094	53.4188
		Percent Difference	0.0%	0.0%	0.0%	0.0%	0.0%
Maximum Percent Difference			2.9%	1.1%	0.3%	0.2%	0.2%

Table 03.07.02-29.24

First Natural Frequency - 3-D Solid Model							
			Aspect Ratio				
			1:1	2:1	4:1	5:1	10:1
Cantilever Subjected to Harmonic Axial Vertical (Z) Force	First Natural Frequency at Top of Cantilever (Hz)	SASSI2000	12.769	9.033	6.372	5.713	4.028
		Theoretical	12.767	9.028	6.383	5.710	4.037
		Percent Difference	0.0%	0.1%	-0.2%	0.1%	-0.2%
Cantilever Subjected to Harmonic Out-of-Plane Horizontal (Y) Force	First Natural Frequency (Hz)	SASSI2000	31.299	11.206	3.979	2.856	1.001
		Theoretical	31.917	11.285	3.990	2.855	1.009
		Percent Difference	-1.9%	-0.7%	-0.3%	0.1%	-0.8%
Shear Wall Subjected to Harmonic In-Plane Horizontal (X) Force	First Natural Frequency (Hz)	SASSI2000	2.124	2.075	2.148	2.100	2.051
		Theoretical	2.087	2.087	2.087	2.087	2.087
		Percent Difference	1.8%	-0.5%	3.0%	0.6%	-1.7%
Maximum Percent Difference			1.9%	0.7%	3.0%	0.6%	1.7%

Table 03.07.02-29.25

Maximum Element Stresses – 2-D Plane Strain Model							
			Aspect Ratio				
			1:1	2:1	4:1	5:1	10:1
Cantilever Subjected to Harmonic Axial Vertical (Z) Force	Vertical Stress at Bottom of Cantilever (kip/ft^2)	SASSI2000	0.100	0.100	0.100	0.100	0.100
		Theoretical	0.100	0.100	0.100	0.100	0.100
		Percent Difference	0.0%	0.0%	0.0%	0.0%	0.0%
	Horizontal Stress at Bottom of Cantilever (kip/ft^2)	SASSI2000	0.020	0.020	0.020	0.020	0.020
		Theoretical	0.020	0.020	0.020	0.020	0.020
		Percent Difference	0.0%	0.0%	0.0%	0.0%	0.0%
Shear Wall Subjected to Harmonic In-Plane Horizontal (X) Force	Shear Stress at Bottom of Wall (kip/ft^2)	SASSI2000	0.020	0.010	0.005	0.004	0.002
		Theoretical	0.020	0.010	0.005	0.004	0.002
		Percent Difference	0.0%	0.0%	0.0%	0.0%	0.0%
Maximum Percent Difference			0.0%	0.0%	0.0%	0.0%	0.0%

Table 03.07.02-29.26

Structural Stiffnesses - 2-D Plane Strain Model							
			Aspect Ratio				
			1:1	2:1	4:1	5:1	10:1
Cantilever Subjected to Harmonic Axial Vertical (Z) Force	Structural Stiffness at Top of Cantilever (kip/ft)	SASSI2000	3.223	1.611	0.806	0.644	0.322
		Theoretical	3.125	1.563	0.781	0.625	0.313
		Percent Difference	3.1%	3.1%	3.1%	3.1%	3.1%
Shear Wall Subjected to Harmonic In-Plane Horizontal (X) Force	Structural Stiffness at Top of Wall (kip/ft)	SASSI2000	1.068	2.137	4.274	5.342	10.684
		Theoretical	1.068	2.137	4.274	5.342	10.684
		Percent Difference	0.0%	0.0%	0.0%	0.0%	0.0%
Maximum Percent Difference			3.1%	3.1%	3.1%	3.1%	3.1%

Table 03.07.02-29.27

First Natural Frequency - Thick Shell Model							
			Aspect Ratio				
			1:1	2:1	4:1	5:1	10:1
Cantilever Subjected to Harmonic Axial Vertical (Z) Force	First Natural Frequency at Top of Cantilever (Hz)	SASSI2000	16.528	11.670	8.252	7.373	5.225
		Theoretical	15.959	11.285	7.979	7.137	5.047
		Percent Difference	3.6%	3.4%	3.4%	3.3%	3.5%
Shear Wall Subjected to Harmonic In-Plane Horizontal (X) Force	First Natural Frequency (Hz)	SASSI2000	9.326	9.326	9.326	9.326	9.326
		Theoretical	9.331	9.331	9.331	9.331	9.331
		Percent Difference	-0.1%	-0.1%	-0.1%	-0.1%	-0.1%
Maximum Percent Difference			3.6%	3.4%	3.4%	3.3%	3.5%

Table 03.07.02-29.28

Maximum Acceleration (g) at Various Locations												
	X Responses Due to X Direction Input Motion				Y Responses Due to Y Direction Input Motion				Z Responses Due to Z Direction Input Motion			
	Top of Bottom Slab	Midheight of 36' Walls	Midheight of 54' Walls	Top of Roof Slab	Top of Bottom Slab	Midheight of 36' Walls	Midheight of 54' Walls	Top of Roof Slab	Top of Bottom Slab	Midheight of 36' Walls	Midheight of 54' Walls	Top of Roof Slab
1:1	0.1441	0.1763	0.1836	0.2350	0.1359	0.1626	0.1654	0.2001	0.1266	0.1316	0.1314	0.1727
1:2	0.1449	0.1767	0.1845	0.2403	0.1361	0.1637	0.1664	0.2022	0.1264	0.1323	0.1321	0.1786
1:3	0.1451	0.1767	0.1846	0.2419	0.1361	0.1638	0.1665	0.2023	0.1262	0.1324	0.1323	0.1797
1:4	0.1452	0.1768	0.1847	0.2425	0.1361	0.1639	0.1666	0.2025	0.1261	0.1326	0.1324	0.1805
1:5	0.1452	0.1766	0.1846	0.2412	0.1361	0.1640	0.1667	0.2027	0.1258	0.1326	0.1324	0.1805
Maximum Difference (%) With Respect to Aspect Ratio 1:1												
	0.8	0.3	0.6	3.2	0.1	0.9	0.8	1.3	-0.6	0.8	0.8	4.5

Table 03.07.02-29.29

Maximum Forces/Moment at Wall Section Above Foundation					
Aspect Ratio	X-Direction Input Motion (along 36' long wall direction)		Y-Direction Input Motion (along 54' long wall direction)		Z-Direction Input Motion
	Total Bending Moment of Two 54 ft Long Walls (ft-kips)	Total In-Plane Shear of Two 36' Long Walls (kips)	Total Bending Moment of Two 36 ft Long Walls (ft-kips)	Total In-Plane Shear of Two 54' Long Walls (kips)	Total Axial Force (kips, 4 Walls)
1:1	554.6	415.6	192.7	508.1	705.5
1:2	541.1	414.1	202.9	500.4	688.6
1:3	536.8	410.0	209.1	505.0	672.8
1:4	534.7	409.6	210.6	504.1	661.2
1:5	533.7	408.2	212.3	504.6	746.2
Maximum Difference (%) With Respect to Aspect Ratio 1:1					
	-3.8	-1.8	10.2	-1.5	-6.3

Table 03.07.02-29.30: Section Forces for Wall Along X - Axis

Aspect Ratio	Wall Along X									
	Axial		In-Plane Shear		In-Plane Moment		Out-of-Plane Shear		Out-of-Plane Moment	
	kip	% Diff	kip	% Diff	kip-ft	% Diff	kip	% Diff	kip-ft	% Diff
X Direction Analysis										
1:1	0.0		272.1		4053.6		0.0		0.0	
1:2	0.0	0.0	273.1	0.4	4190.0	3.4	0.0	0.0	0.0	0.0
1:3	0.0	0.0	273.3	0.4	4232.3	4.4	0.0	0.0	0.0	0.0
1:4	0.0	0.0	273.4	0.5	4242.6	4.7	0.0	0.0	0.0	0.0
1:5	0.0	0.0	273.4	0.5	4253.7	4.9	0.0	0.0	0.0	0.0
Y Direction Analysis										
1:1	565.0		0.0		0.0		200.3		286.9	
1:2	568.8	0.7	0.0	0.0	0.0	0.0	200.4	0.1	285.6	0.5
1:3	569.8	0.8	0.0	0.0	0.0	0.0	200.3	0.0	285.7	0.4
1:4	570.0	0.9	0.0	0.0	0.0	0.0	200.3	0.0	285.8	0.4
1:5	570.3	0.9	0.0	0.0	0.0	0.0	200.3	0.0	285.8	0.4
Z Direction Analysis										
1:1	218.1		0.0		0.0		60.0		234.4	
1:2	220.5	1.1	0.0	0.0	0.0	0.0	59.3	1.3	228.2	2.6
1:3	221.2	1.4	0.0	0.0	0.0	0.0	59.0	1.7	227.4	3.0
1:4	221.3	1.5	0.0	0.0	0.0	0.0	59.0	1.7	227.0	3.1
1:5	221.5	1.6	0.0	0.0	0.0	0.0	58.9	1.8	226.9	3.2

Table 03.07.02-29.31: Section Forces for Wall Along Y - Axis

Aspect Ratio	Wall Along Y									
	Axial		In-Plane Shear		In-Plane Moment		Out-of-Plane Shear		Out-of-Plane Moment	
	kip	% Diff	kip	% Diff	kip-ft	% Diff	kip	% Diff	kip-ft	% Diff
X Direction Analysis										
1:1	292.9		0.0		0.0		80.7		117.7	
1:2	285.7	2.4	0.0	0.0	0.0	0.0	81.4	1.0	118.9	1.0
1:3	283.8	3.1	0.0	0.0	0.0	0.0	81.5	1.1	119.0	1.1
1:4	283.4	3.2	0.0	0.0	0.0	0.0	81.6	1.1	119.1	1.1
1:5	282.9	3.4	0.0	0.0	0.0	0.0	81.6	1.1	119.1	1.2
Y Direction Analysis										
1:1	0.0		221.1		2574.5		0.0		0.0	
1:2	0.0	0.0	222.1	0.5	2536.4	1.5	0.0	0.0	0.0	0.0
1:3	0.0	0.0	222.3	0.5	2529.2	1.8	0.0	0.0	0.0	0.0
1:4	0.0	0.0	222.4	0.6	2536.4	1.5	0.0	0.0	0.0	0.0
1:5	0.0	0.0	222.4	0.6	2527.7	1.8	0.0	0.0	0.0	0.0
Z Direction Analysis										
1:1	137.8		0.0		0.0		34.4		116.1	
1:2	134.3	2.6	0.0	0.0	0.0	0.0	34.4	0.0	116.7	0.5
1:3	133.4	3.2	0.0	0.0	0.0	0.0	34.3	0.2	116.8	0.6
1:4	133.2	3.3	0.0	0.0	0.0	0.0	34.3	0.2	116.8	0.6
1:5	133.0	3.5	0.0	0.0	0.0	0.0	34.3	0.2	116.8	0.6

Table 03.07.02-29.32

Comparison of section cut shear results:

	Expected Results	SAP2000 Results	Difference (%)
From fixed end	Shear (kips)	Shear (kips)	
0"	20.63	20.64	< 1
75"	20.63	20.64	< 1
150"	-9.38	-9.36	< 1
225"	-9.38	-9.36	< 1
300"	9.38	9.36	< 1

Comparison of section cut moment results:

	Expected Results	SAP2000 Results	Difference (%)
From fixed end	Moment (kips-in)	Moment (kips-in)	
0"	-1688	-1691	< 1
75"	-140.6	-143.0	2
150"	1406	1405	< 1
225"	703.1	702.3	< 1
300"	0	0	0

In addition, the section axial force at every section is 30 kips, as expected.

Table 03.07.02-29.33

Comparison of modal frequency results:

	Expected Results (ANSYS)	SAP2000 Results	Difference (%)
Mode No.	Frequency (Hz)	Frequency (Hz)	
1	9.06037	9.071	< 1
2	18.8171	18.803	< 1
3	26.5053	26.427	< 1
4	35.1965	34.980	< 1
5	35.9126	35.853	< 1

Comparison of plate center displacement results:

	Expected Results (ANSYS)	SAP2000 Results	Difference (%)
Minimum Displacement (in)	-0.003120	-0.003118	< 1
Maximum Displacement (in)	0.002915	0.002873	1.5

Comparison of support reaction results:

	Expected Results (ANSYS)	SAP2000 Results	Difference (%)
Minimum Reaction at Corner (lbs)	-132.348	-123.72	7.0
Maximum Reaction at Corner (lbs)	87.208	80.30	8.6
Minimum Reaction at Short side Center (lbs)	-41.40	-41.21	< 1
Maximum Reaction at Short side Center (lbs)	62.62	63.26	1.0
Minimum Reaction at Long side Center (lbs)	-35.79	-36.28	1.4
Maximum Reaction at Long side Center (lbs)	44.40	45.31	2.1

Table 03.07.02-29.34

Comparison of modal frequency results:

	Expected Results (ANSYS)	SAP2000 Results	Difference (%)
Mode No.	Frequency (Hz)	Frequency (Hz)	
1	8.35560	8.332	< 1
2	9.62216	9.604	< 1
3	10.5209	10.46	< 1
4	11.9669	11.96	< 1
5	13.1260	13.08	< 1
6	15.0105	14.86	1
7	18.2422	18.19	< 1
8	19.8132	19.65	< 1
9	20.3556	20.17	< 1
10	24.3296	24.39	< 1
11	24.7822	24.66	< 1
12	25.9027	25.78	< 1
13	26.9772	26.76	< 1
14	27.5210	27.30	< 1
15	29.9460	29.43	2
16	30.5292	30.46	< 1
17	31.7276	31.26	2
18	31.8323	31.61	< 1
19	35.5686	35.16	1
20	36.1959	35.91	< 1
21	36.9213	36.56	1
22	37.9936	37.93	< 1
23	41.8152	41.45	1
24	43.6486	42.83	2
25	43.7251	42.84	2
26	43.9963	43.40	1
27	44.3450	43.98	< 1
28	44.5701	44.55	< 1

Tube displacement results at top center of long side:

	Expected Results (ANSYS)	SAP2000 Results	Difference (%)
Minimum Displacement (in)	-0.09197	-0.092618	< 1
Maximum Displacement (in)	0.1051	0.106377	1

Table 03.07.02-29.35

Support reaction results at base center of long side:

	Expected Results (ANSYS)	SAP2000 Results	Difference (%)
Minimum Reaction (lbs)	-582.7	-623.79	7.1
Maximum Reaction (lbs)	551.8	593.46	7.6
Minimum Moment (lbs-in)	-40280	-43545.49	8.1
Maximum Moment (lbs-in)	41830	41992.80	< 1

Table 03.07.02-29.36
Comparison of Iterated Strain Dependent Shear Modulus and Damping Values
(SHAKE2000 – 116 Layer Validation Problem 1)

validation-problem1					validation-problem1-116 layers						
Layer No.	Layer Thickness (ft)	Mid Layer Depth (ft)	Shear Modulus (ksf)	Damping	Layer No.	Layer Thickness (ft)	Mid Layer Depth (ft)	Shear Modulus (ksf)	Damping	Difference Shear Modulus (%)	Difference Damping (%)
1	7	3.5	4470.4	0.045	4	1	3.5	4471	0.044	0.013%	2.22%
2	13	13.5	813.7	0.112	14	1	13.5	816.8	0.111	0.381%	0.89%
3	10	25	3058.9	0.089	25	1	24.5	3067.3	0.088	0.054%	0.56%
					See Note 1		25	3060.55	0.0885		
					26	1	25.5	3053.8	0.089		
4	12	36	393.4	0.191	36	1	35.5	401.5	0.189	0.483%	0.26%
					See Note 1		36	395.3	0.1905		
					37	1	36.5	389.1	0.192		
5	15	49.5	648.4	0.177	50	1	49.5	649.1	0.177	0.108%	0.00%
6	14	64	3007.3	0.114	64	1	63.5	3013	0.113	0.035%	0.44%
					See Note 1		64	3008.35	0.1135		
					65	1	64.5	3003.7	0.114		
7	20	81	3521.8	0.117	81	1	80.5	3530.5	0.116	0.104%	0.43%
					See Note 1		81	3525.45	0.1165		
					82	1	81.5	3520.4	0.117		
8	25	103.5	842.6	0.193	104	1	103.5	845.1	0.193	0.297%	0.00%

Note 1) The values reported are the average of the values for the above and below layers.

Table 03.07.02-29.37
Comparison of Maximum Accelerations
(SHAKE2000 – 116 Layer Validation Problem 1)

validation-problem1			validation-problem1-116 layers			
Layer No.	Top Layer Depth (ft)	Max. Accel. (g)	Layer No.	Top Layer Depth (ft)	Max. Accel. (g)	Difference Max. Accel. (%)
1	0	0.2626	1	0	0.26067	0.735%
2	7	0.26178	8	7	0.25992	0.711%
3	20	0.25081	21	20	0.24969	0.447%
4	30	0.24765	31	30	0.24666	0.400%
5	42	0.23005	43	42	0.22978	0.117%
6	57	0.23926	58	57	0.23811	0.481%
7	71	0.23325	72	71	0.2323	0.407%
8	91	0.20981	92	91	0.20865	0.553%
9	116	0.178	117	116	0.178	0.000%

Table 03.07.02-29.38
Comparison of Iterated Strain Dependent Shear Modulus and Damping Values
(SHAKE2000 – 116 Layer Validation Problem 2)

validation-problem2					validation-problem2-116 layers						
Layer No.	Layer Thickness (ft)	Mid Layer Depth (ft)	Shear Modulus (ksf)	Damping	Layer No.	Layer Thickness (ft)	Mid Layer Depth (ft)	Shear Modulus (ksf)	Damping	Difference Shear Modulus (%)	Difference Damping (%)
1	7	3.5	4509.3	0.04	4	1	3.5	4509.3	0.04	0.000%	0.00%
2	13	13.5	1157	0.073	14	1	13.5	1154.4	0.073	0.225%	0.00%
3	10	25	3229.5	0.067	25	1	24.5	3231.7	0.066	0.002%	0.75%
					See Note 1		25	3229.55	0.0665		
					26	1	25.5	3227.4	0.067		
4	12	36	952.9	0.108	36	1	35.5	957.4	0.108	0.037%	0.46%
					See Note 1		36	952.55	0.1085		
					37	1	36.5	947.7	0.109		
5	15	49.5	1479.7	0.099	50	1	49.5	1476.8	0.099	0.196%	0.00%
6	14	64	3380.3	0.077	64	1	63.5	3385.1	0.076	0.065%	0.65%
					See Note 1		64	3382.5	0.0765		
					65	1	64.5	3377.9	0.077		
7	20	81	4016.3	0.076	81	1	80.5	4019	0.076	0.021%	0.00%
					See Note 1		81	4017.15	0.076		
					82	1	81.5	4015.3	0.076		
8	25	103.5	2528.2	0.088	104	1	103.5	2530.6	0.088	0.095%	0.00%

Note 1) The values reported are the average of the values for the above and below layers.

Table 03.07.02-29.39
Comparison of Maximum Accelerations
(SHAKE2000 – 116 Layer Validation Problem 2)

validation-problem2			validation-problem2-116 layers			
Layer No.	Top Layer Depth (ft)	Max. Accel. (g)	Layer No.	Top Layer Depth (ft)	Max. Accel. (g)	Difference Max. Accel. (%)
1	0	0.16147	1	0	0.16147	0.000%
2	7	0.15306	8	7	0.15304	0.013%
3	20	0.1652	21	20	0.16875	2.149%
4	30	0.14368	31	30	0.14749	2.652%
5	42	0.2446	43	42	0.2474	1.145%
6	57	0.36329	58	57	0.35371	2.637%
7	71	0.32167	72	71	0.3112	3.255%
8	91	0.41379	92	91	0.40235	2.765%
9	116	0.83661	117	116	0.83035	0.748%

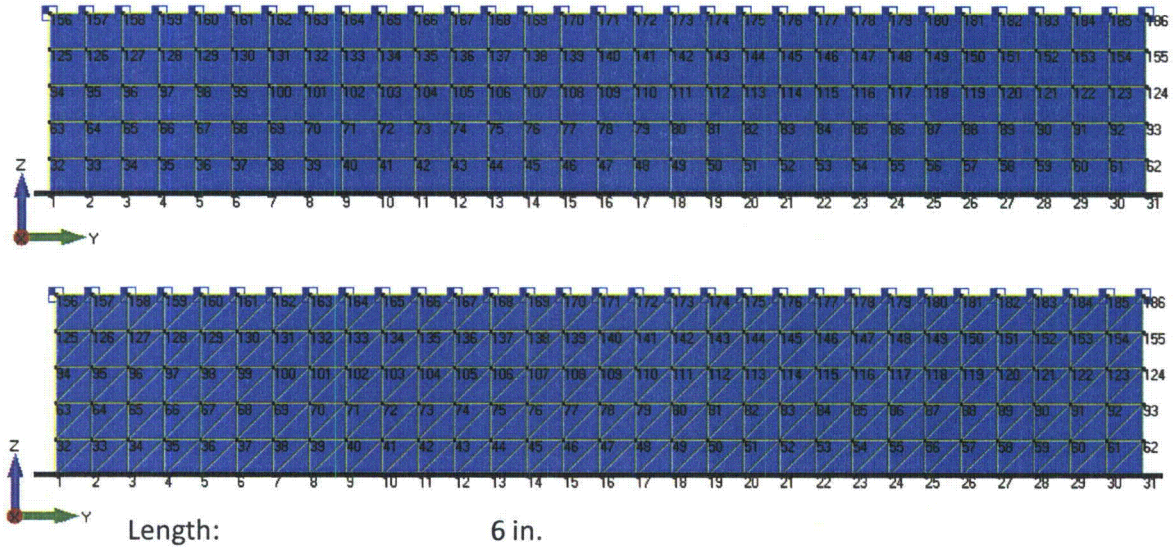

Length:	6 in.
Height:	1 in.
Thickness:	0.1 in.
Young's Modulus:	3,000 psi
Poisson's Ratio:	0.3
Density of Wall:	0 (lb-s^2/in)/in^3
Total Mass at Top of Wall:	0.2 lbf-sec^2/in

Figure 03.07.02-29.1: Cantilever Thick Shell Finite Element Models for In-Plane Loading, Node Numbers are Shown, Rectangular Element Model (top) and Triangular Element Model (bottom)

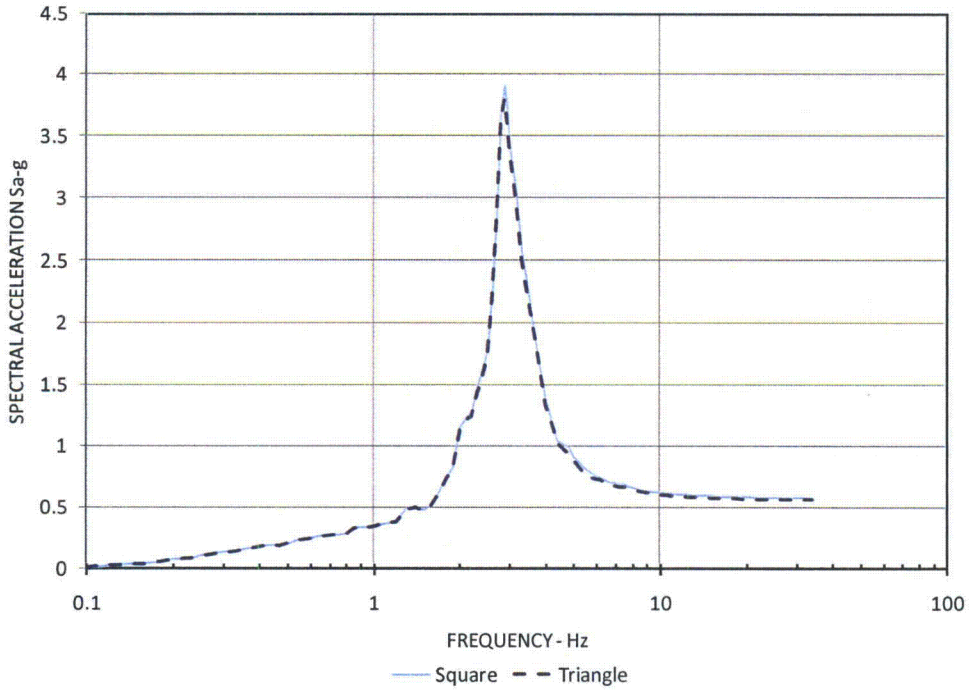

Figure 03.07.02-29.2: Acceleration Response Spectrum for Thick Shell Element Model for In-Plane Loading – Node 158

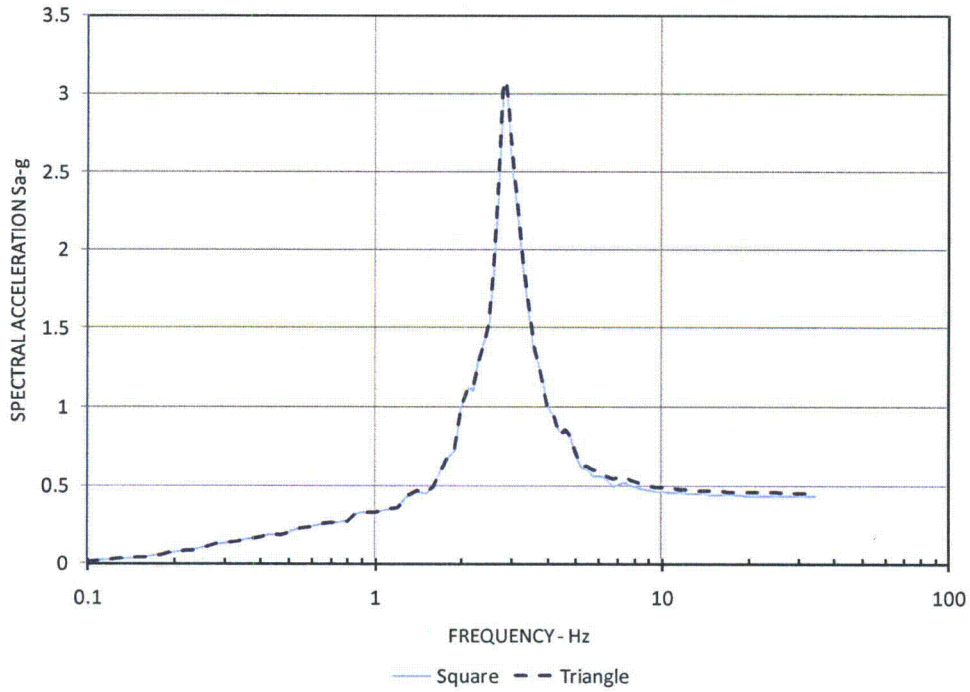

Figure 03.07.02-29.3: Acceleration Response Spectrum for Thick Shell Element Model for In-Plane Loading – Node 171

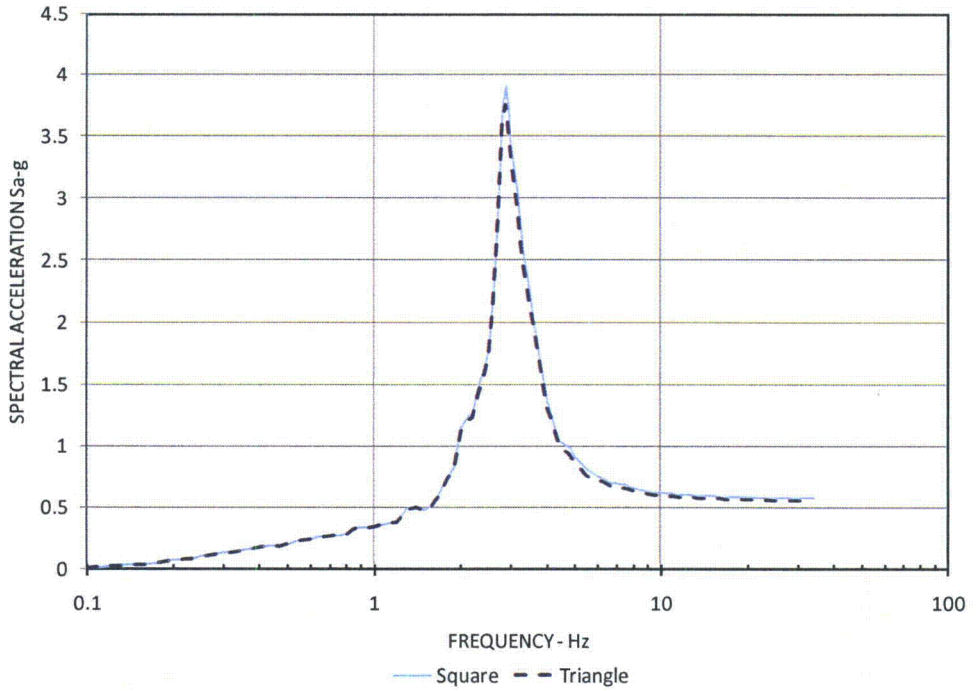

Figure 03.07.02-29.4: Acceleration Response Spectrum for Thick Shell Element Model for In-Plane Loading – Node 184

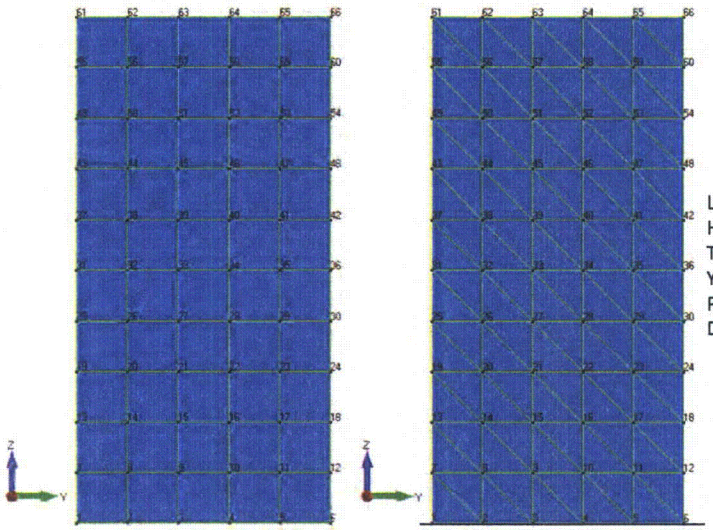

Length:	5 ft
Height:	10 ft
Thickness:	6 in. or 4 ft
Young's Modulus:	432 ksf
Poisson's Ratio:	0.3
Density of Plate:	$2.0*10^{-4}$ lbf-sec^2/in^4
	0.133 kip/ft^3

Figure 03.07.02-29.5: Cantilever Thick Shell Finite Element Models for Out-of-Plane Loading, Node Numbers are Shown, Rectangular Element Model (left) and Triangular Element Model (right)

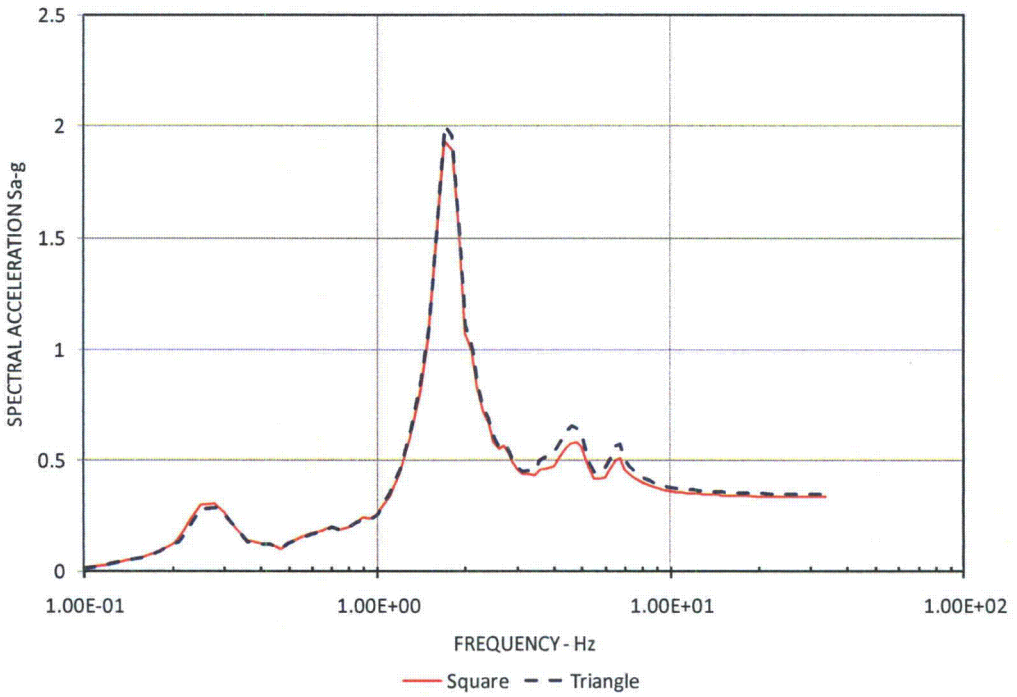

Figure 03.07.02-29.6: Acceleration Response Spectrum for Thick Shell Element Model for Out-of-Plane Loading – Node 31 – 6 in. Wall

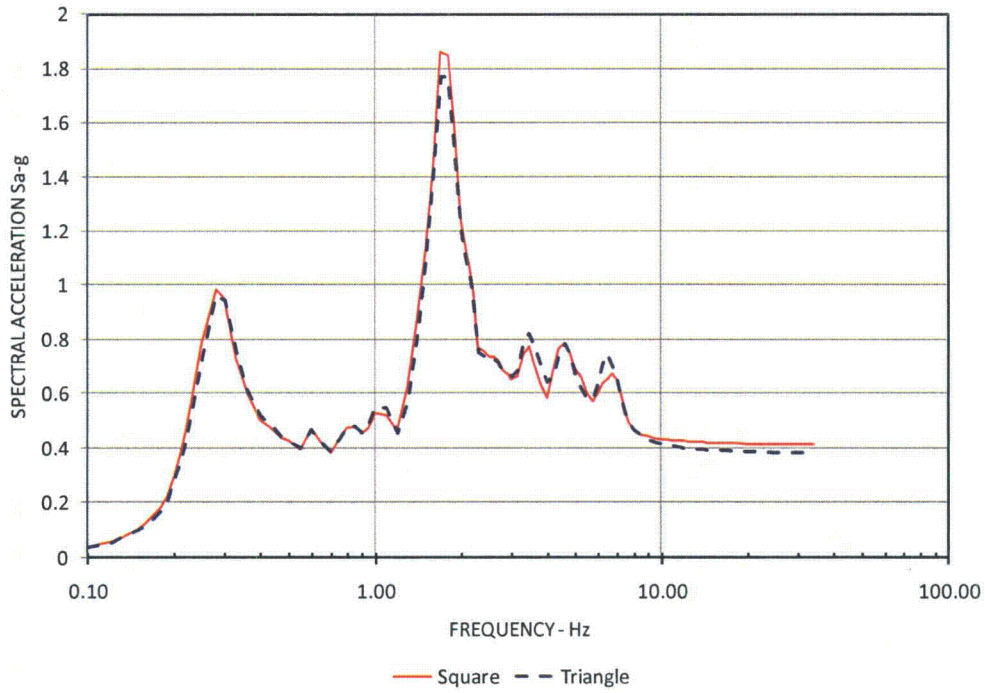

Figure 03.07.02-29.7: Acceleration Response Spectrum for Thick Shell Element Model for Out-of-Plane Loading – Node 61 – 6 in. Wall

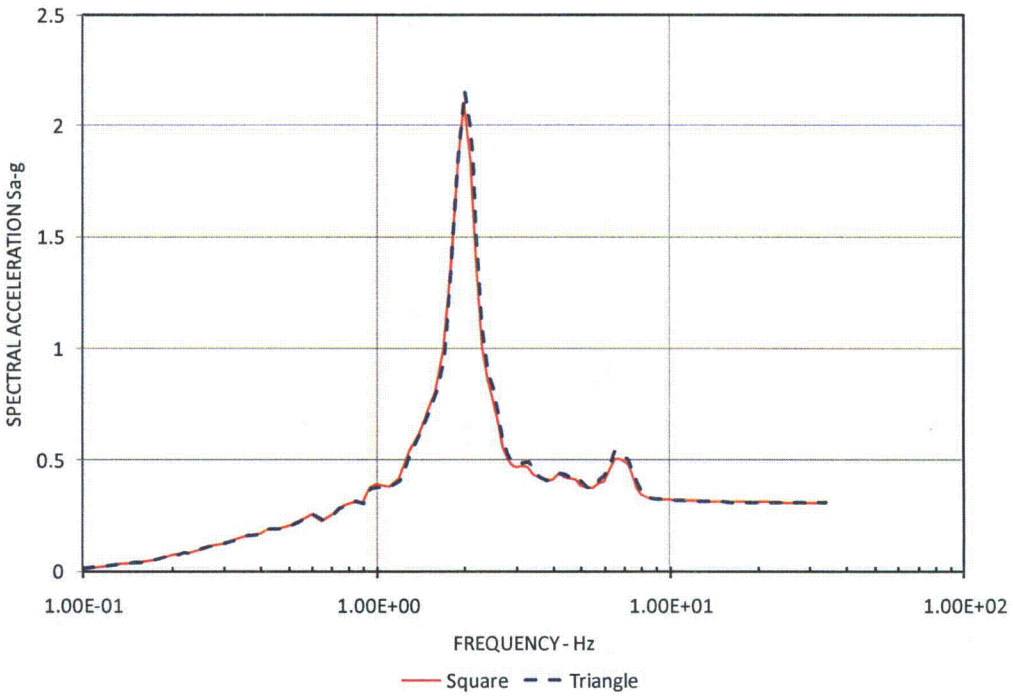

Figure 03.07.02-29.8: Acceleration Response Spectrum for Thick Shell Element Model for Out-of-Plane Loading – Node 31 –4 ft Wall

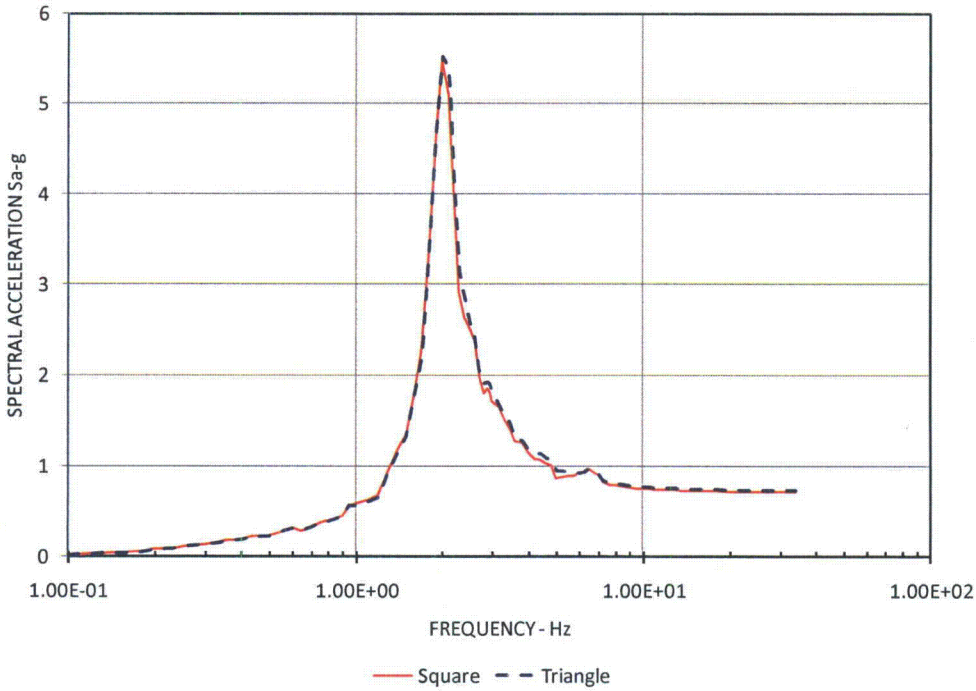

Figure 03.07.02-29.9: Acceleration Response Spectrum for Thick Shell Element Model for Out-of-Plane Loading – Node 61 –4 ft Wall

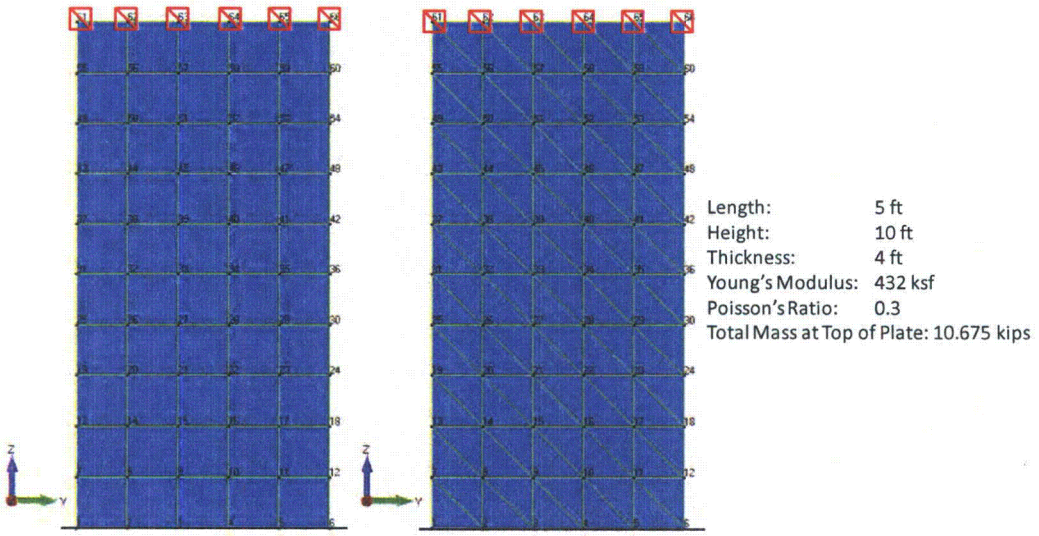

Figure 03.07.02-29.10: Cantilever Thick Shell Finite Element Models for Axial Loading, Node Numbers are Shown, Rectangular Element Model (left) and Triangular Element Model (right)

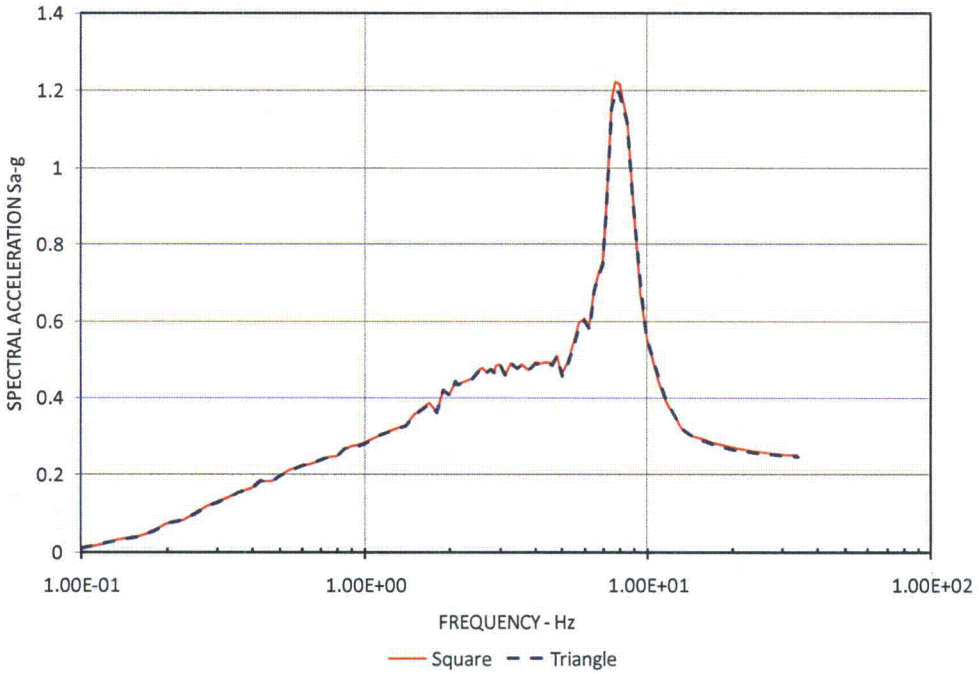

Figure 03.07.02-29.11: Acceleration Response Spectrum for Thick Shell Element Model with Vertical Axial Load – Node 31 –4 ft Wall

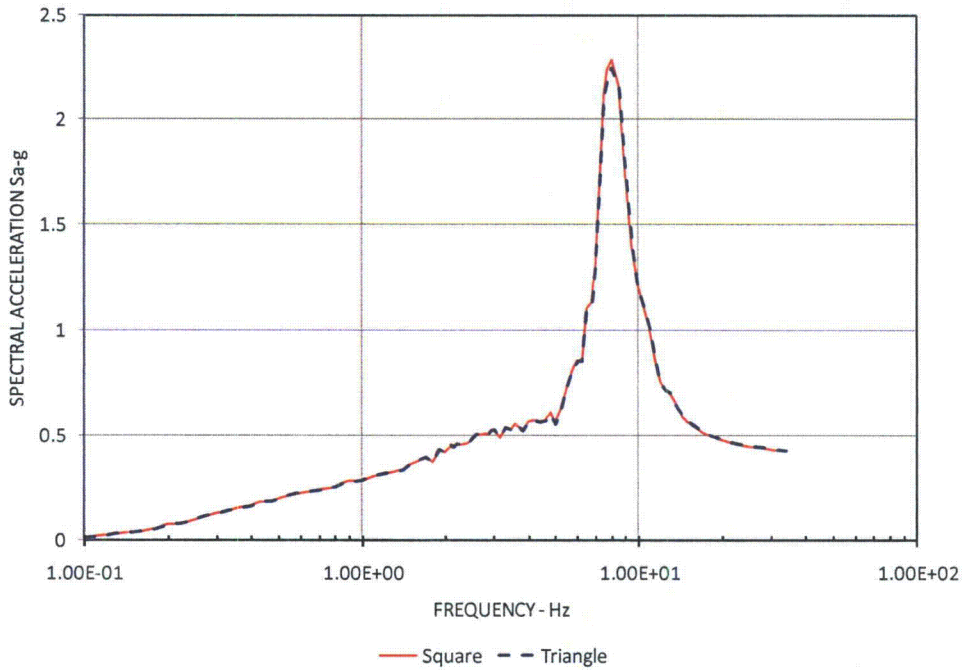

Figure 03.07.02-29.12: Acceleration Response Spectrum for Thick Shell Element Model with Vertical Axial Load – Node 61 –4 ft Wall

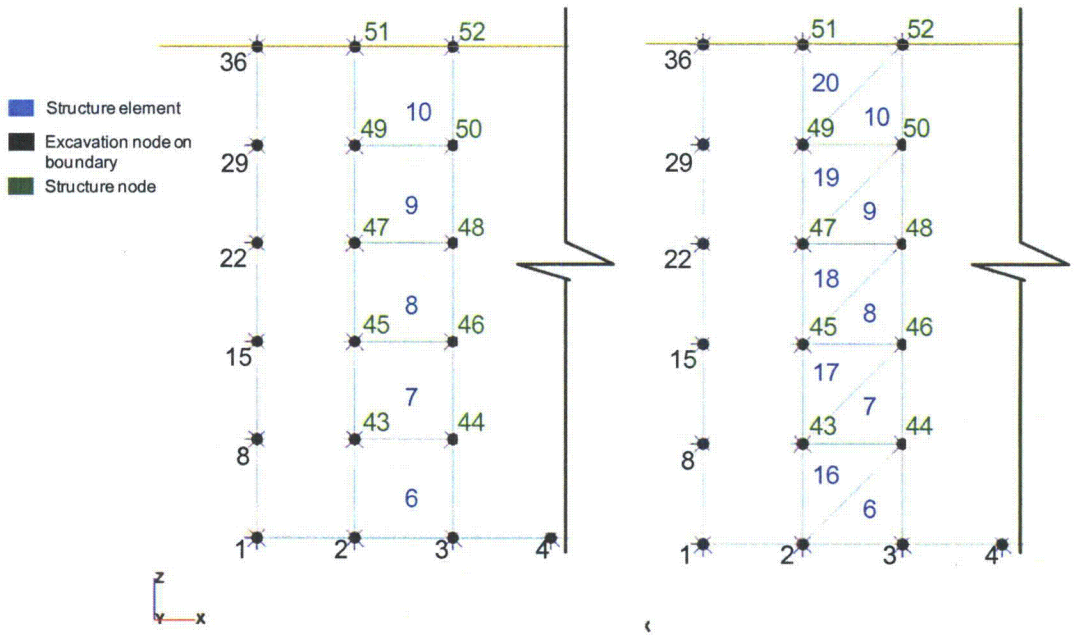

Figure 03.07.02-29.13: SASSI Model - Rectangular Element Structure shown on Left and Triangular Element Structure Shown on Right (Right Edge of Excavation Not Shown)

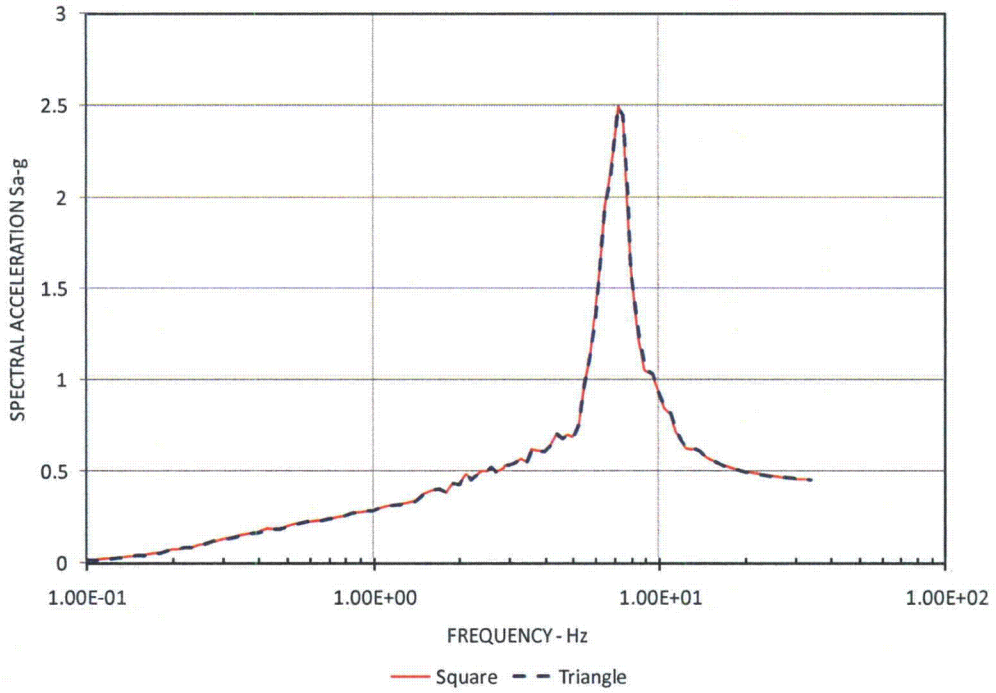

Figure 03.07.02-29.14: Acceleration Response Spectrum for 2-D Plane Strain Element Model with In-Plane Load – Node 52

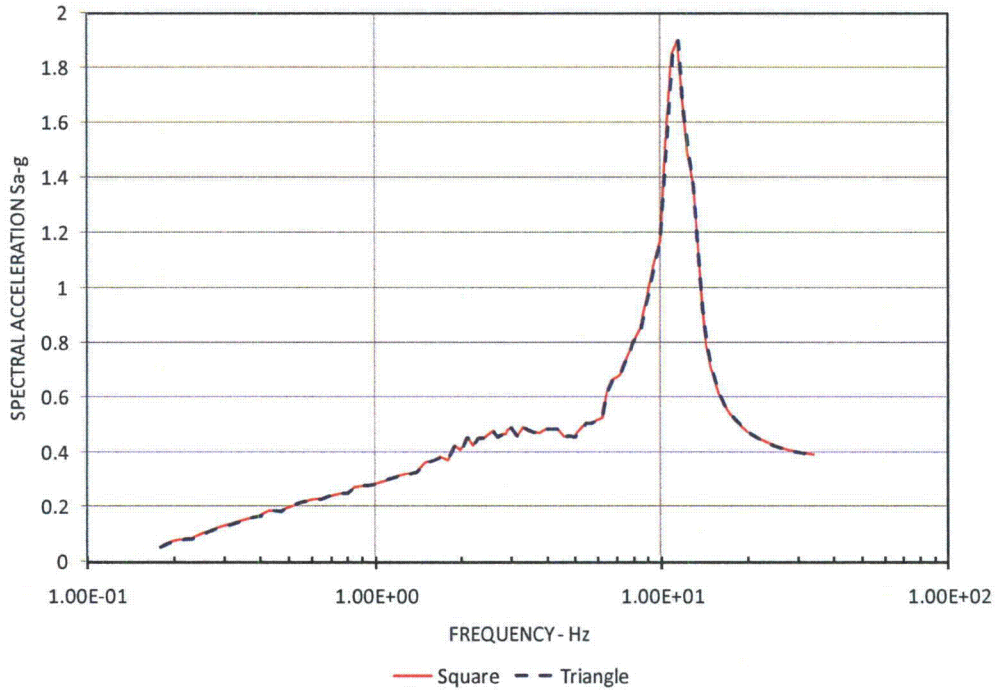

Figure 03.07.02-29.15: Acceleration Response Spectrum for the 2-D Plane Strain Element Model with Vertical Axial Load – Node 52

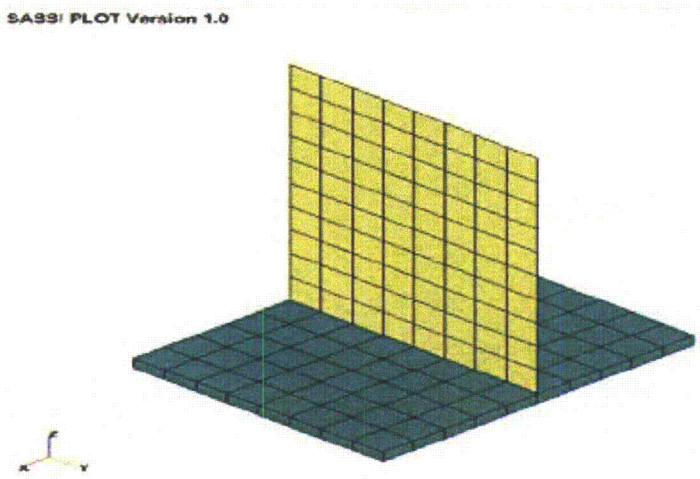

Figure 4.26-1: Tilted View of Model 1 - Aspect Ratio 1:1

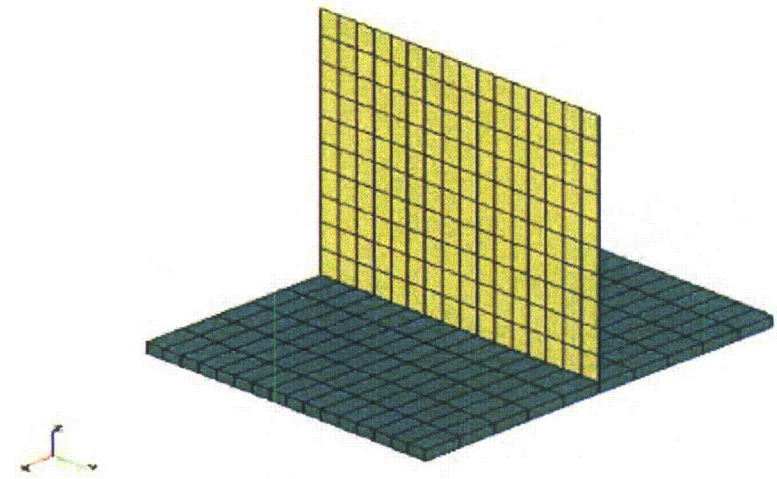

Figure 4.26-2: Tilted View of Model 2 - Aspect Ratio 1:2

Figure 03.07.02-29.16: Thin Shell Element Models for Element Aspect Ratios of 1:1 and 1:2

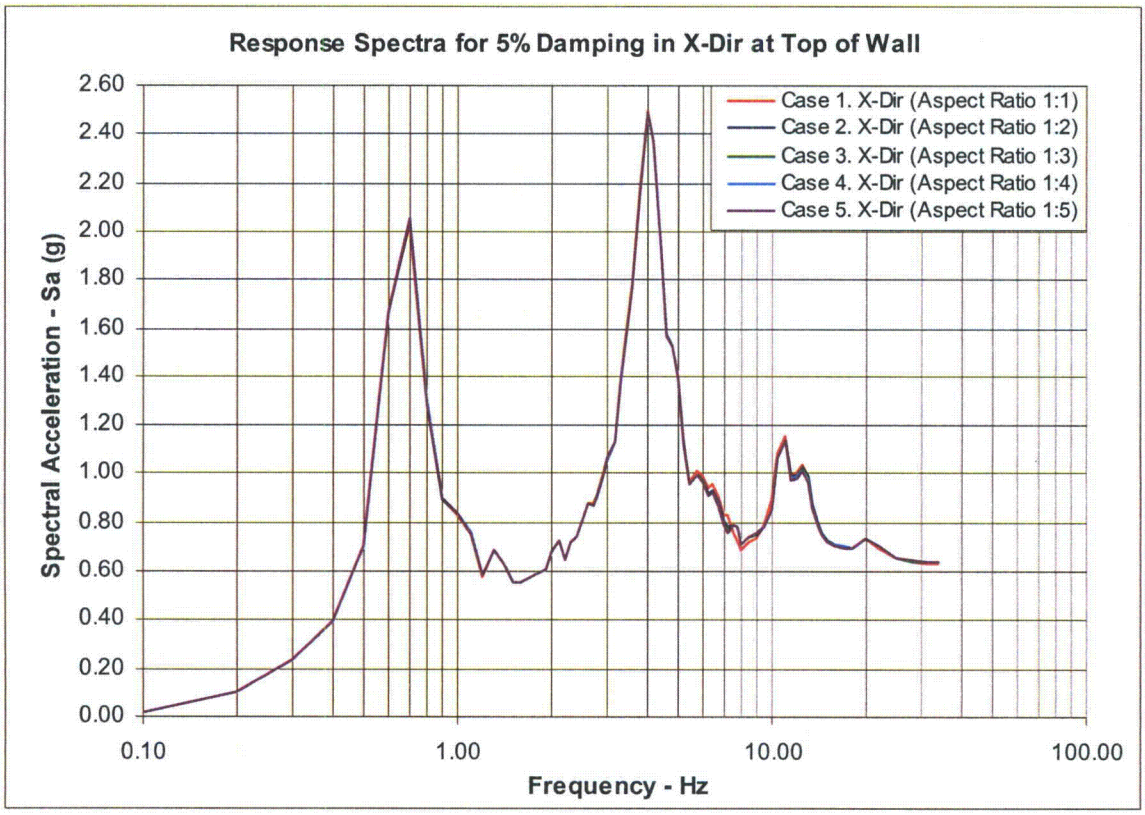

Figure 03.07.02-29.17: Comparison of 5% damped X-Direction Response Spectra at the Top of the Wall for Various aspect Ratios of Thin Plate Elements

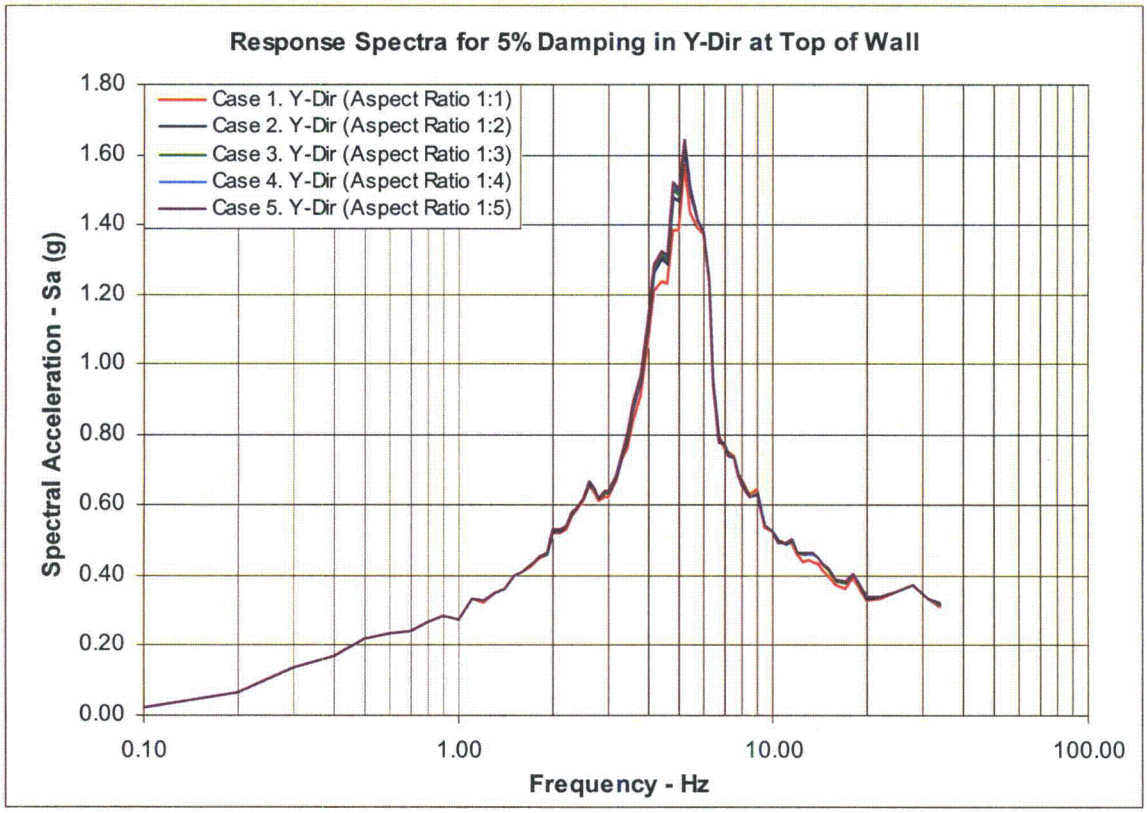

Figure 03.07.02-29.18: Comparison of 5% damped Y-Direction Response Spectra at the Top of the Wall for Various aspect Ratios of Thin Plate Elements

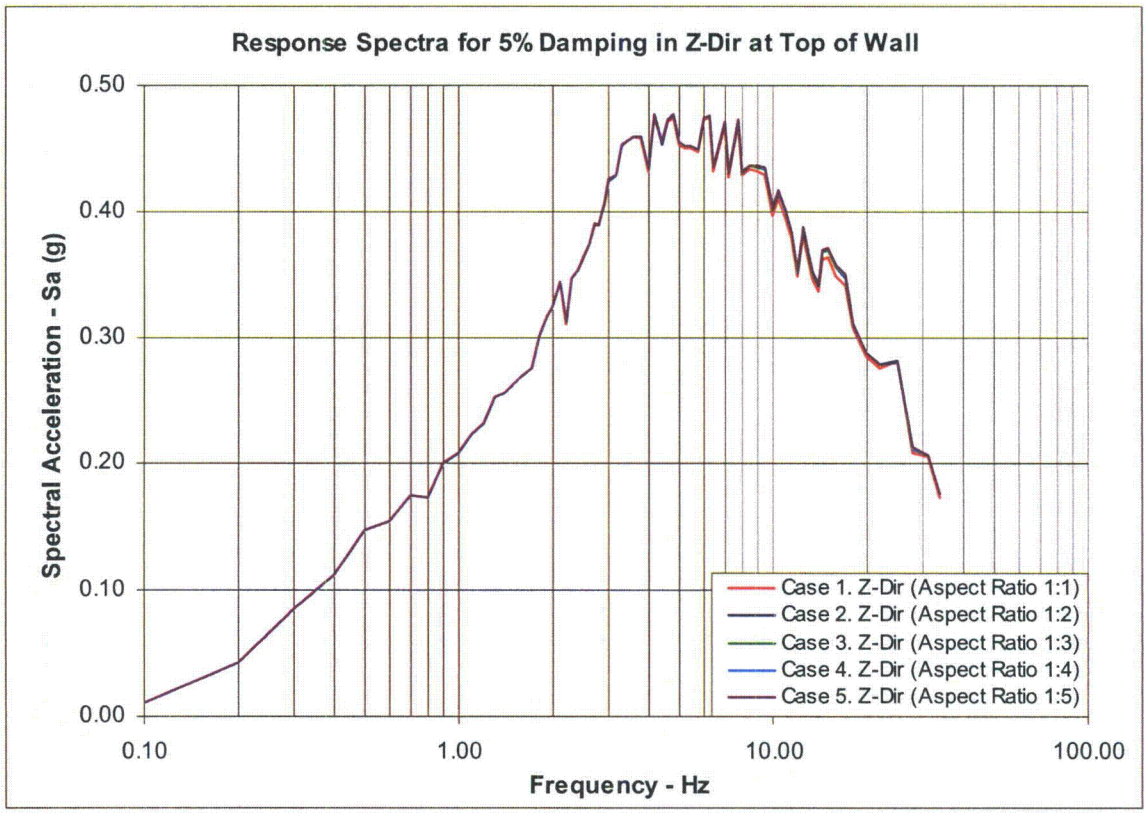

Figure 03.07.02-29.19: Comparison of 5% damped Z-Direction Response Spectra at the Top of the Wall for Various aspect Ratios of Thin Plate Elements

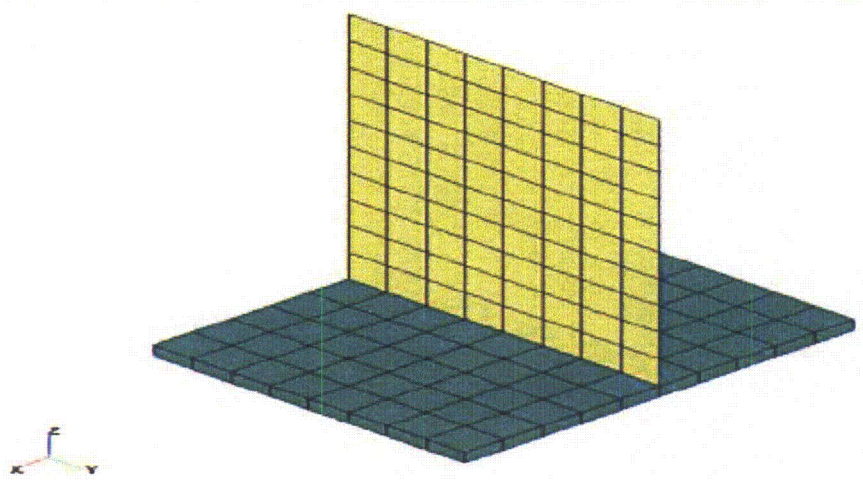

Figure 4.27-1: Tilted View of Model 1 - Aspect Ratio 1:1

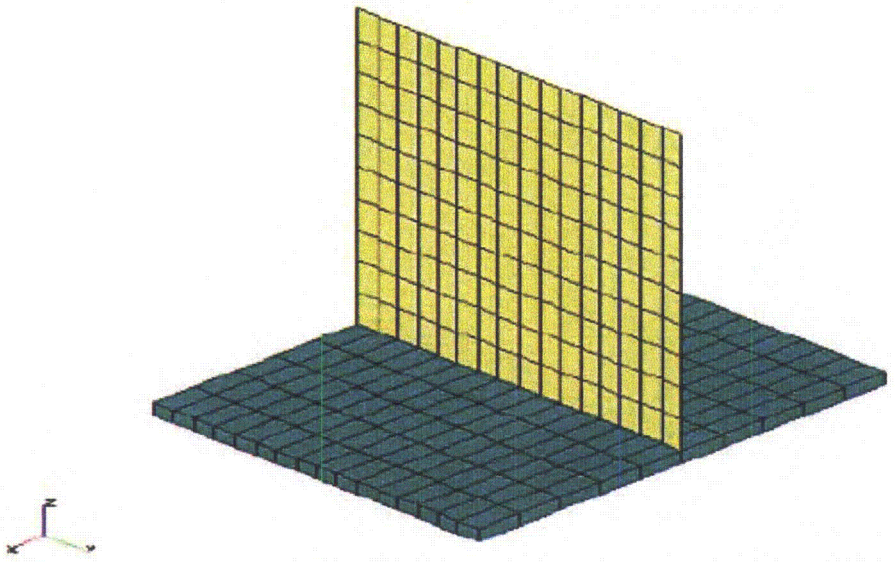

Figure 4.27-2: Tilted View of Model 2 - Aspect Ratio 1:2

Figure 03.07.02-29.20: Thick Shell Element Models for Element Aspect Ratios of 1:1 and 1:2

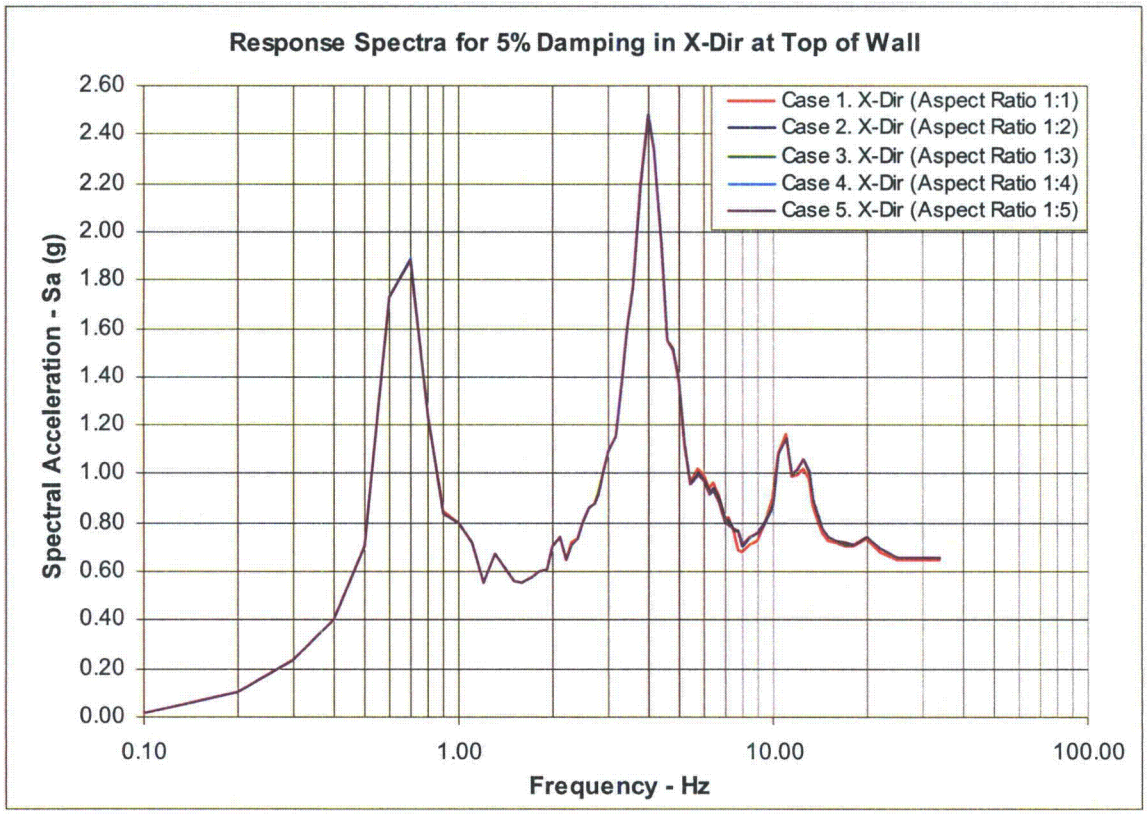

Figure 03.07.02-29.21: Comparison of 5% damped X-Direction Response Spectra at the Top of Wall for Various aspect Ratios of Thick Plate Elements

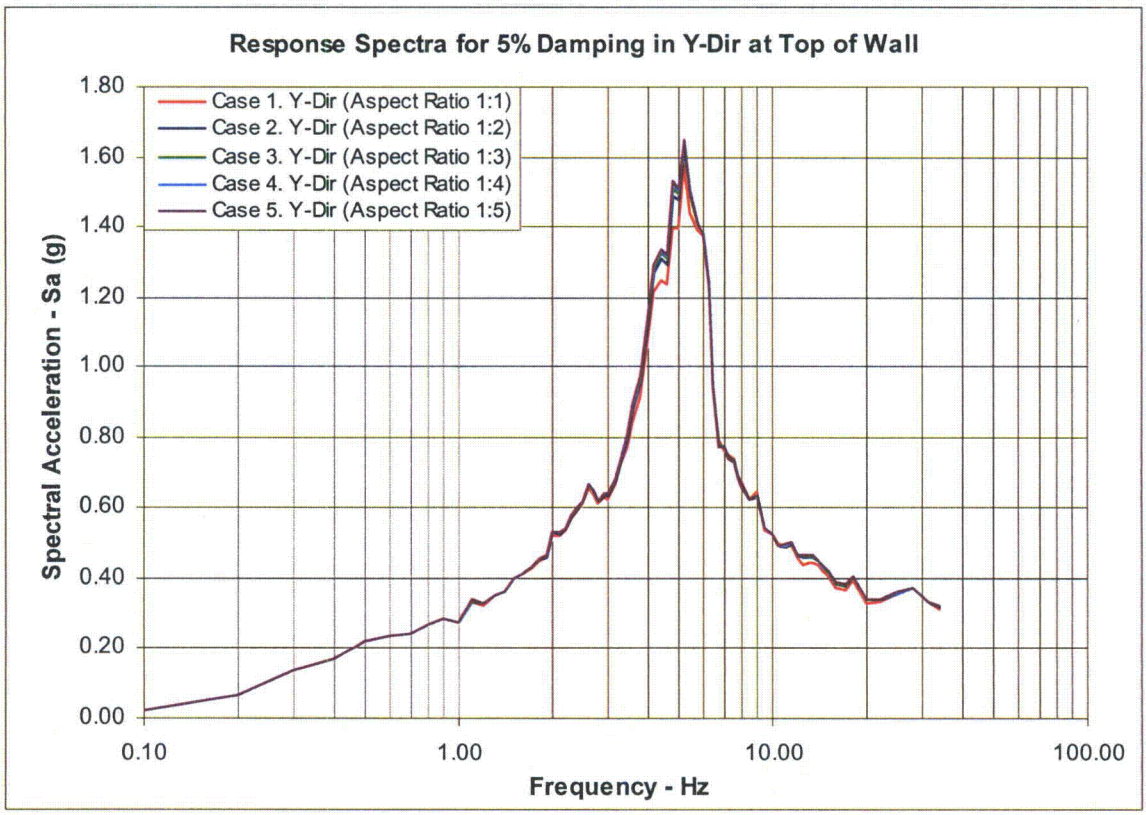

Figure 03.07.02-29.22: Comparison of 5% damped Y-Direction Response Spectra at the Top of Wall for Various aspect Ratios of Thick Plate Elements

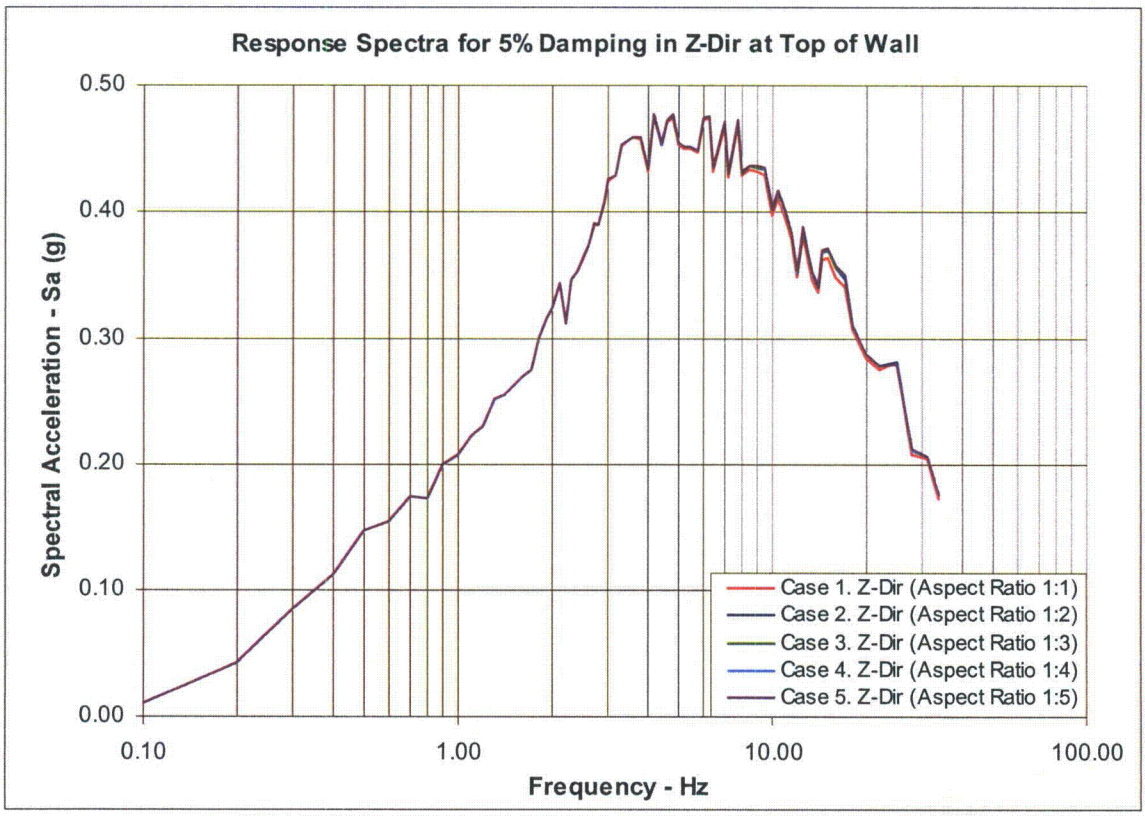

Figure 03.07.02-29.23: Comparison of 5% damped Z-Direction Response Spectra at the Top of Wall for Various aspect Ratios of Thick Plate Elements

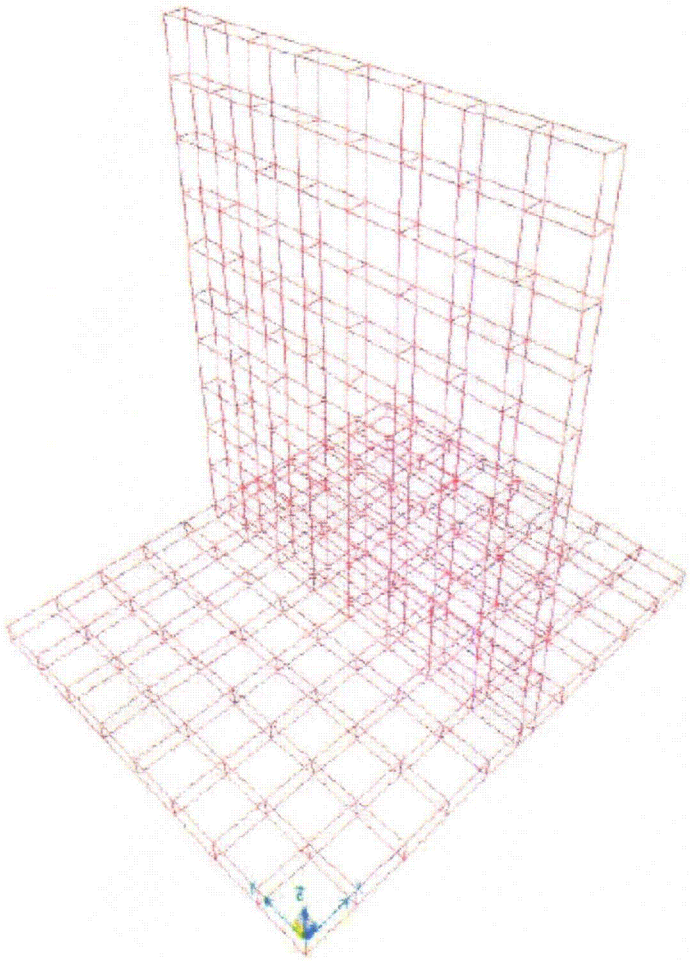

Figure 03.07.02-29.24: Solid Element Model for Element Aspect Ratio of 1:1

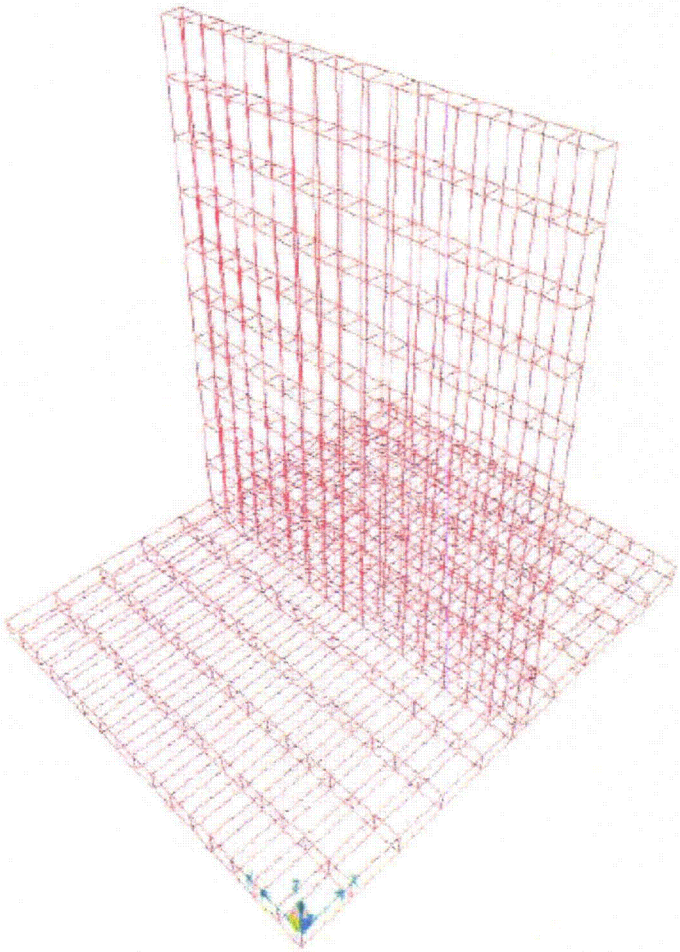

Figure 03.07.02-29.25: Solid Element Model for Element Aspect Ratio of 1:2

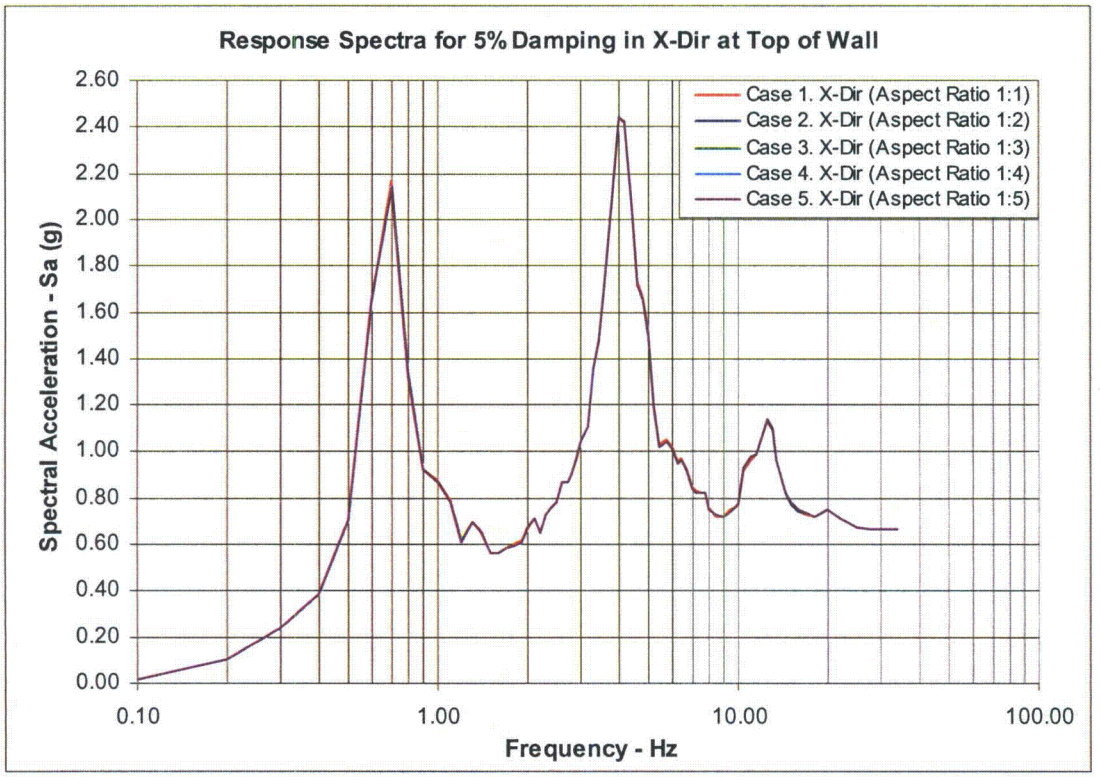

Figure 03.07.02-29.26: Comparison of 5% damped X-Direction Response Spectra at the Top of Wall for Various aspect Ratios of 8-Node Solid Elements

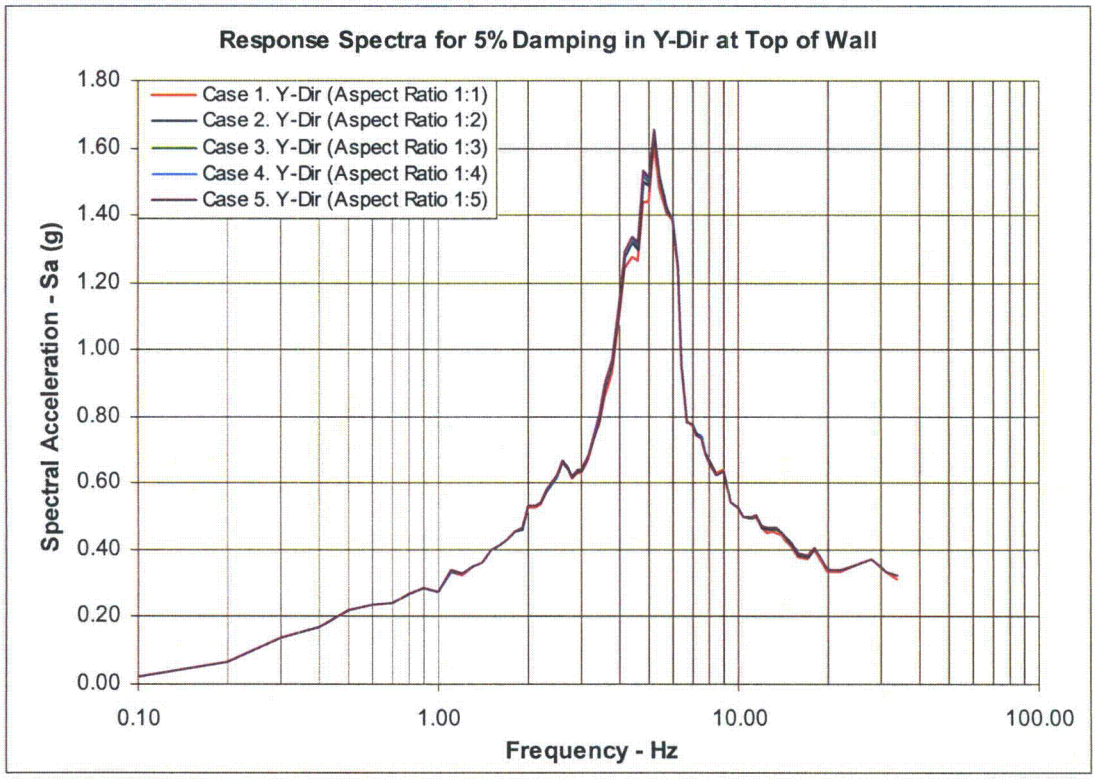

Figure 03.07.02-29.27: Comparison of 5% damped Y-Direction Response Spectra at the Top of Wall for Various aspect Ratios of 8-Node Solid Elements

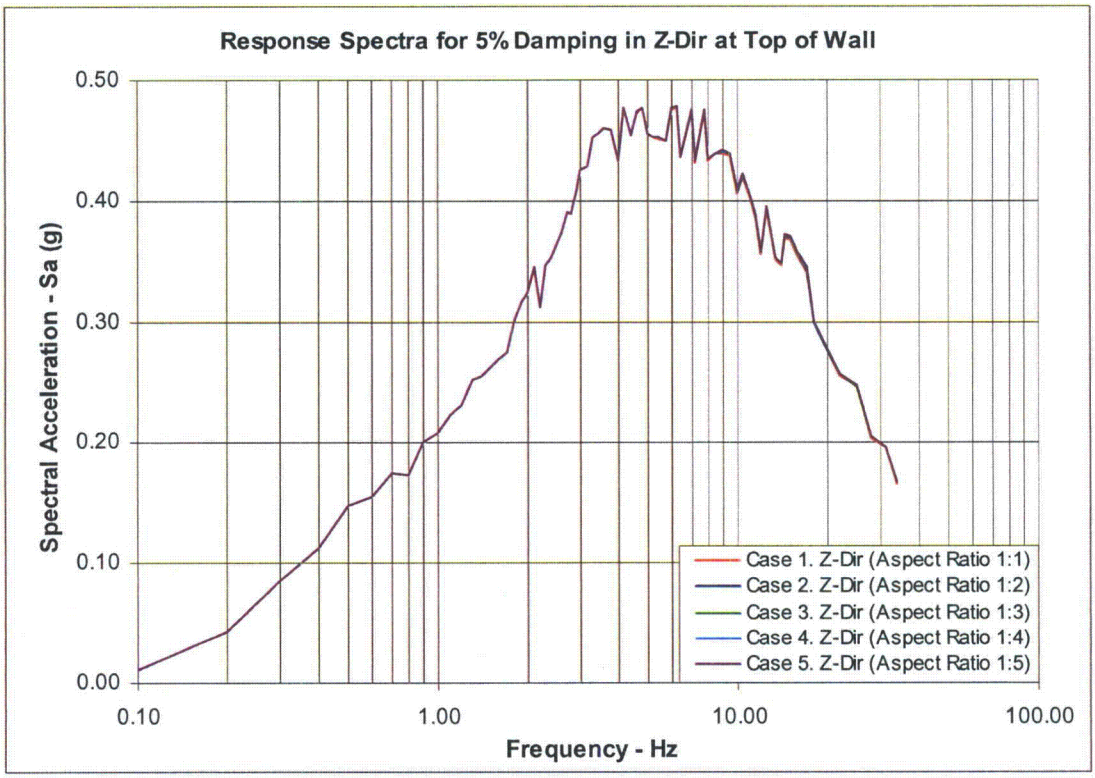

Figure 03.07.02-29.28: Comparison of 5% damped Z-Direction Response Spectra at the Top of Wall for Various aspect Ratios of 8-Node Solid Elements

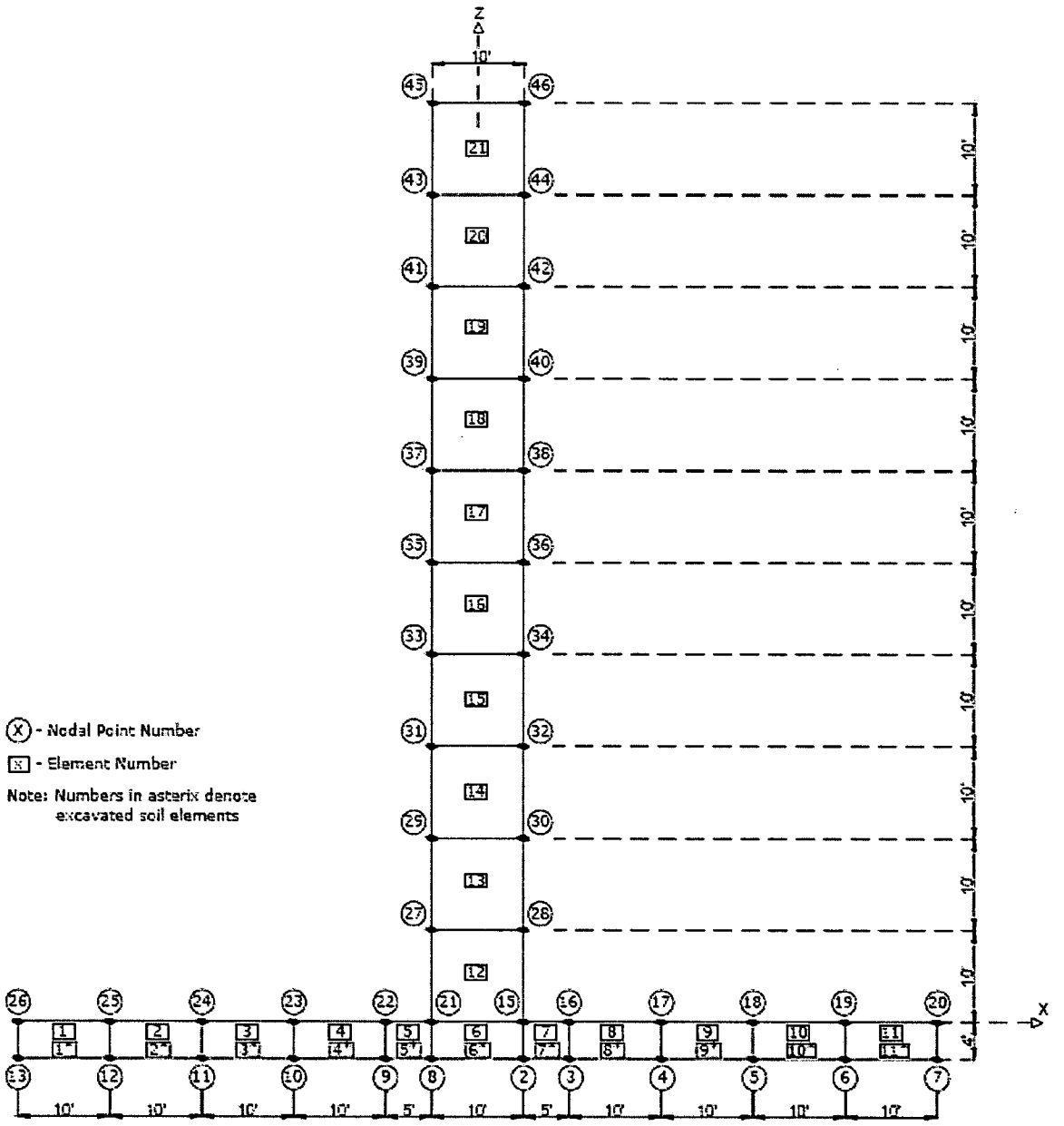

Figure 03.07.02-29.29: 2-D Plane Strain Model for Element Aspect Ratios of 1:1

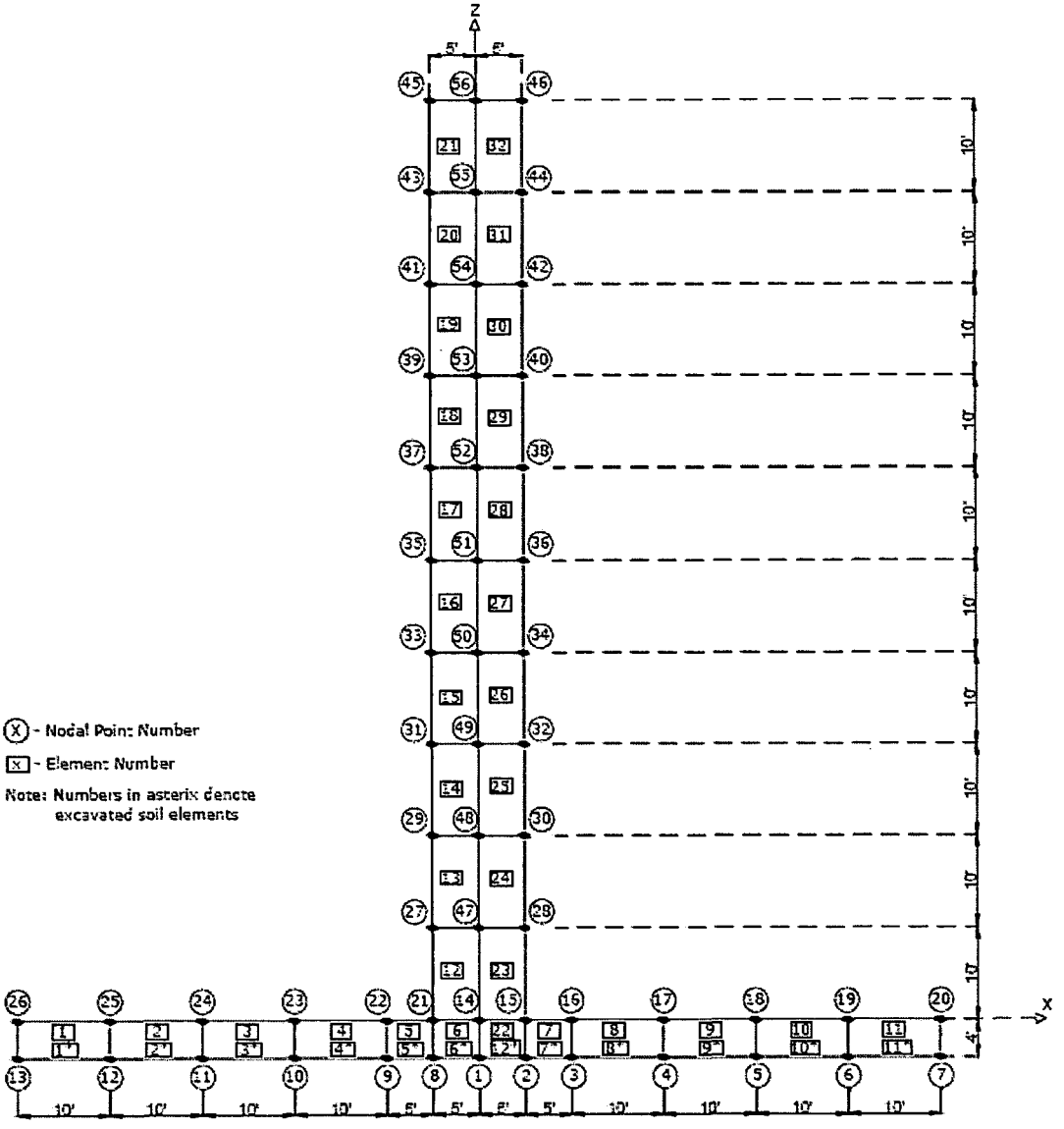

Figure 03.07.02-29.30: 2-D Plane Strain Model for Element Aspect Ratios of 1:2

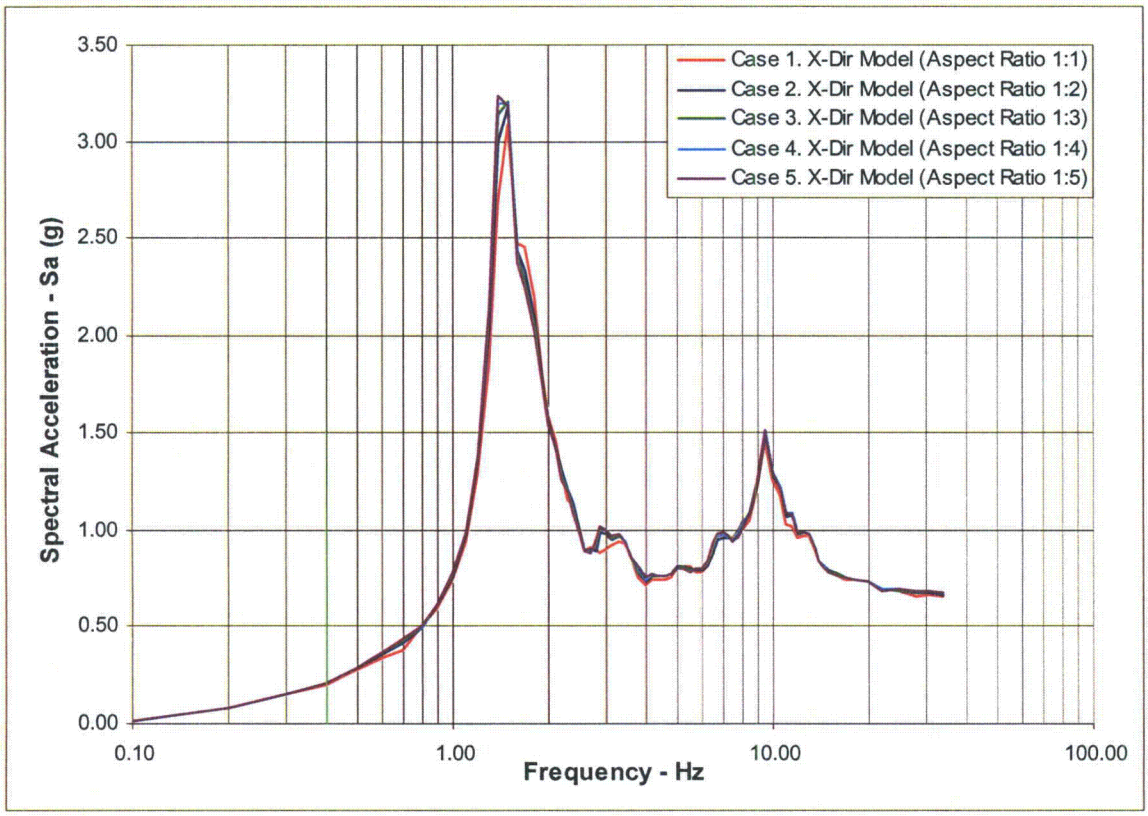

Figure 03.07.02-29.31: Comparison of 5% damped X-Direction Response Spectra at the Top of Wall for Various aspect Ratios of 2-D plane-Strain Elements

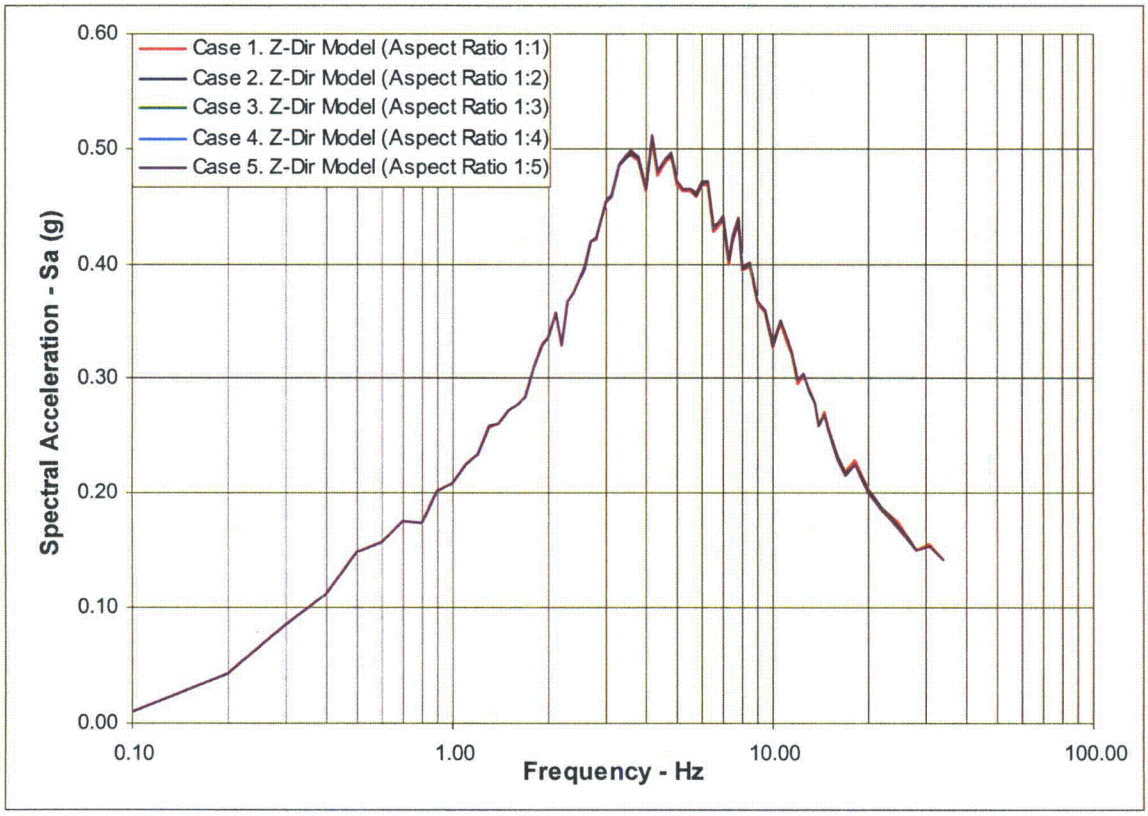

Figure 03.07.02-29.32: Comparison of 5% damped Y-Direction Response Spectra at the Top of Wall for Various aspect Ratios of 2-D plane-Strain Elements

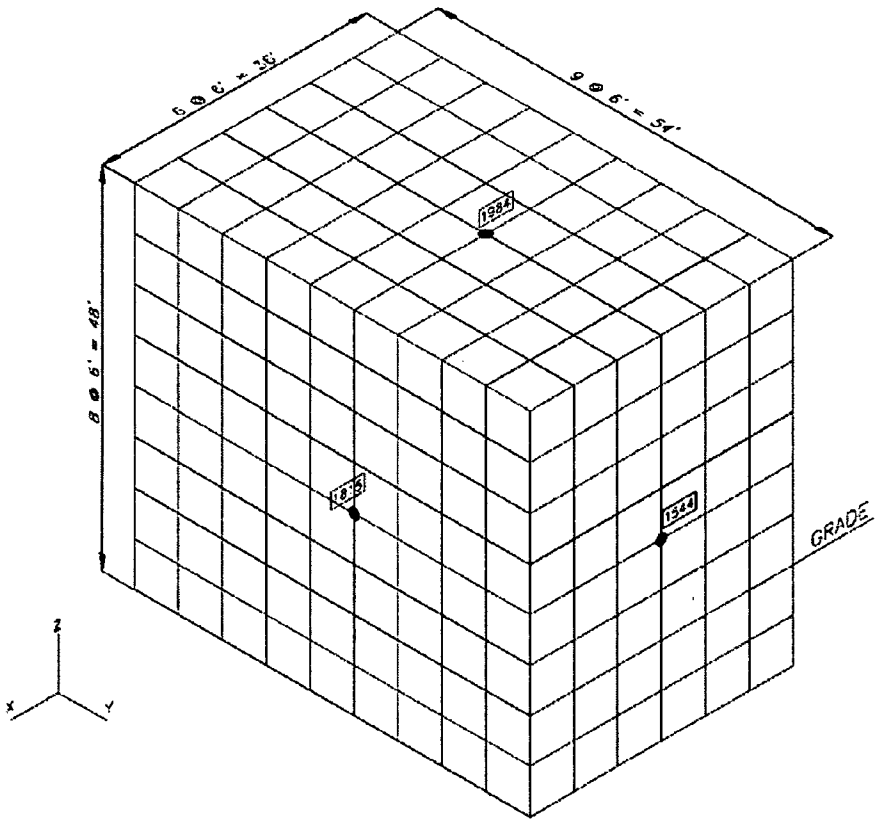

Figure 03.07.02-29.33: Thick Shell Box-Structure Model with Element Aspect Ratio of 1:1

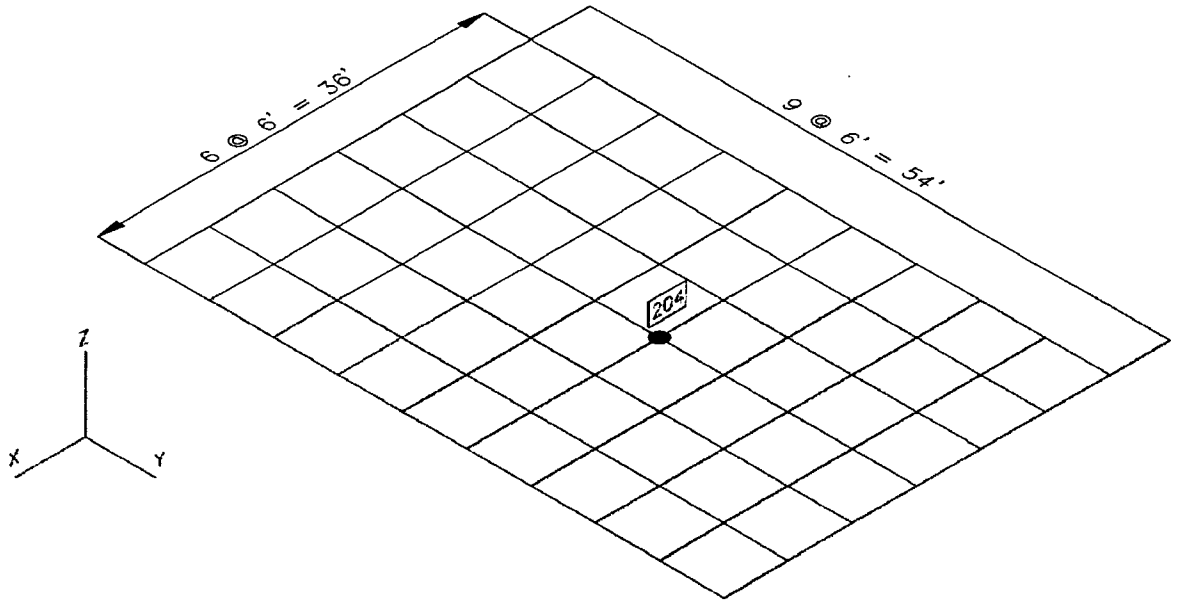

Figure 03.07.02-29.34: Thick Shell Box-Structure Base Mat Model with Element Aspect Ratio of 1:1

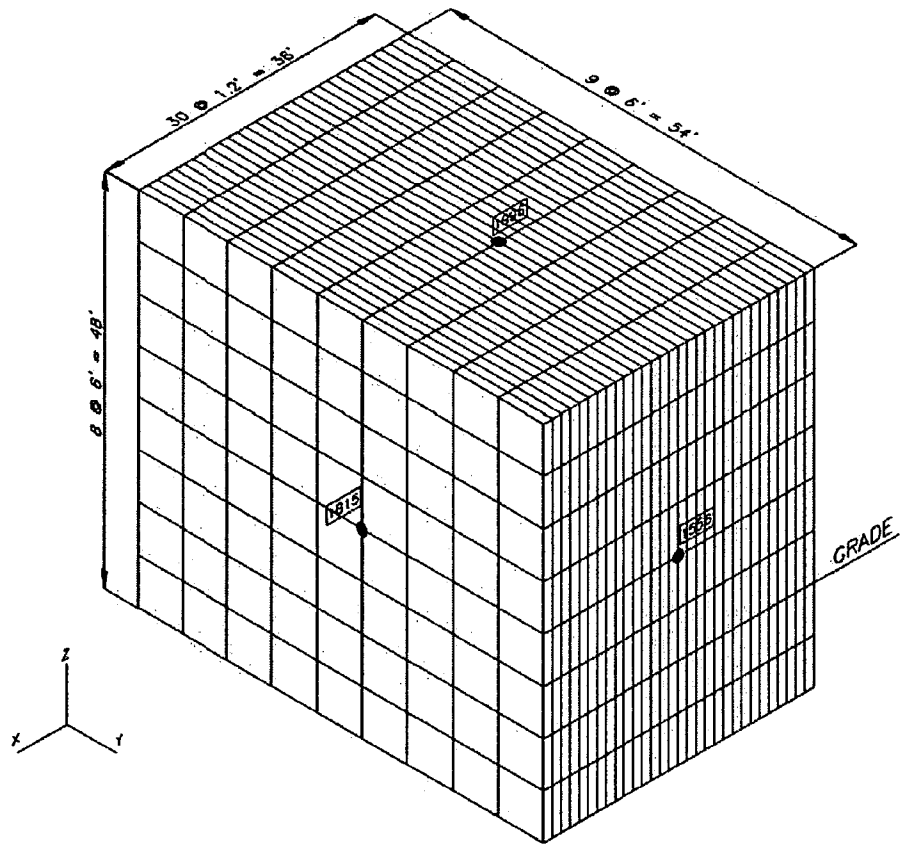

Figure 03.07.02-29.35: Thick Shell Box-Structure Model with Element Aspect Ratio of 1:5

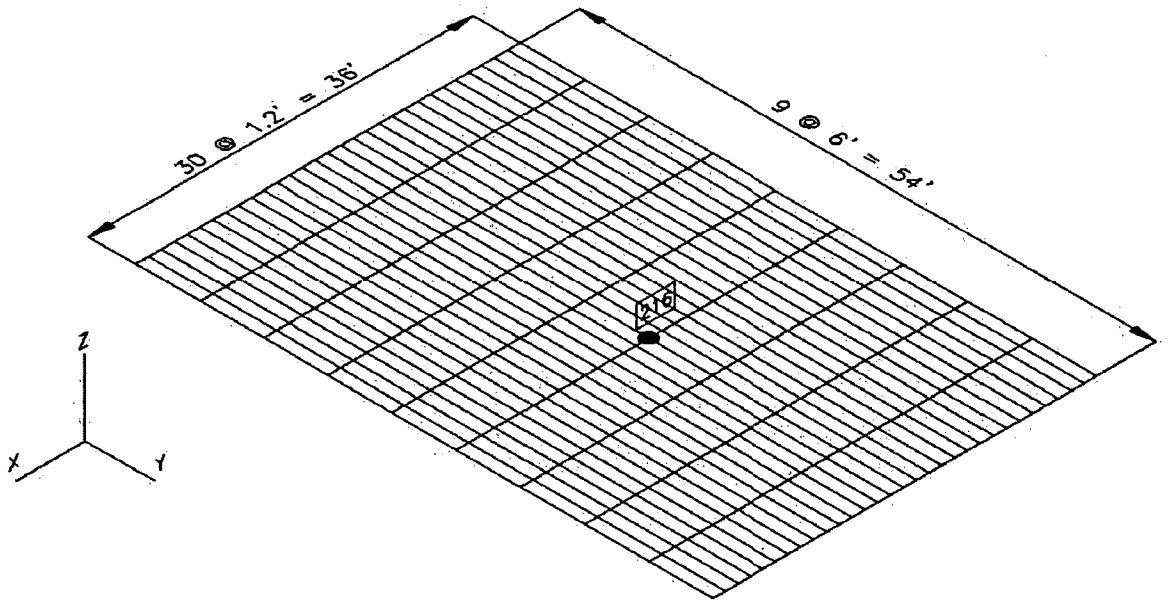

Figure 03.07.02-29.36: Thick Shell Box-Structure Base Mat Model with Element Aspect Ratio of 1:1

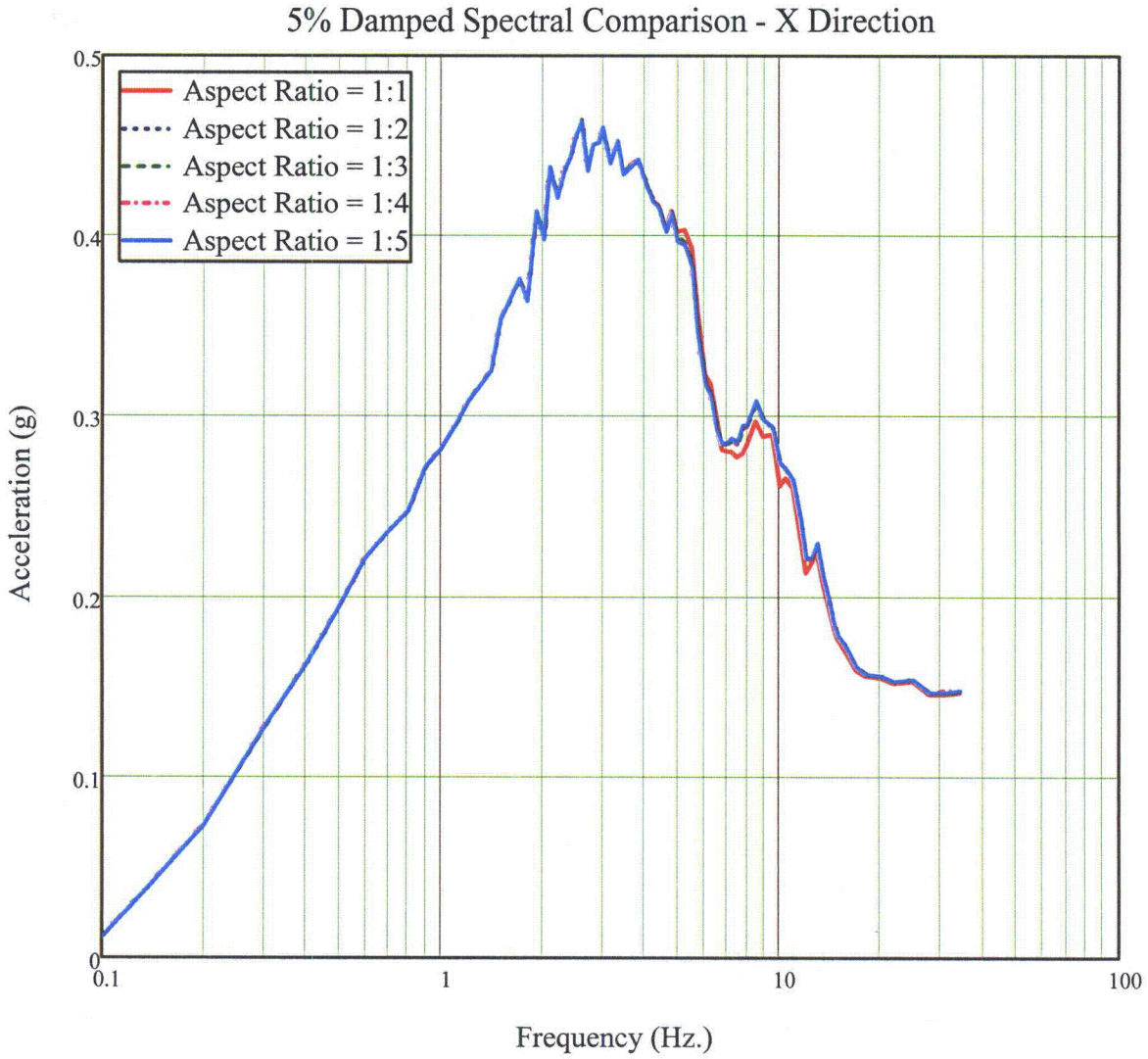

Figure 03.07.02-29.37: Comparison of Spectra – Base Mat X-Direction

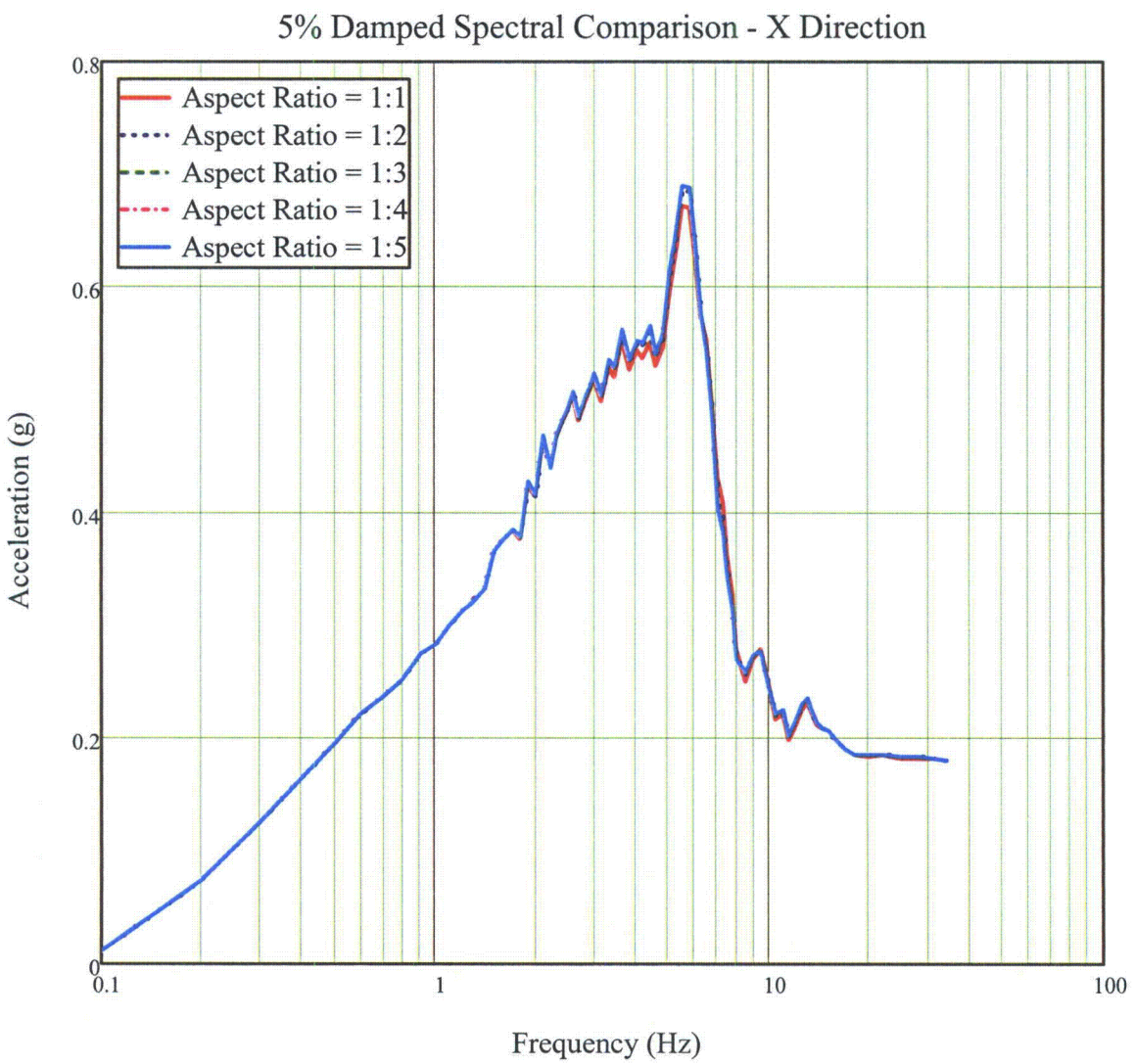

Figure 03.07.02-29.38: Comparison of Spectra – Mid height of 36 ft Long Wall X Direction

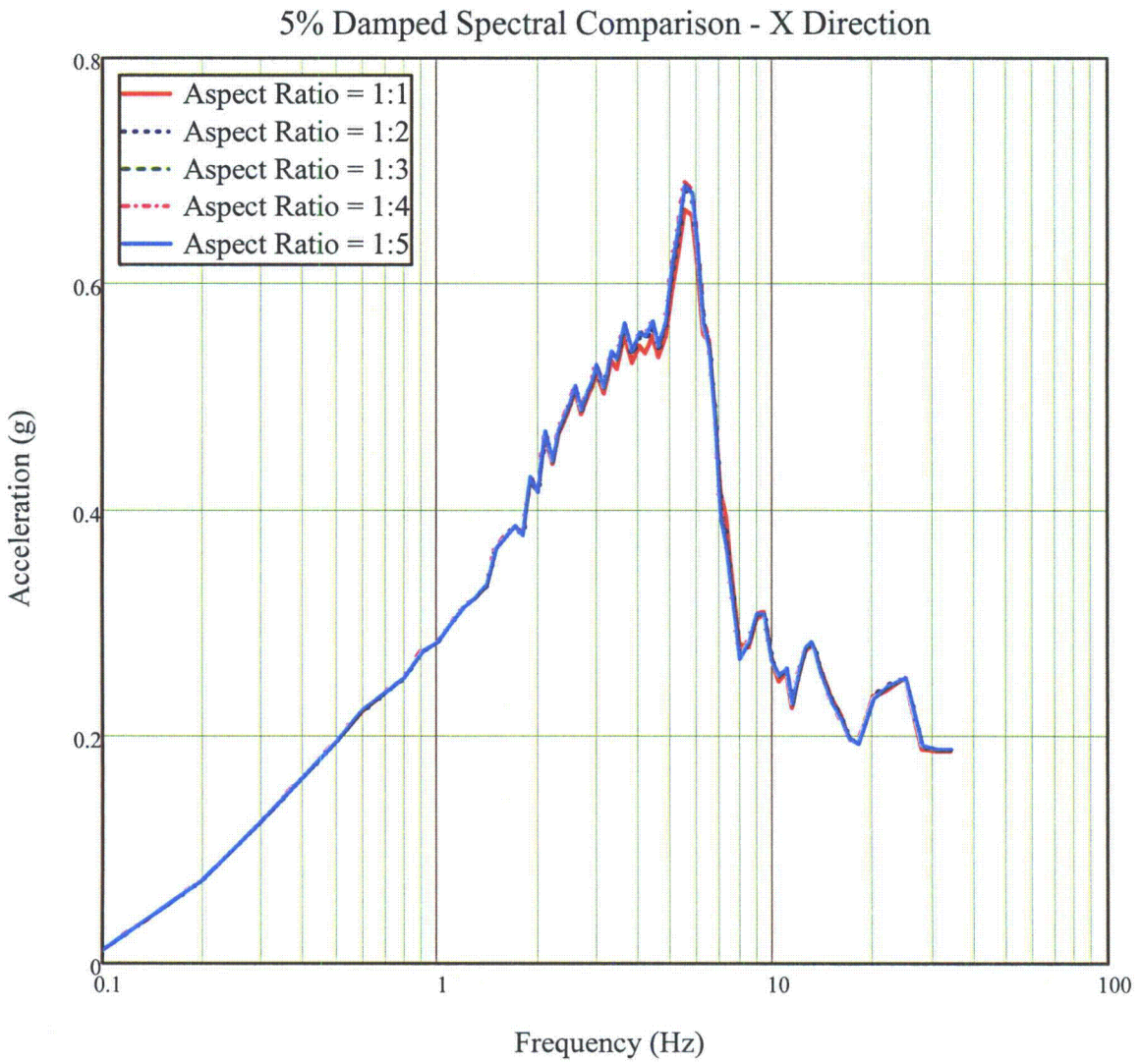

Figure 03.07.02-29.39: Comparison of Spectra – Mid height of 54 ft Long Wall X Direction

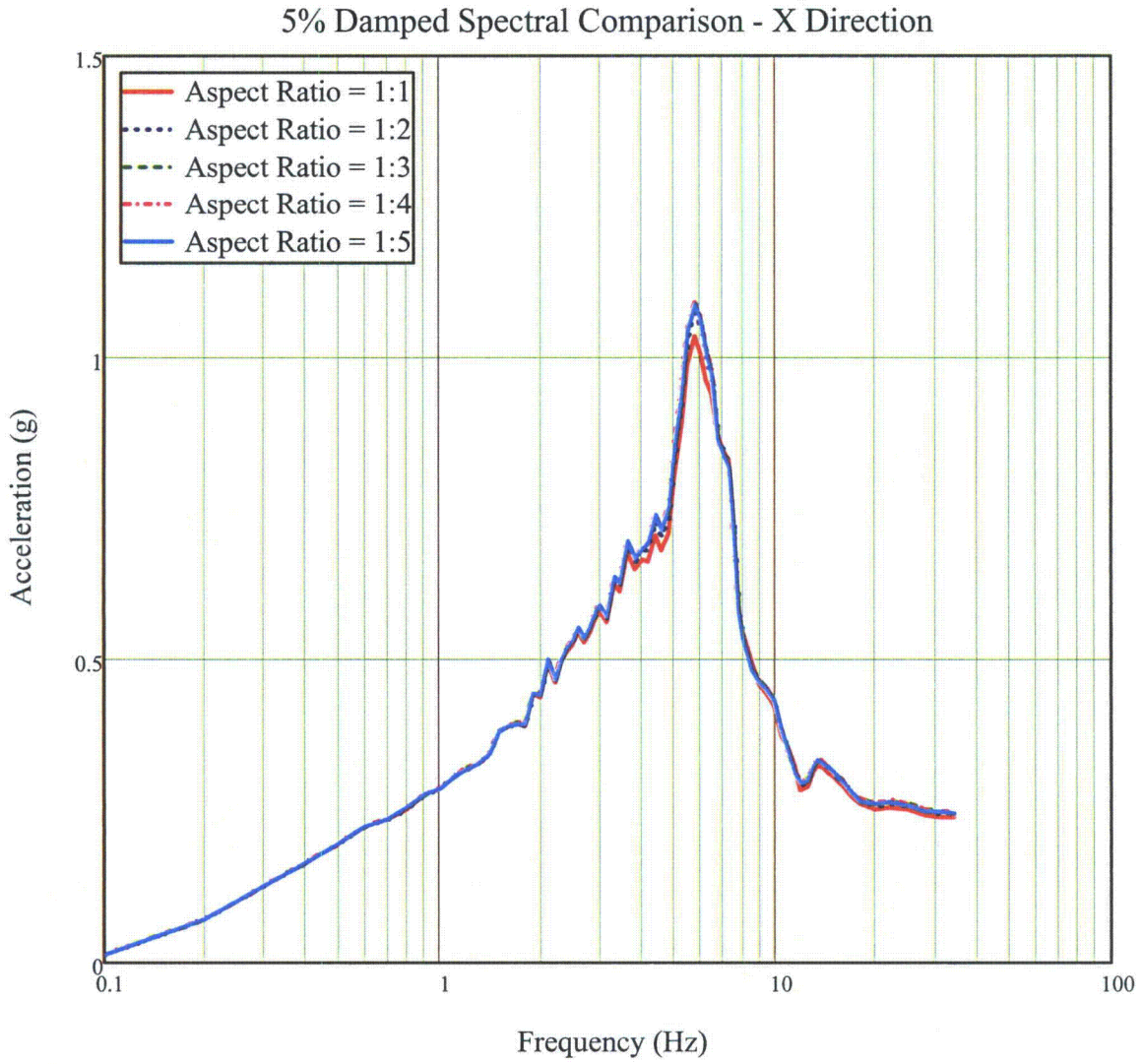

Figure 03.07.02-29.40: Comparison of Spectra – Roof Slab X Direction

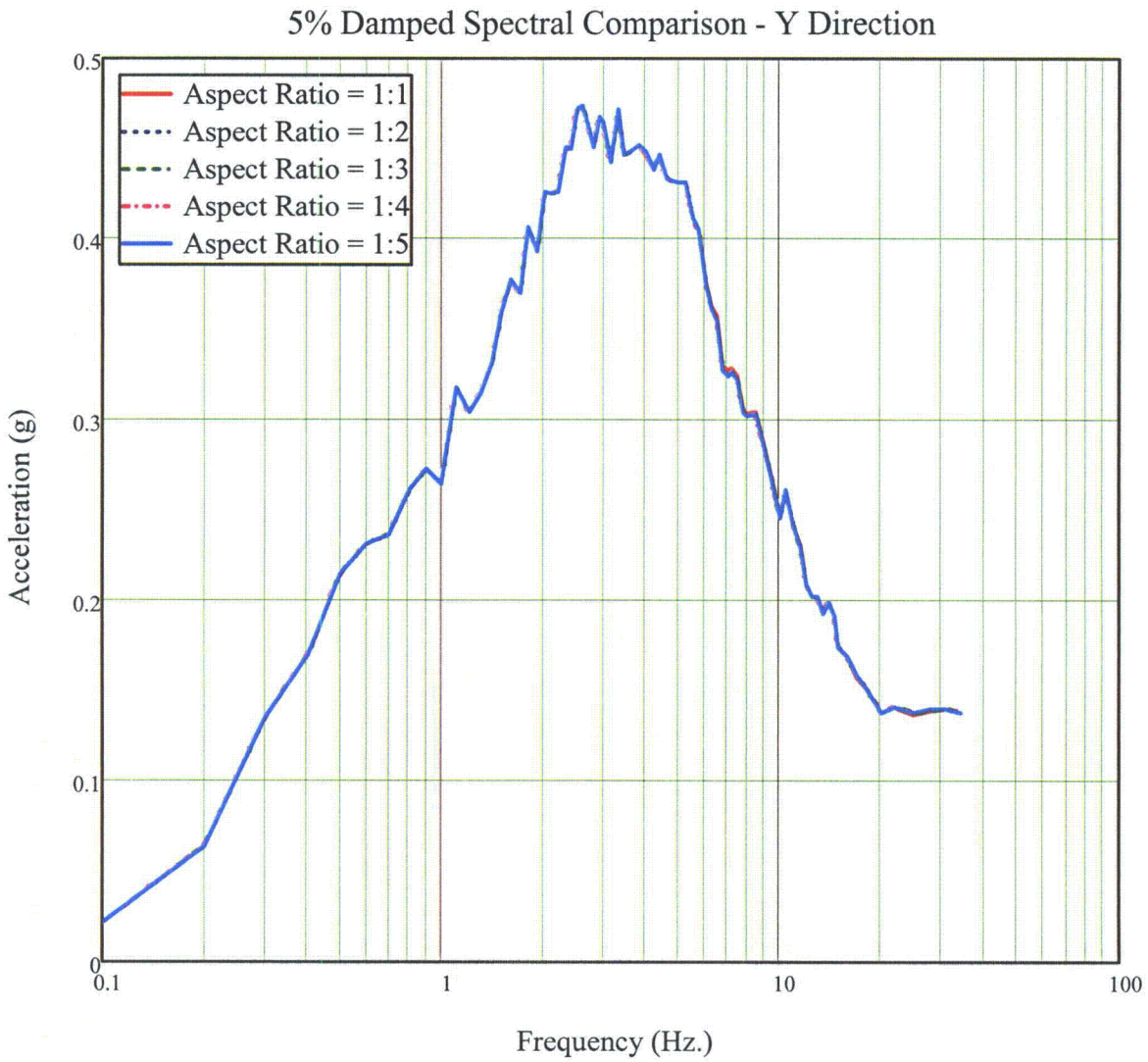

Figure 03.07.02-29.41: Comparison of Spectra – Base Mat Y Direction

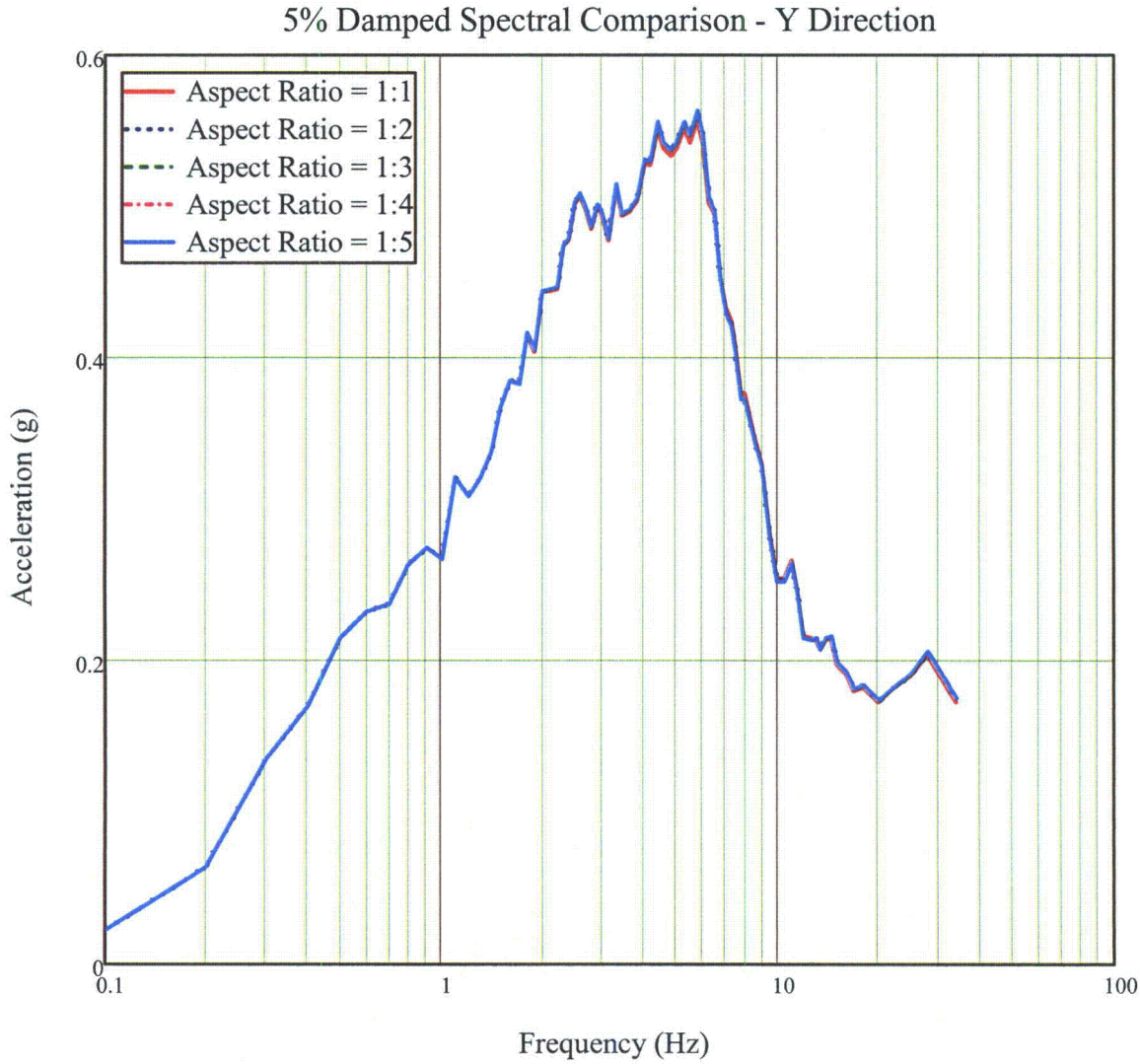

Figure 03.07.02-29.42: Comparison of Spectra – Mid height of 36 ft Long Wall Y Direction

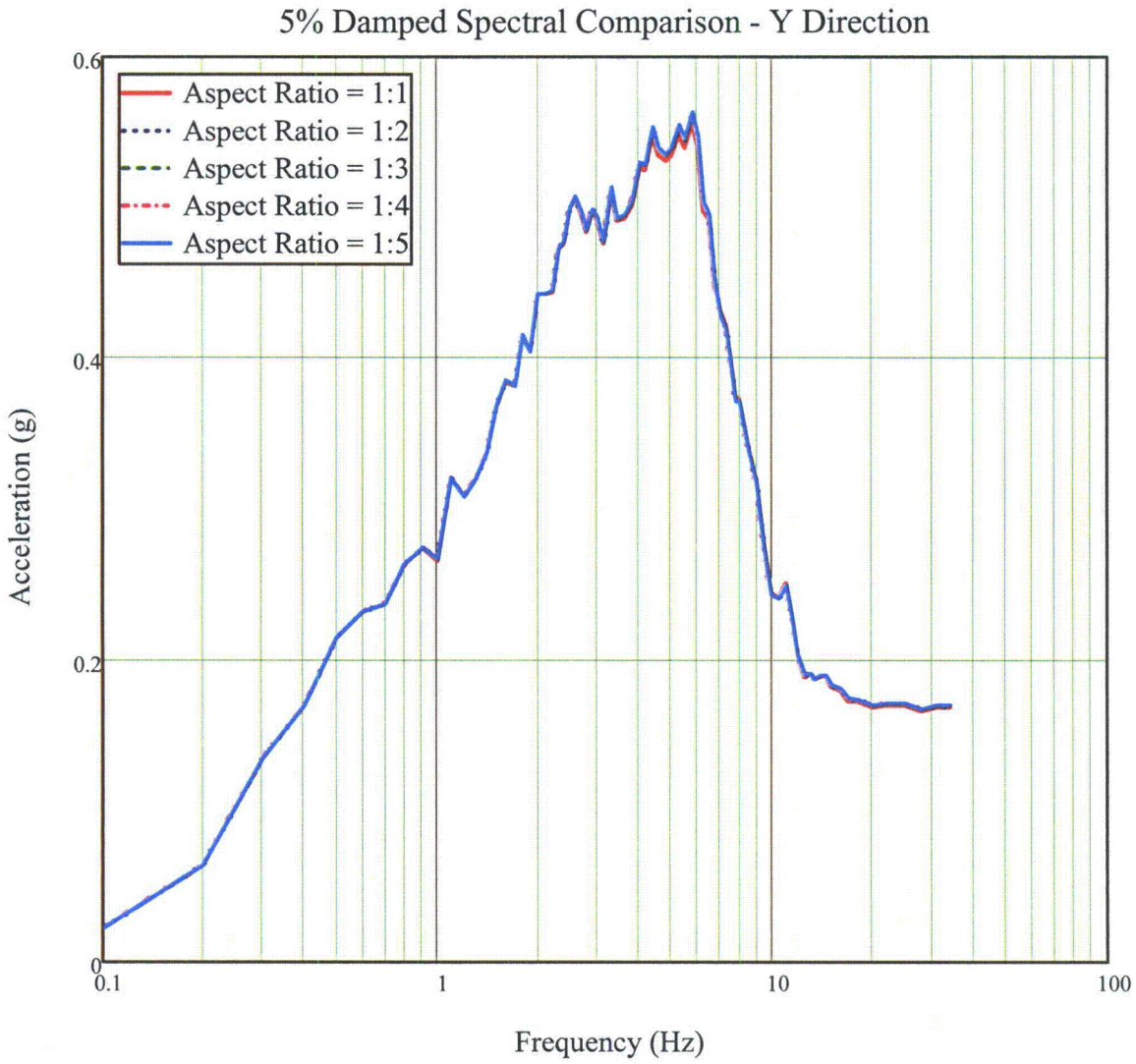

Figure 03.07.02-29.43: Comparison of Spectra – Mid height of 54 ft Long Wall Y Direction

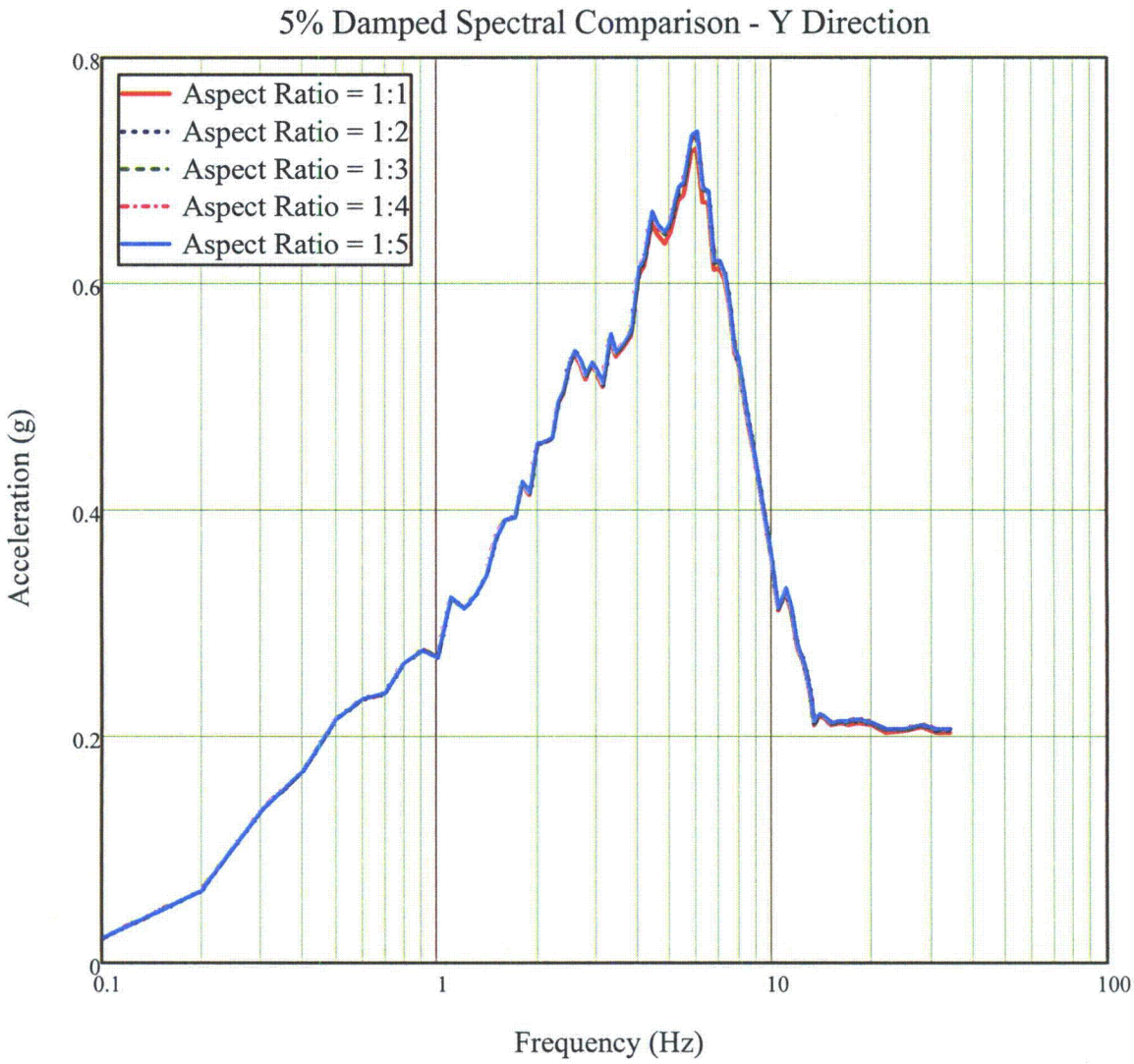

Figure 03.07.02-29.44: Comparison of Spectra – Roof Slab Y Direction

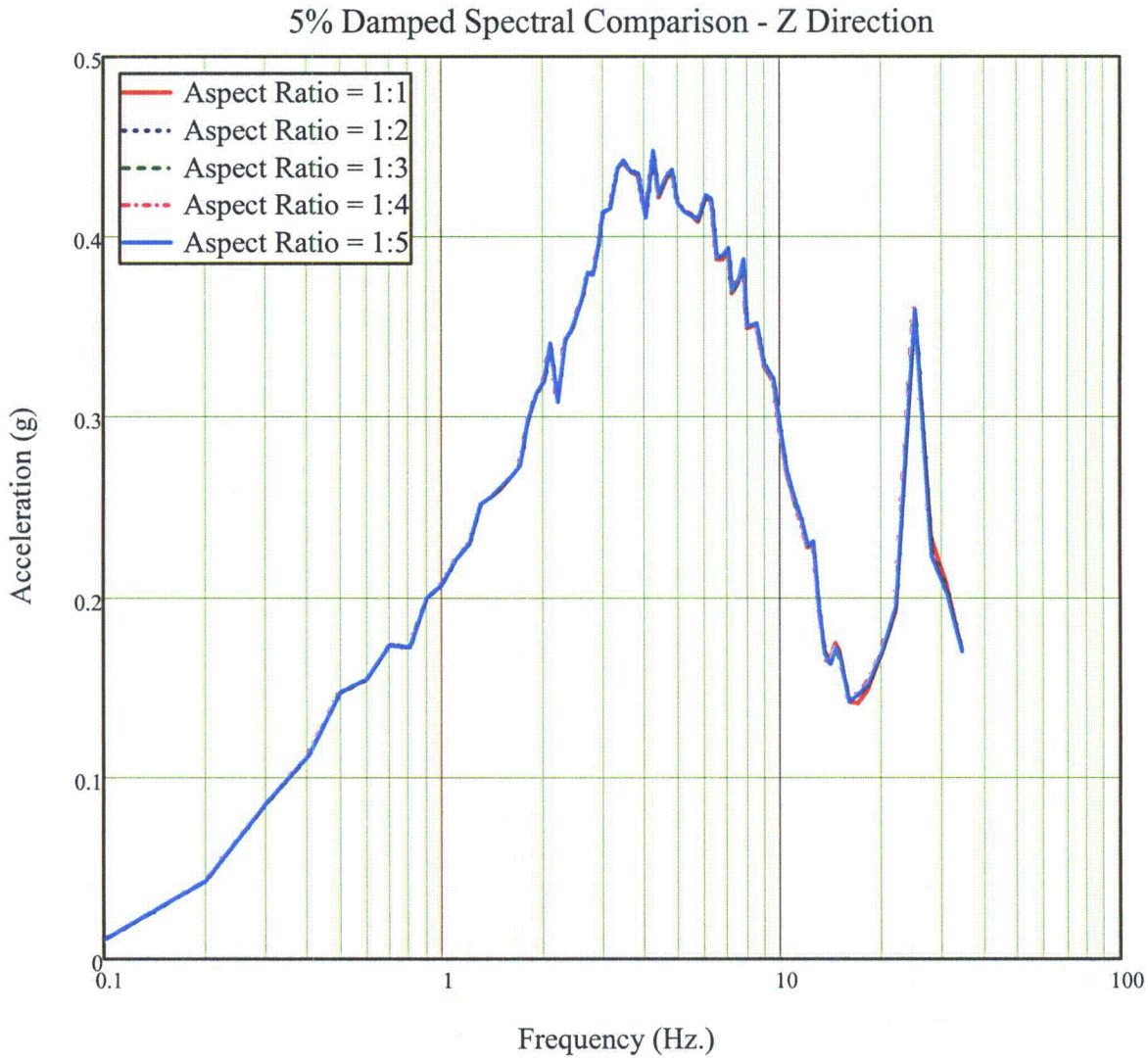

Figure 03.07.02-29.45: Comparison of Spectra – Base Mat Z Direction

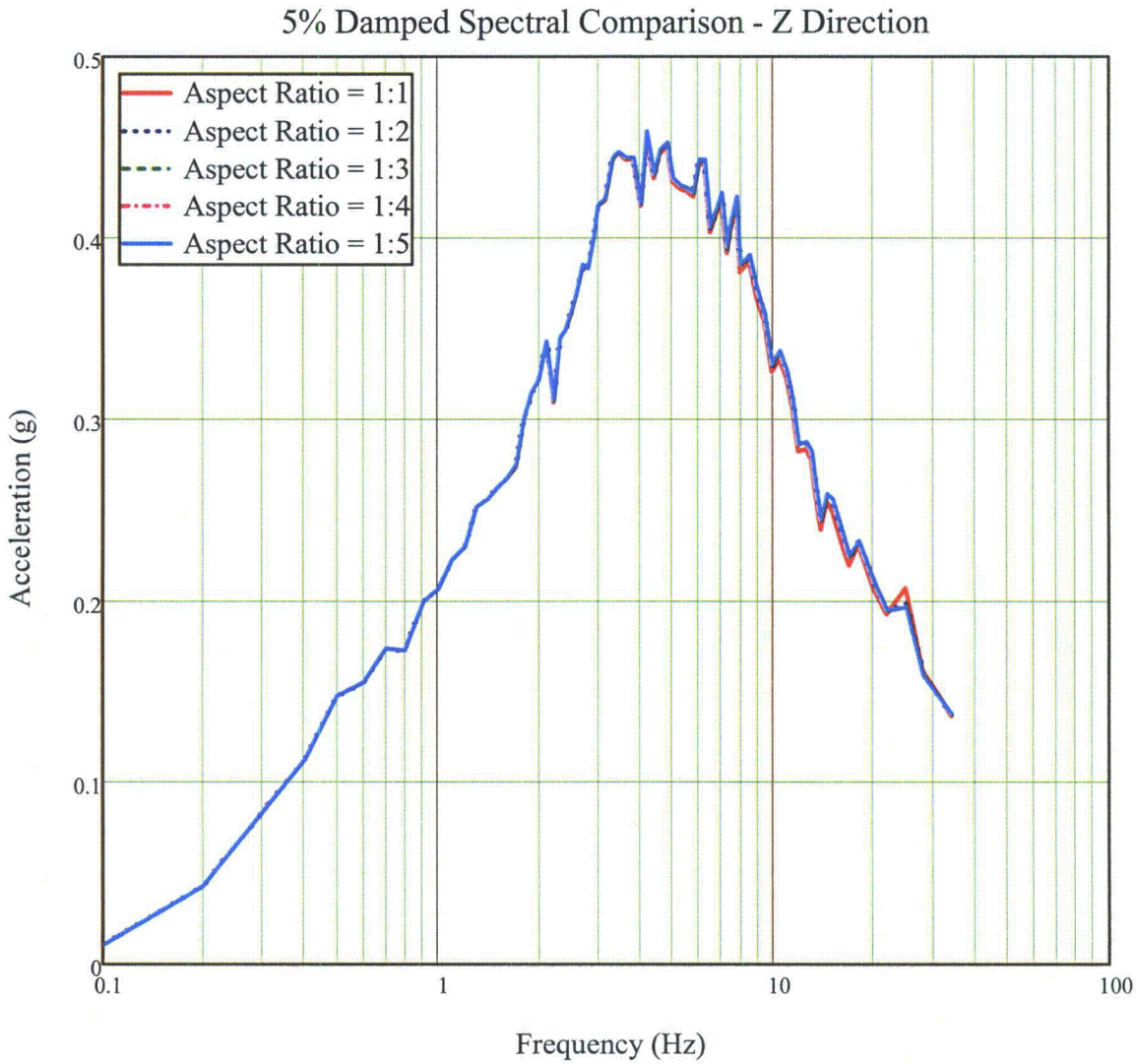

Figure 03.07.02-29.46: Comparison of Spectra – Mid height of 36 ft Long Wall Z Direction

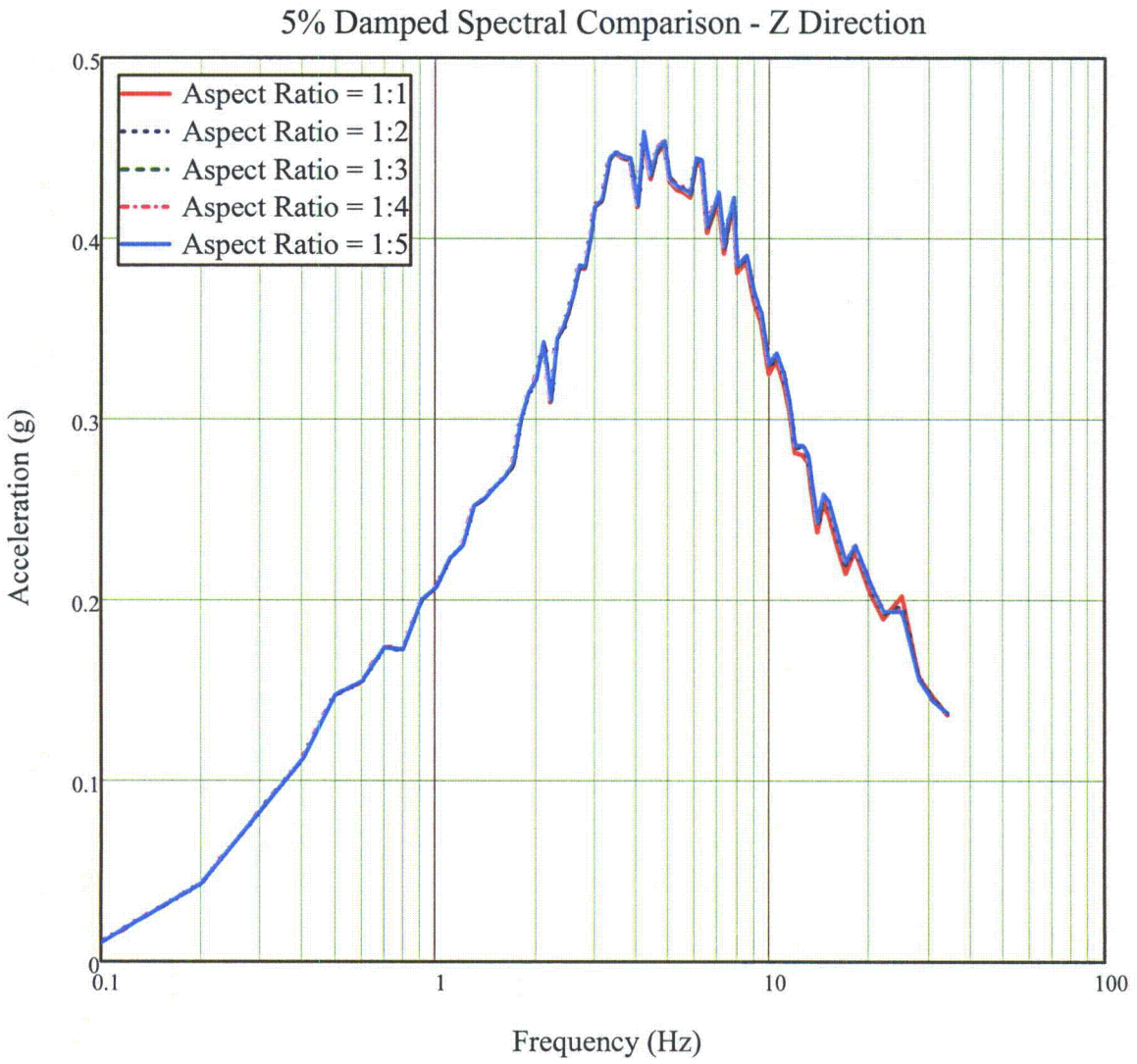

Figure 03.07.02-29.47: Comparison of Spectra – Mid Height of 54 ft Long Wall Z Direction

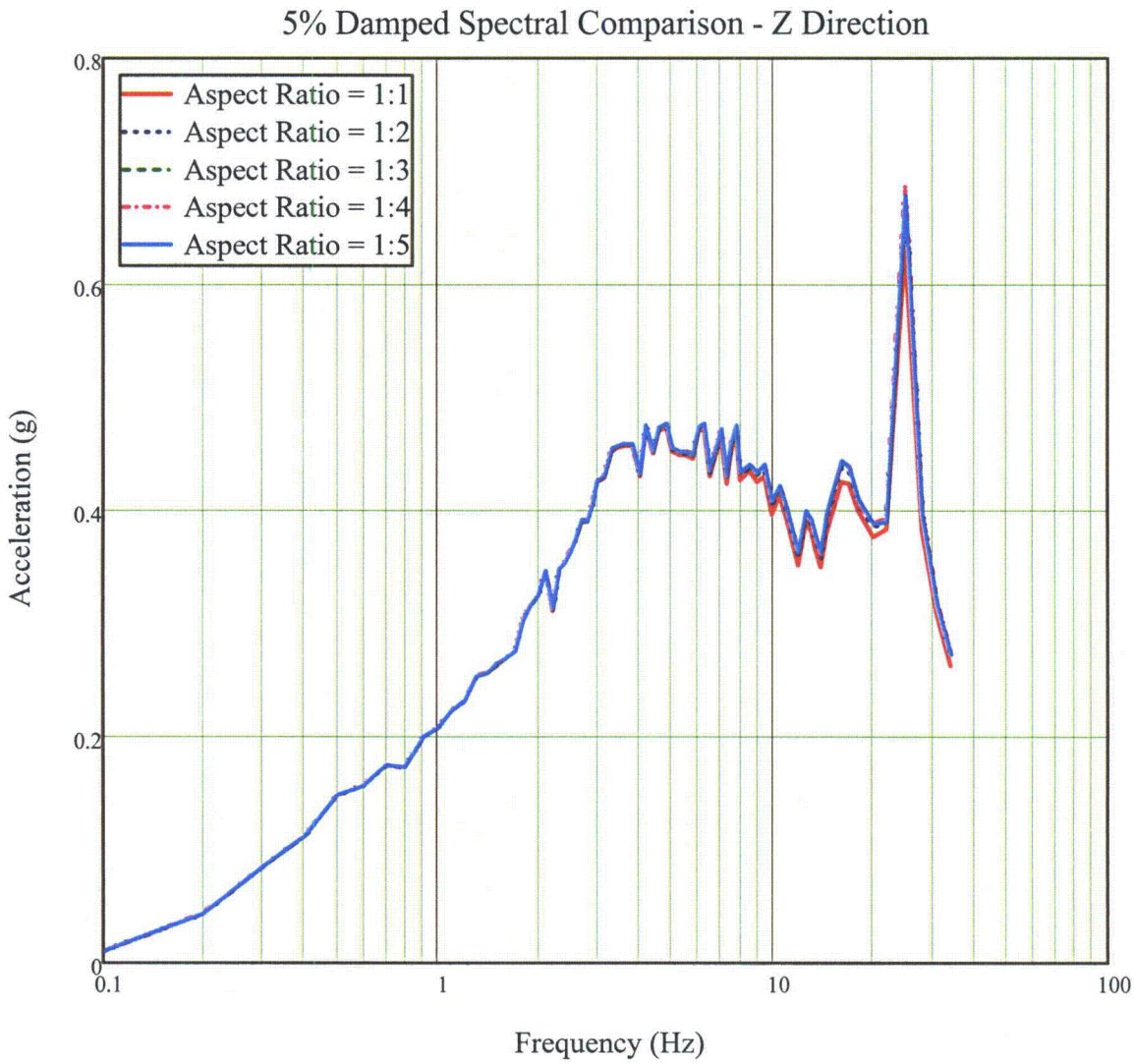

Figure 03.07.02-29.48: Comparison of Spectra – Roof Slab Z Direction

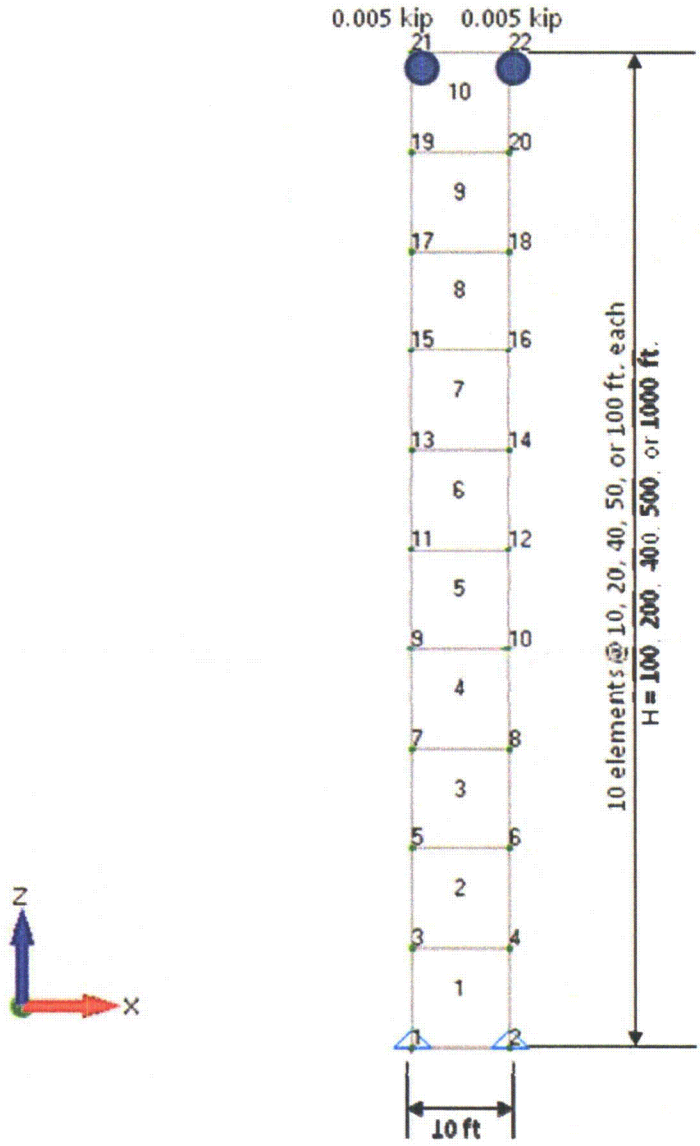

Figure 03.07.02-29.49: Model of Cantilever Subjected to Vertical (Z) Seismic Excitation

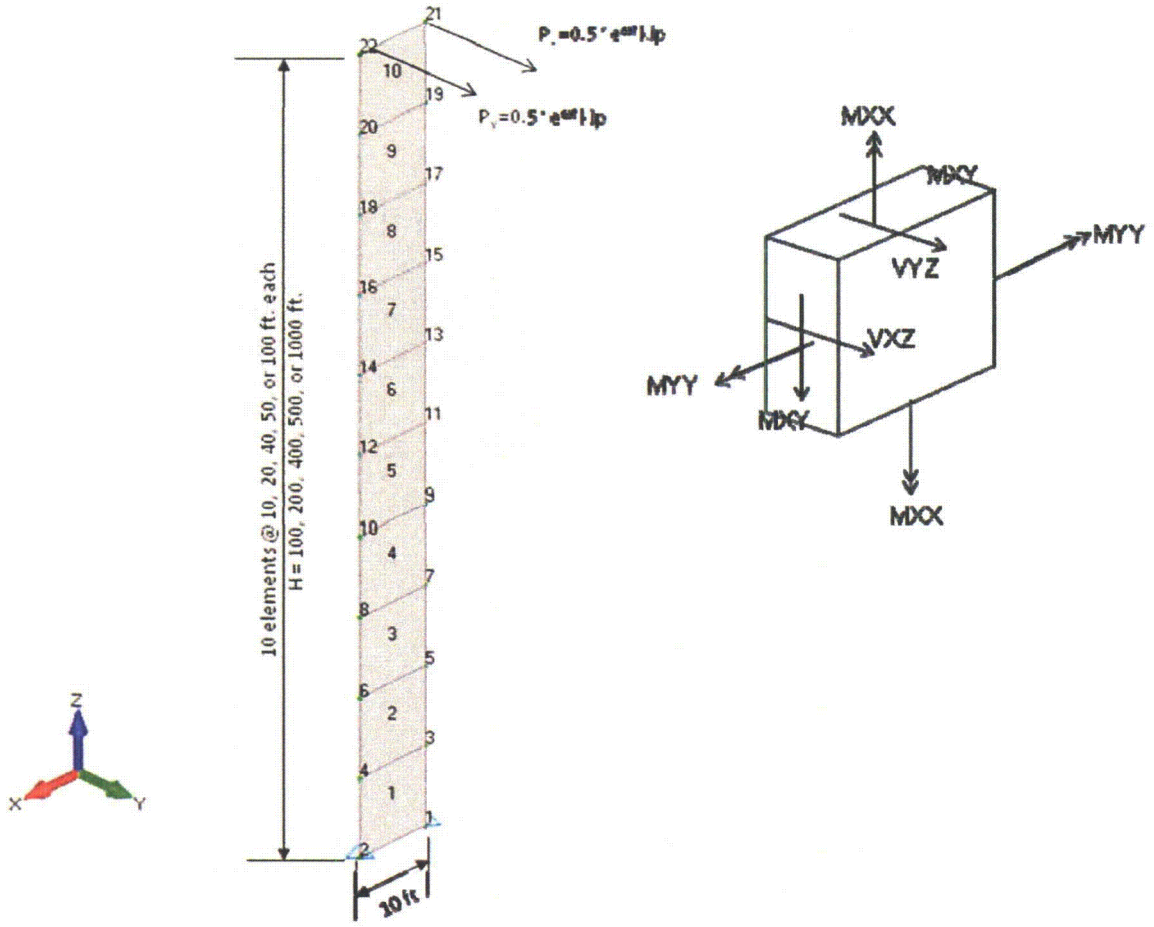

Figure 03.07.02-29.50: Model of Cantilever Subjected to Harmonic Out-of-Plane Shear Force, and Element Force and Moment Orientation

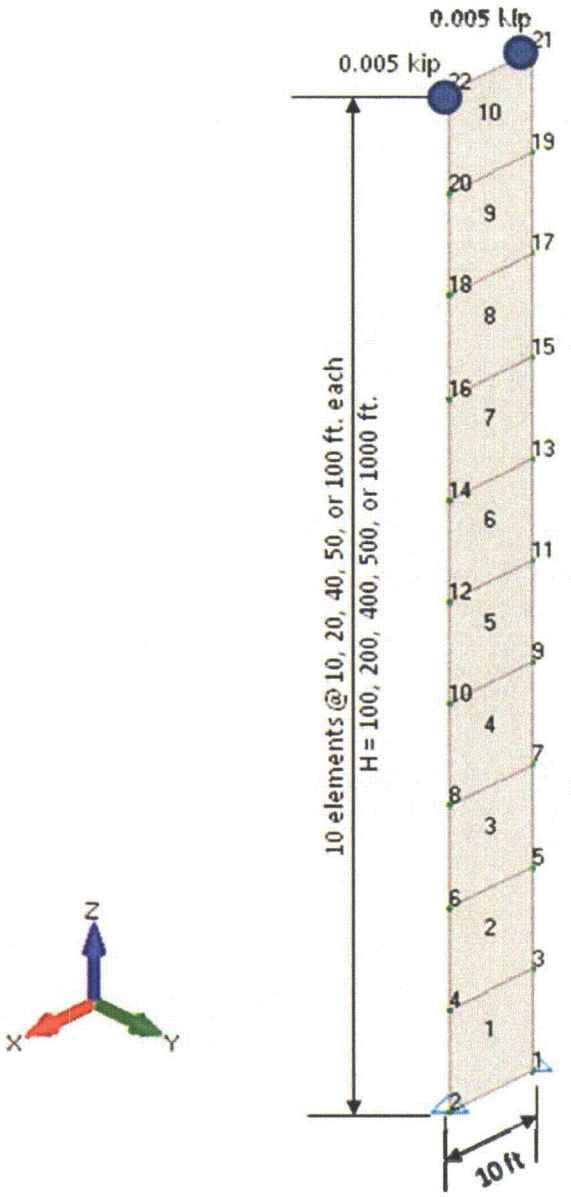

Figure 03.07.02-29.51: Model of Cantilever Subjected to Out-of-Plane Horizontal (Y) Seismic Excitation

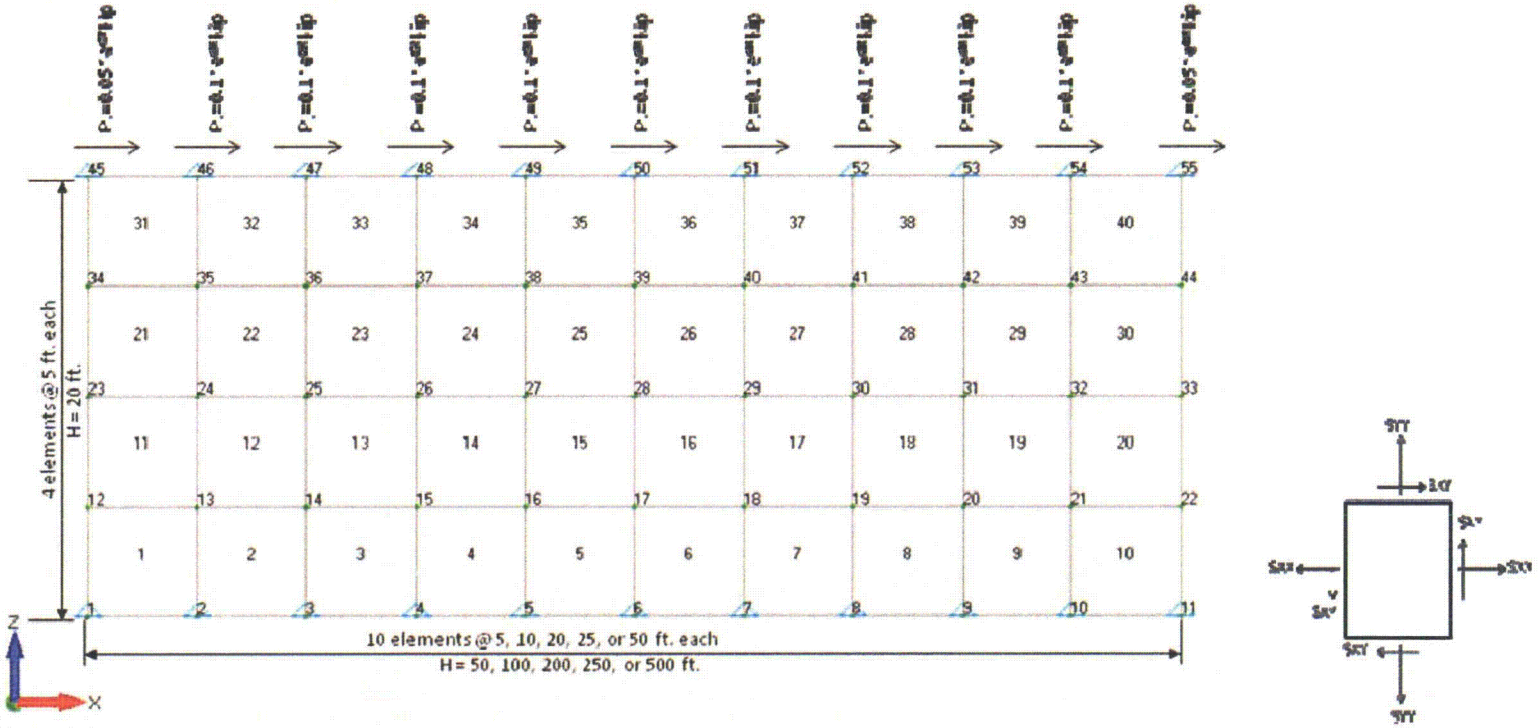

Figure 03.07.02-29.52: Model of Shear Wall Subjected to Harmonic In-Plane Shear Force, and Element Force Orientation

STI 32833064

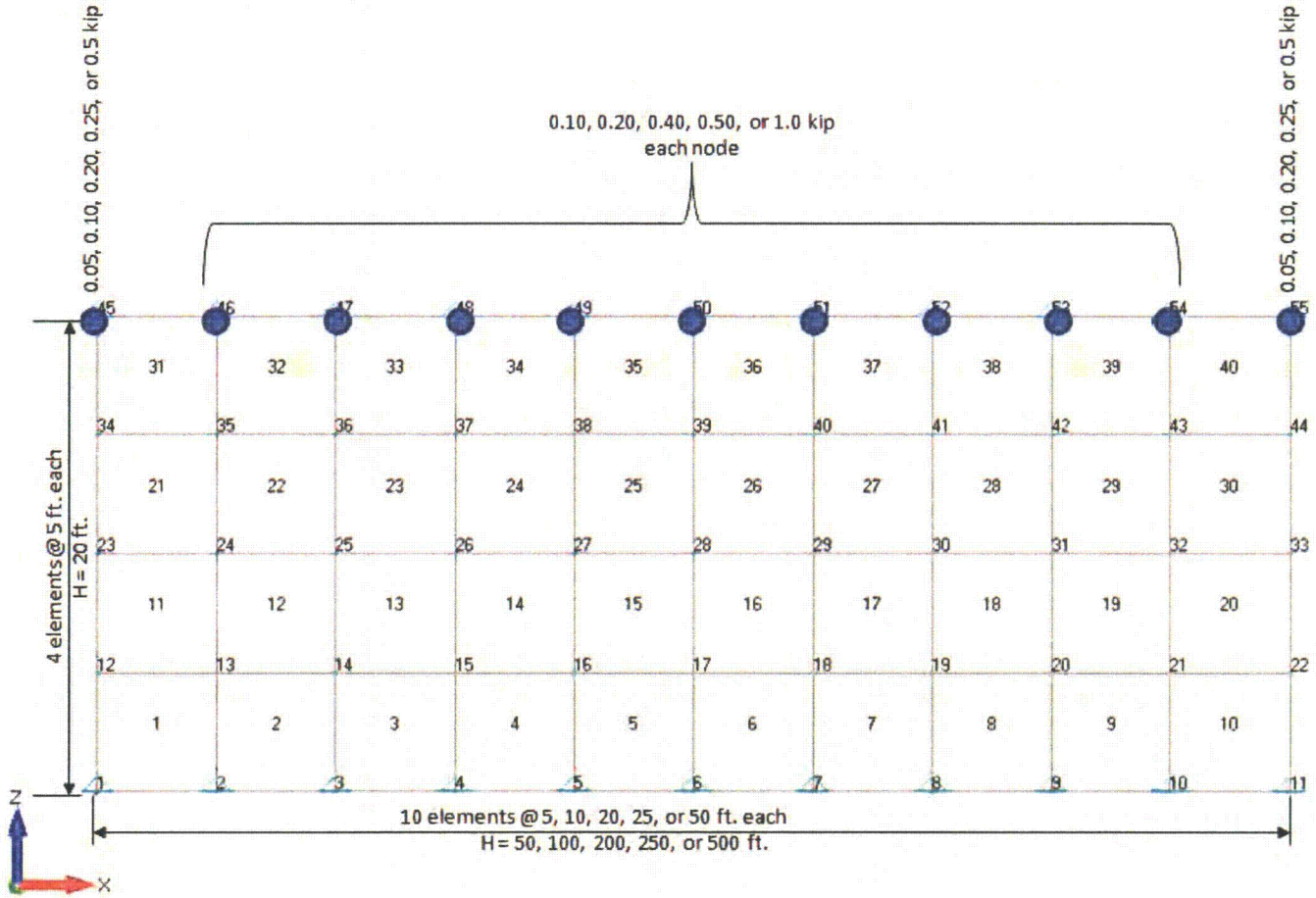

Figure 03.07.02-29.53: Model of Shear Wall Subjected to In-Plane Horizontal (X) Seismic Excitation

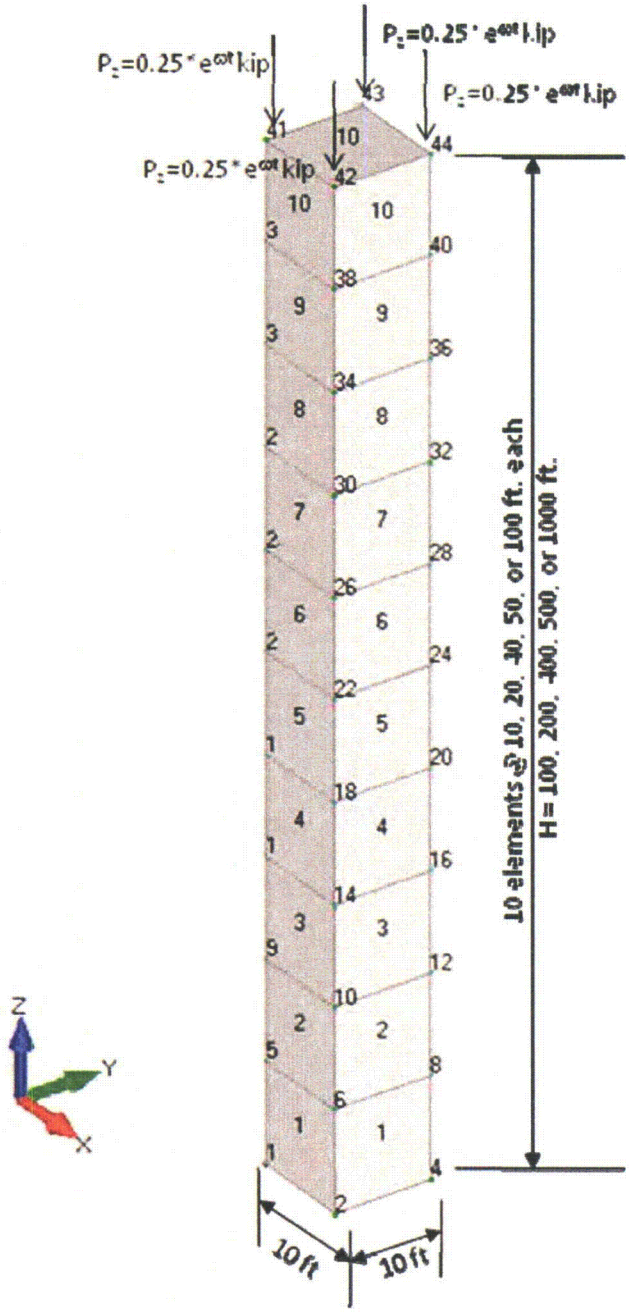

Figure 03.07.02-29.54: Model of Cantilever Subjected to Harmonic Axial Force

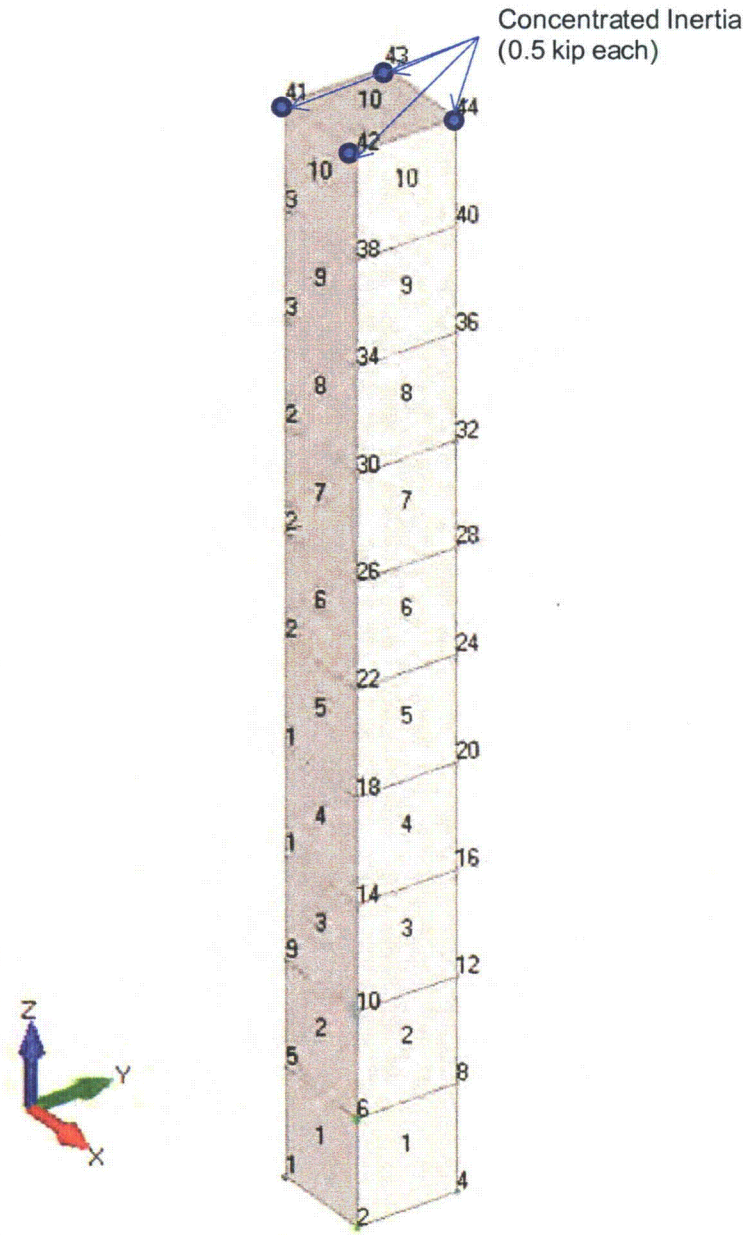

Figure 03.07.02-29.55: Model of Cantilever Subjected to Vertical Seismic Excitation

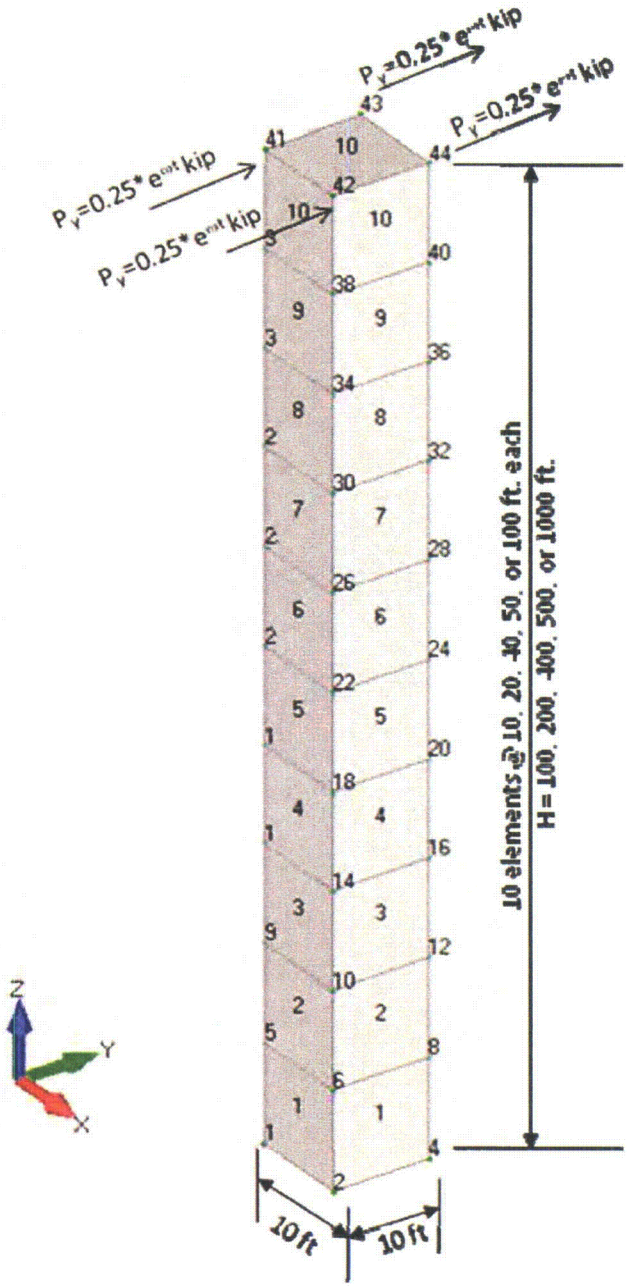

Figure 03.07.02-29.56: Model of Cantilever Subjected to Harmonic Horizontal Shear Force

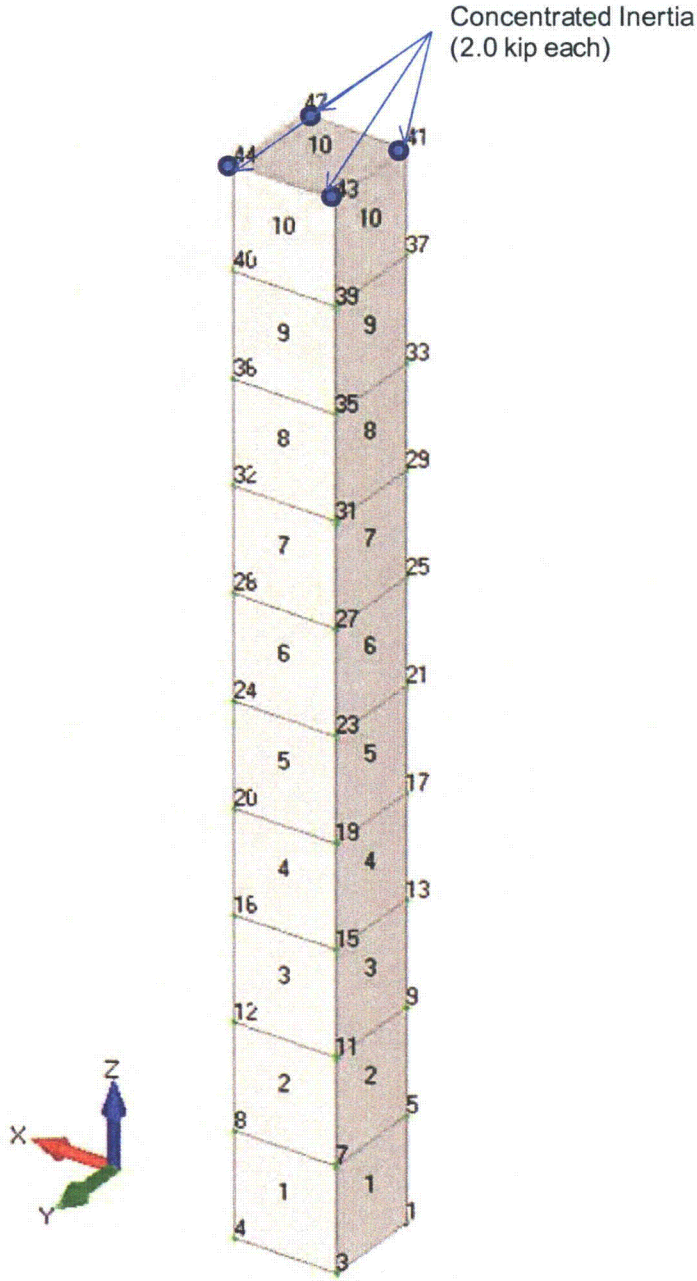

Figure 03.07.02-29.57: Model of Cantilever Subjected to Horizontal Seismic Excitation

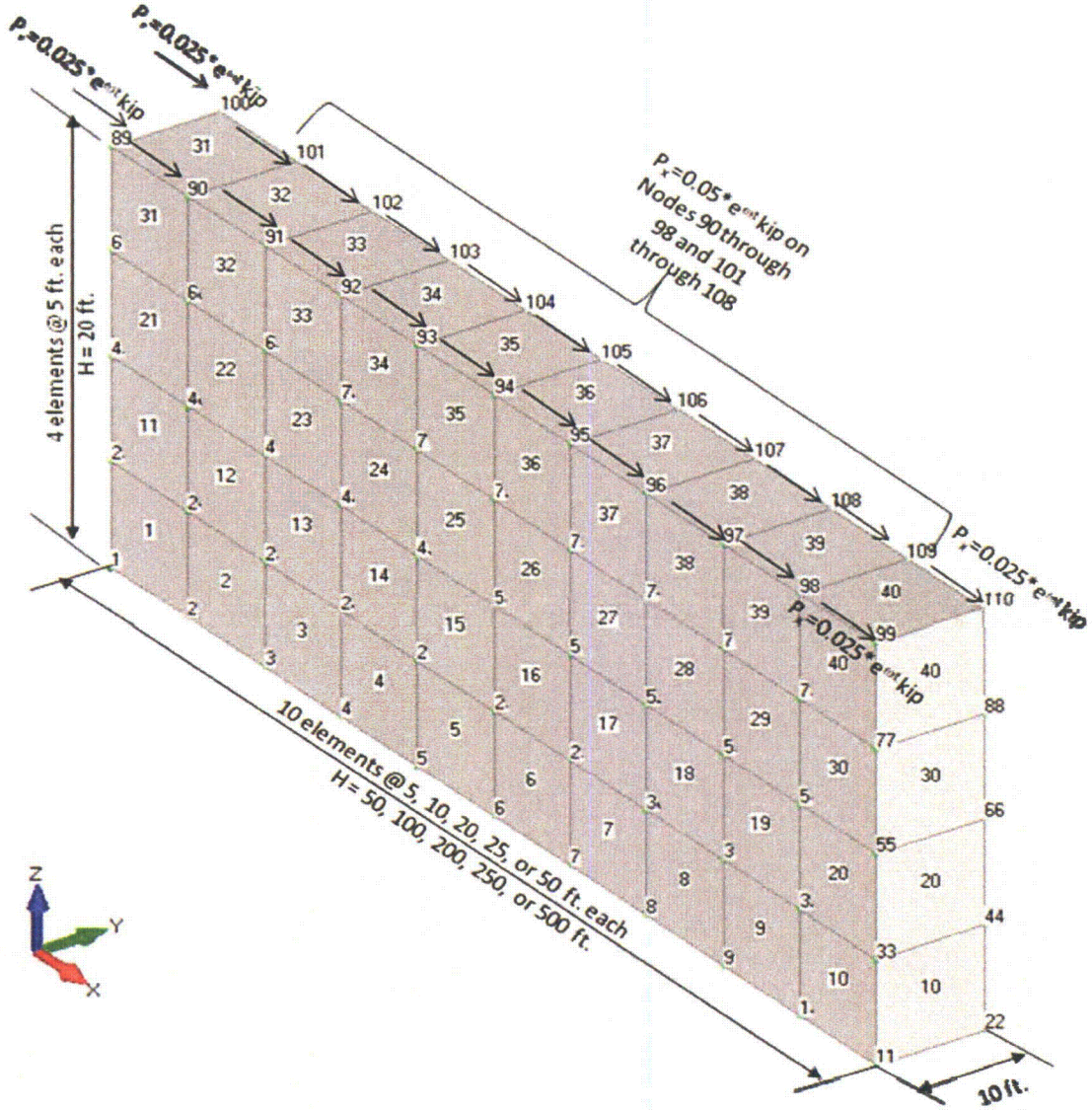

Figure 03.07.02-29.58: Model of Shear Wall Subjected to Harmonic In-Plane Shear Force

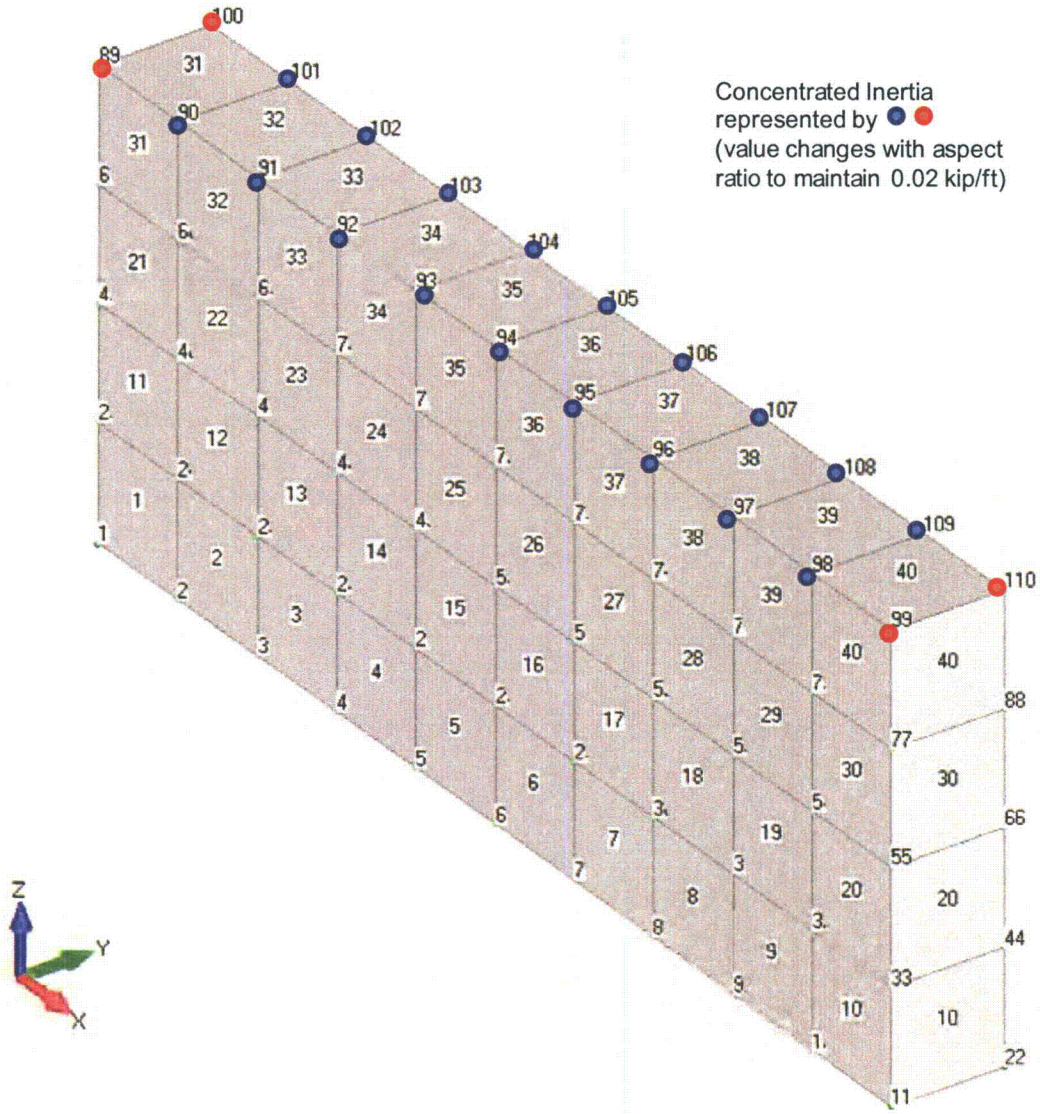

Figure 03.07.02-29.59: Model of Shear Wall Subjected to In-Plane Seismic Excitation

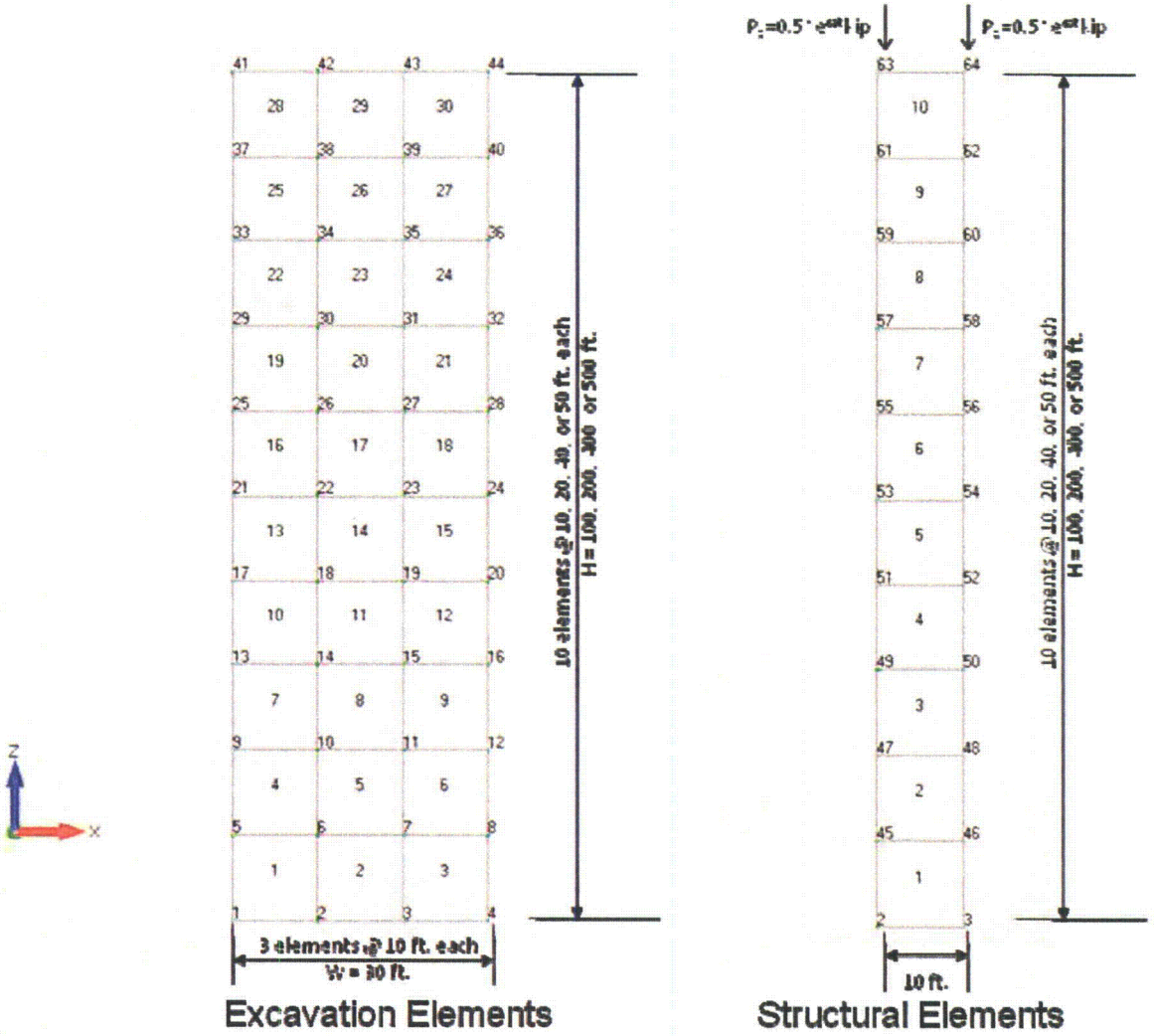

Figure 03.07.02-29.60: Model of Cantilever Subjected to Harmonic Axial Force, Aspect Ratios 1:1, 2:1, 4:1, and 5:1 (Not to Scale)

Note: Aspect ratio only applies to structural elements

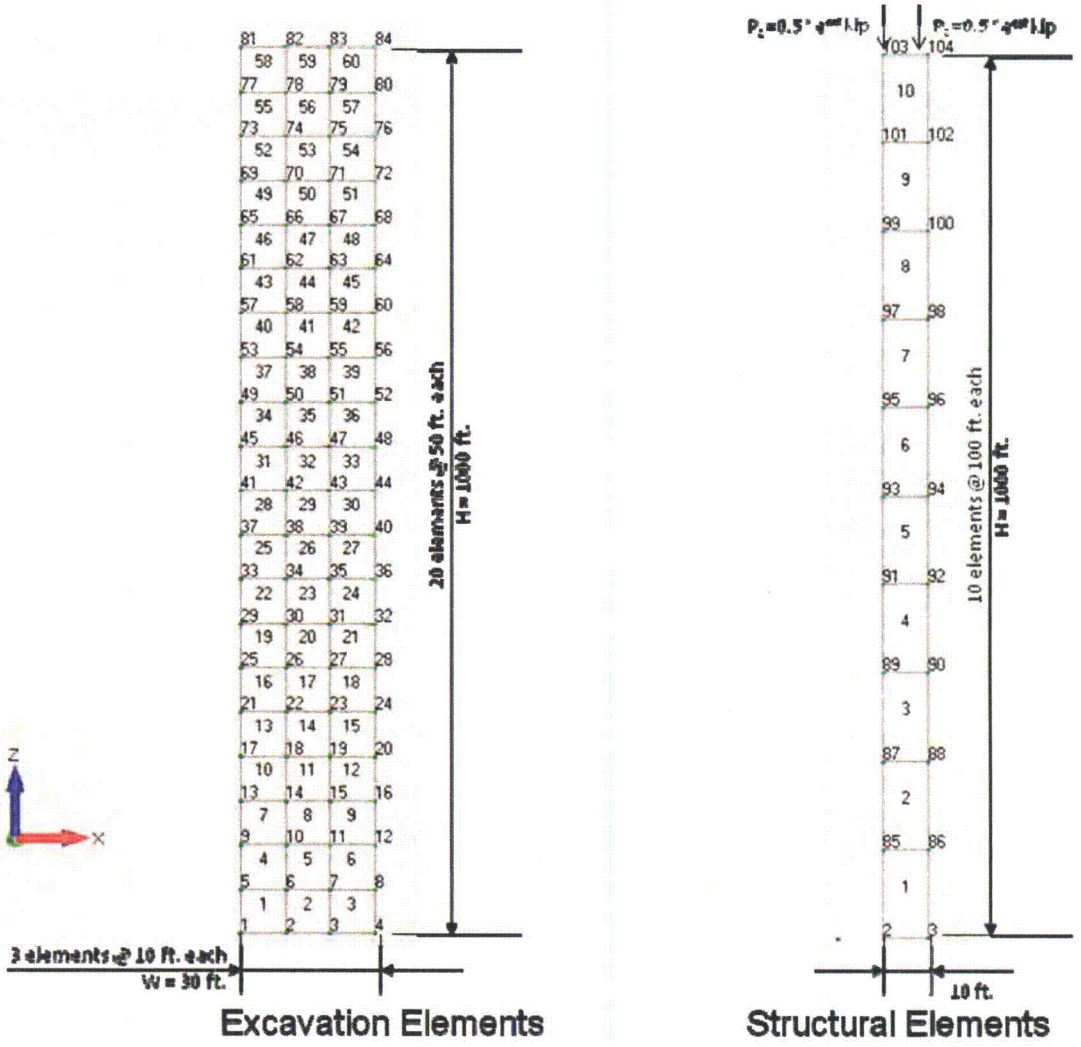

Figure 03.07.02-29.61: Model of Cantilever Subjected to Harmonic Axial Force, Aspect Ratio 10:1 (Not to Scale)

Note: Aspect ratio only applies to structural elements

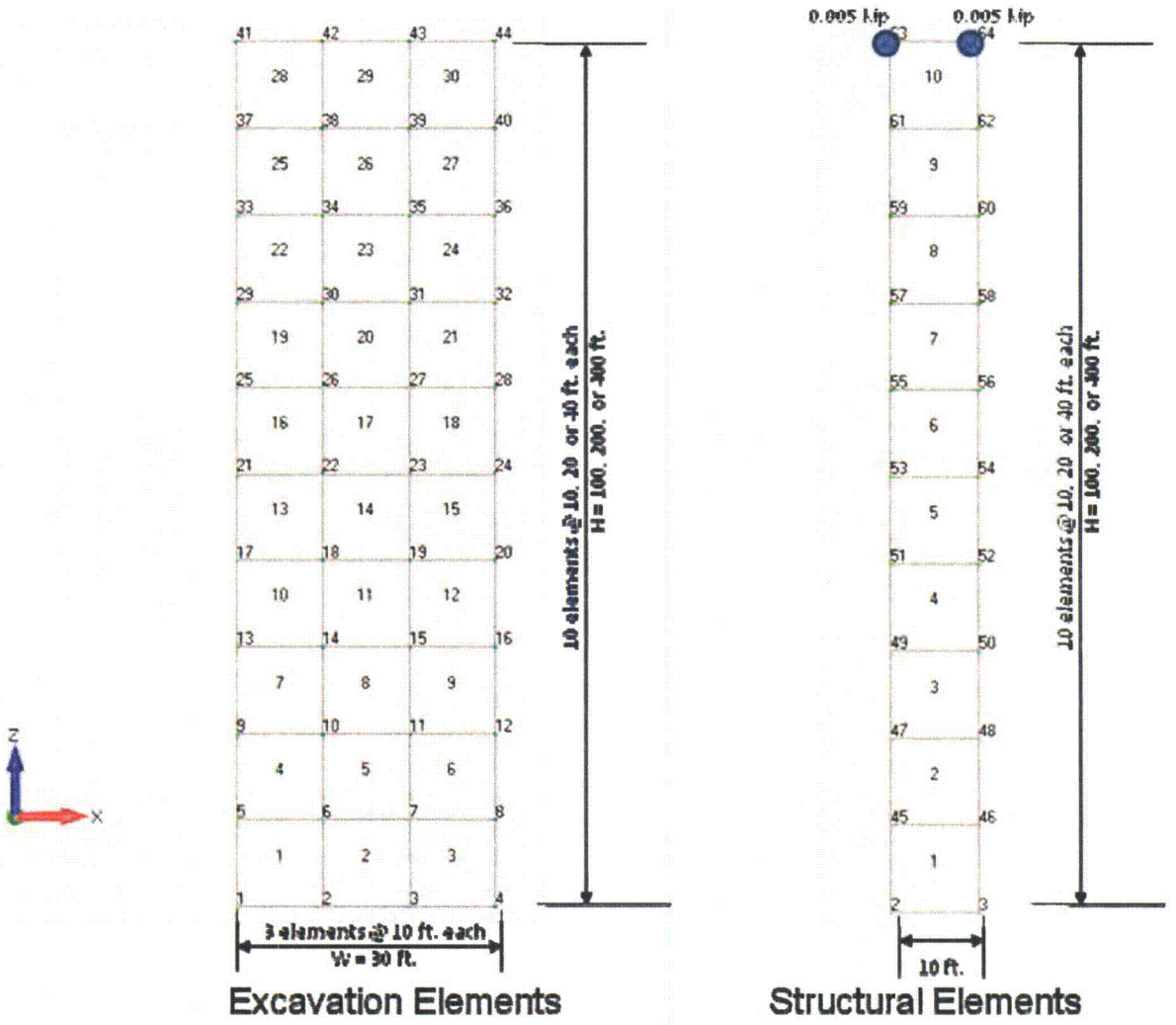

Figure 03.07.02-29.62: Model of Cantilever Subjected to Vertical (Z) Seismic Excitation, Aspect Ratios 1:1, 2:1, and 4:1 (Not to Scale)

Note: Aspect ratio only applies to structural elements

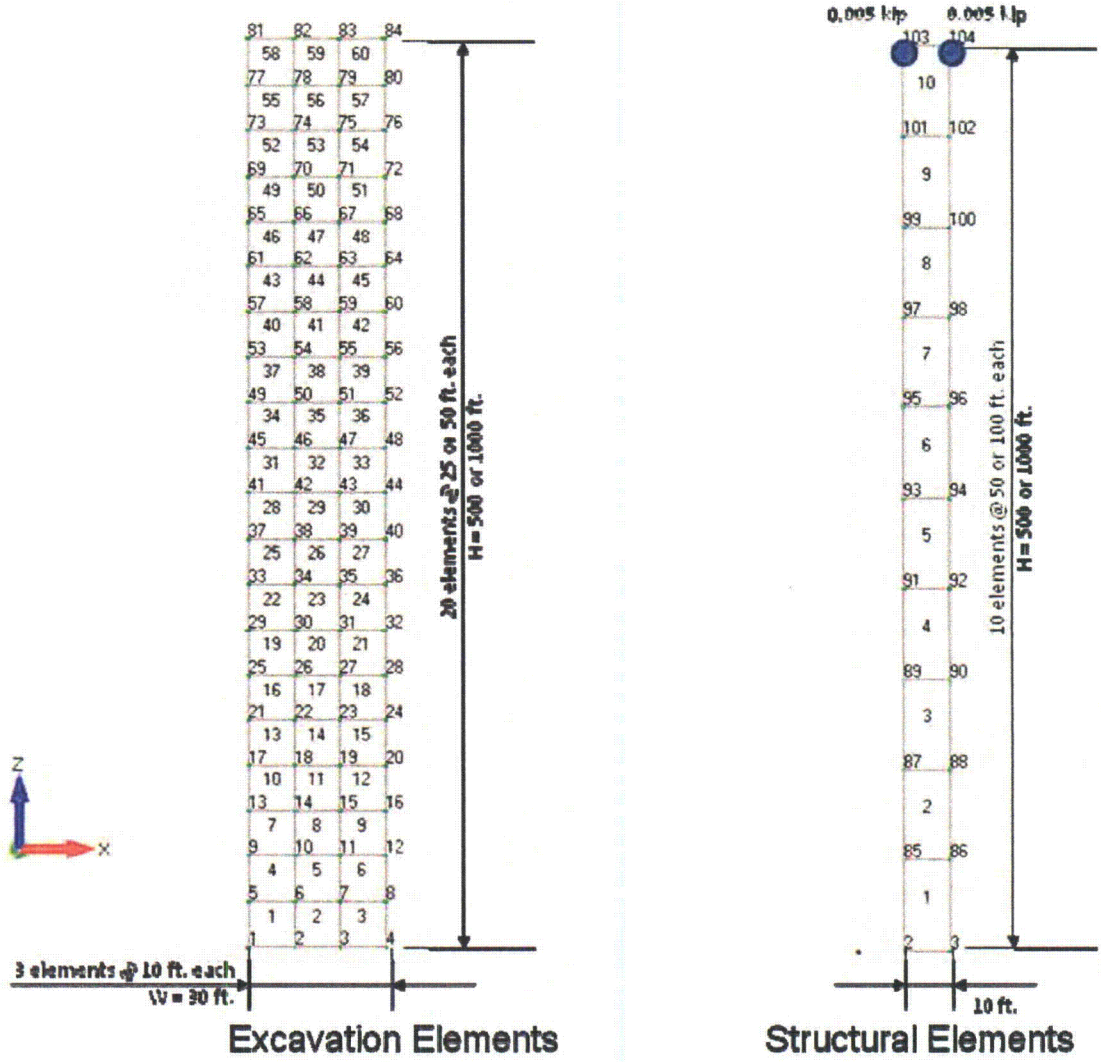

Figure 03.07.02-29.63: Model of Cantilever Subjected to Vertical (Z) Seismic Excitation, Aspect Ratios 5:1 and 10:1 (Not to Scale)

Note: Aspect ratio only applies to structural elements

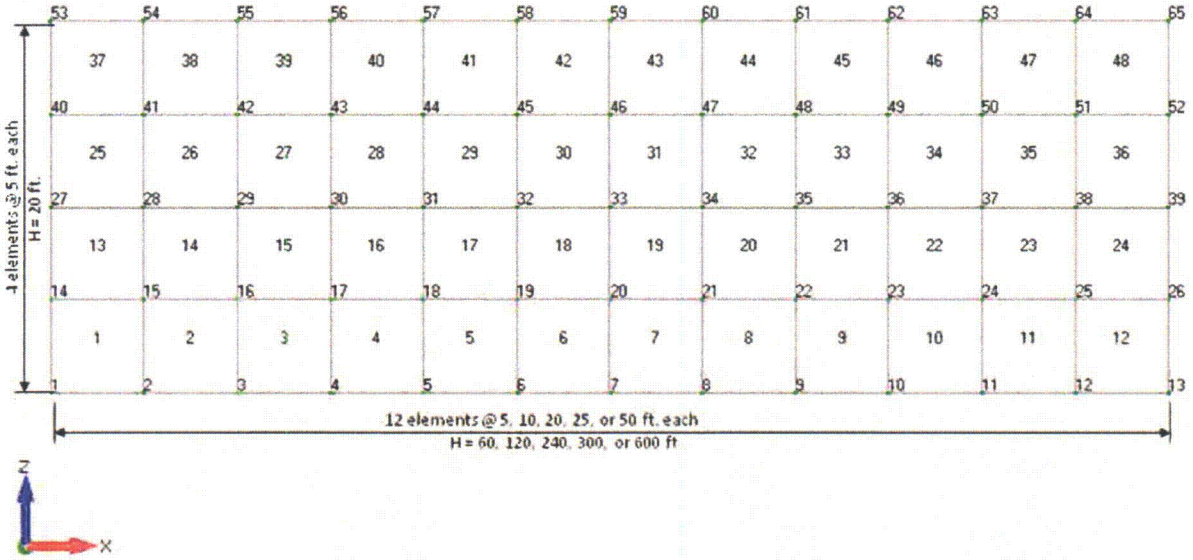

Figure 03.07.02-29.64: Model of Shear Wall Subjected to Harmonic In-Plane Shear Force, Excavation Elements

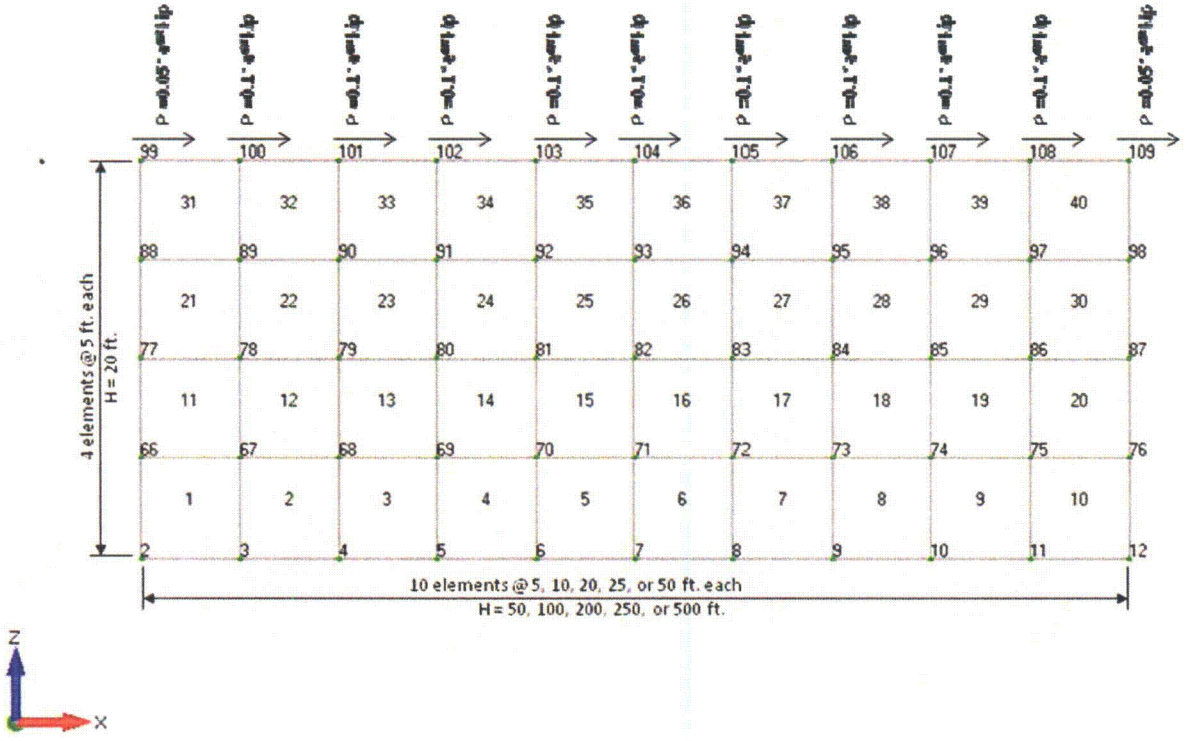

Figure 03.07.02-29.65: Model of Shear Wall Subjected to Harmonic In-Plane Shear Force, Structural Elements

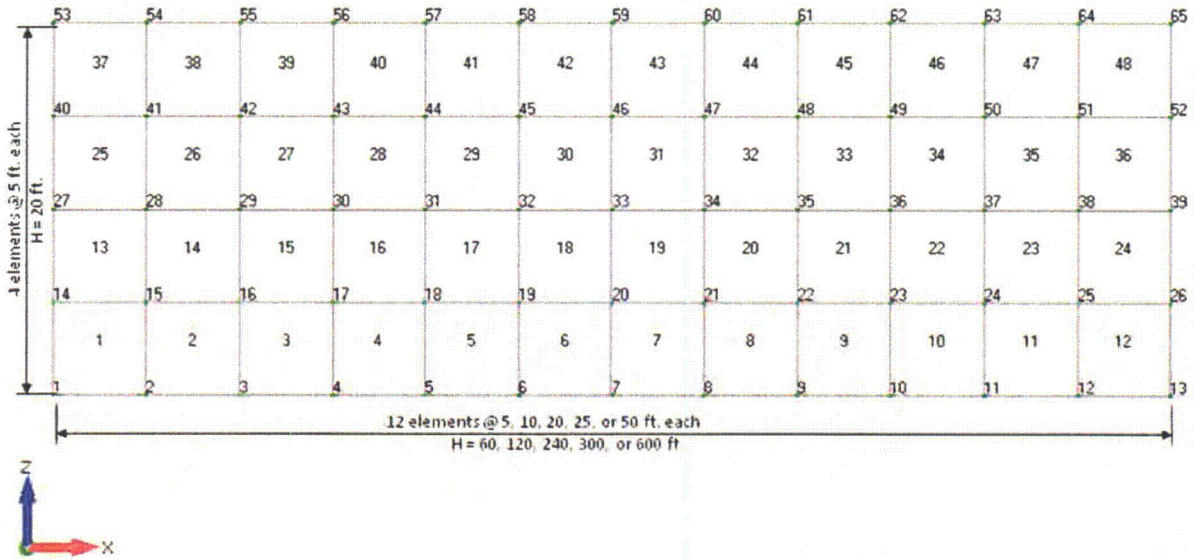

Figure 03.07.02-29.66: Model of Shear Wall Subjected to In-Plane Horizontal (X) Seismic Excitation, Excavation Elements

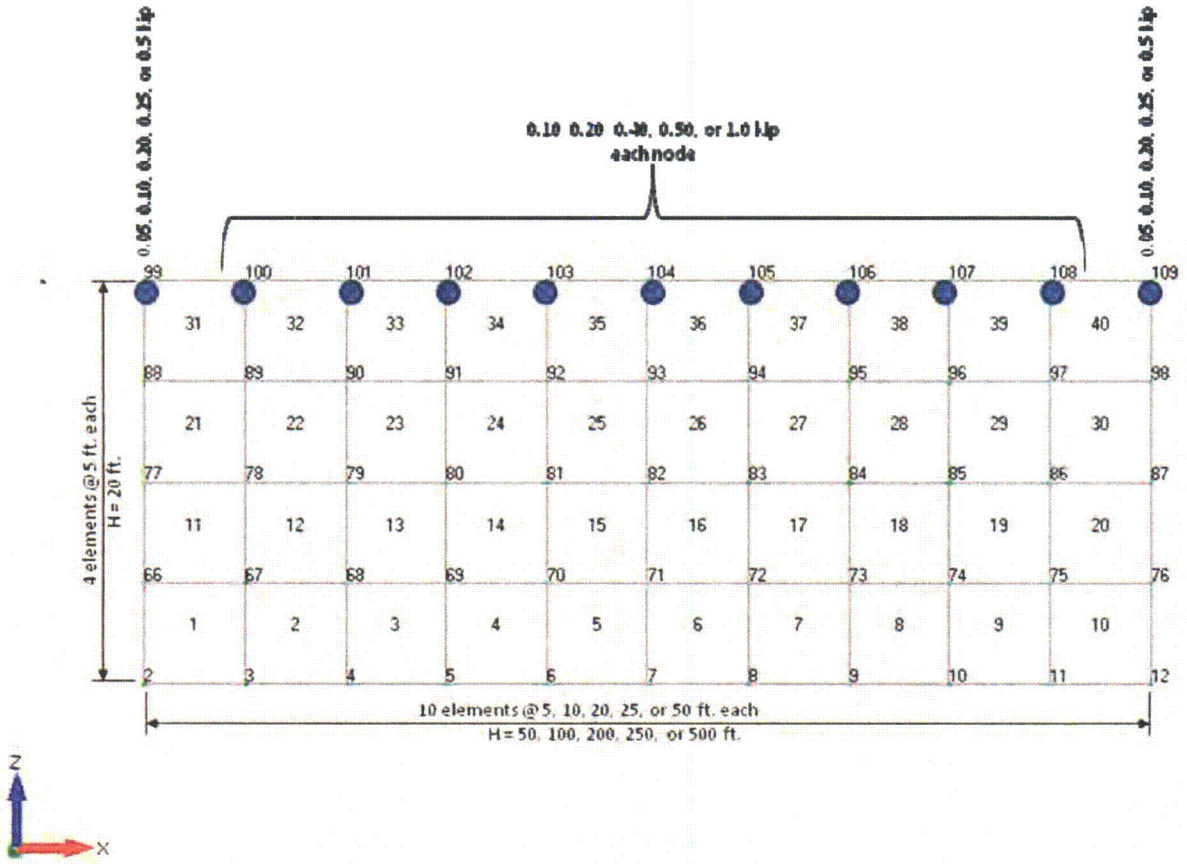

Figure 03.07.02-29.67: Model of Shear Wall Subjected to In-Plane Horizontal (X) Seismic Excitation, Structural Elements

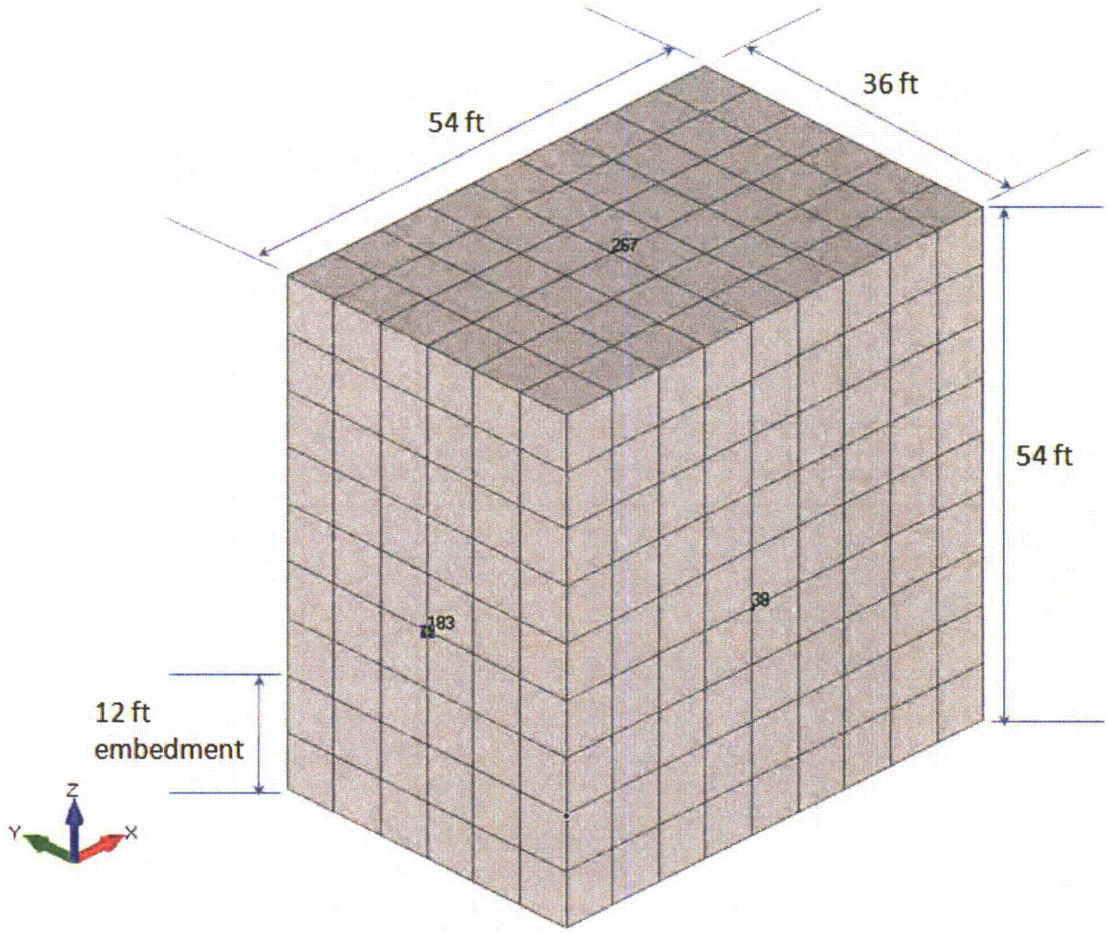

Figure 03.07.02-29.68: Isometric View of the Box Structure (Element Aspect Ratio 1:1), Indicating the Nodes of Interest on Long Wall, Short Wall and Roof

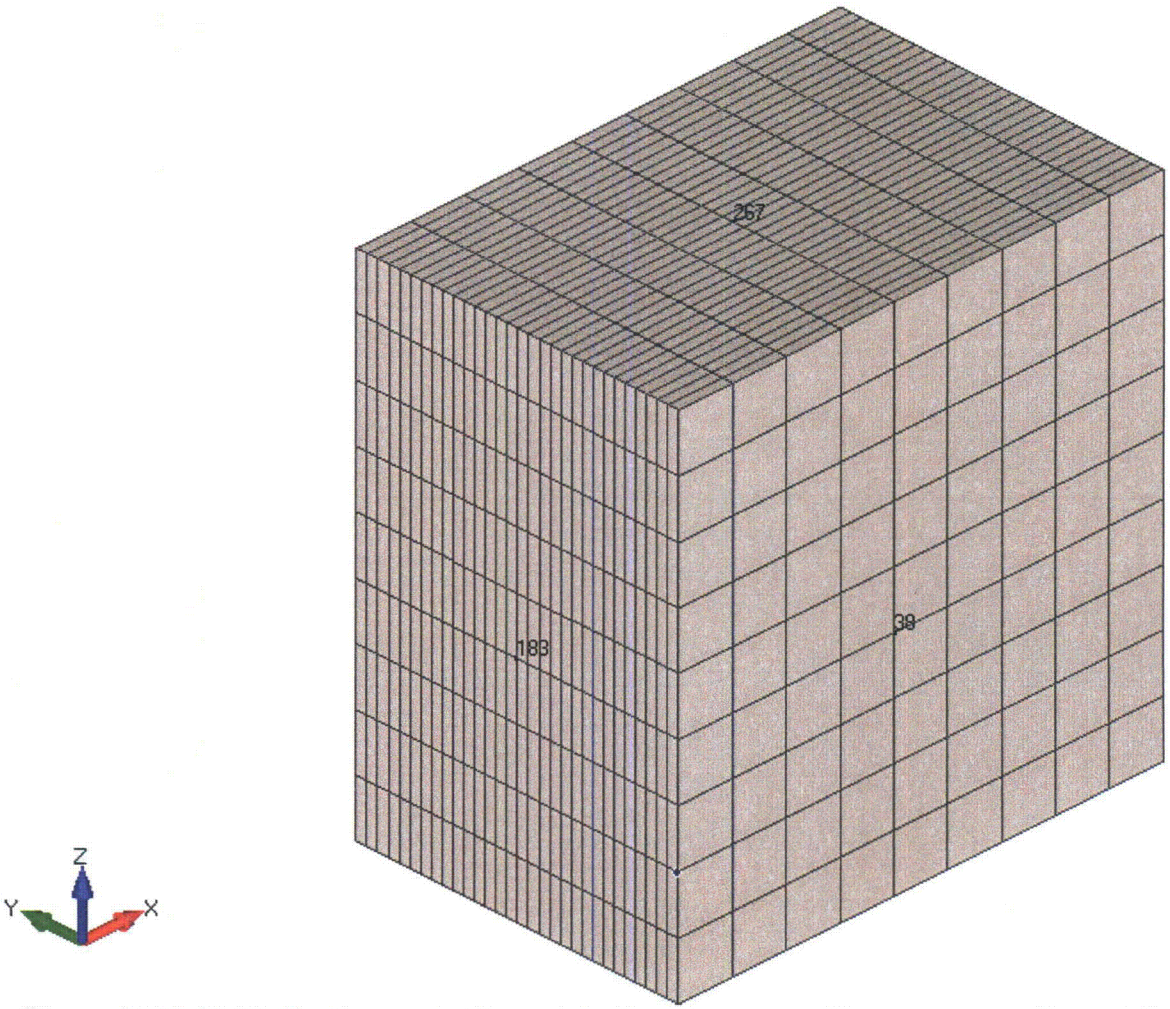

Figure 03.07.02-29.69: Isometric View of the Box Structure (Element Aspect Ratio 1:5), Indicating the Nodes of Interest on Long Wall, Short Wall and Roof

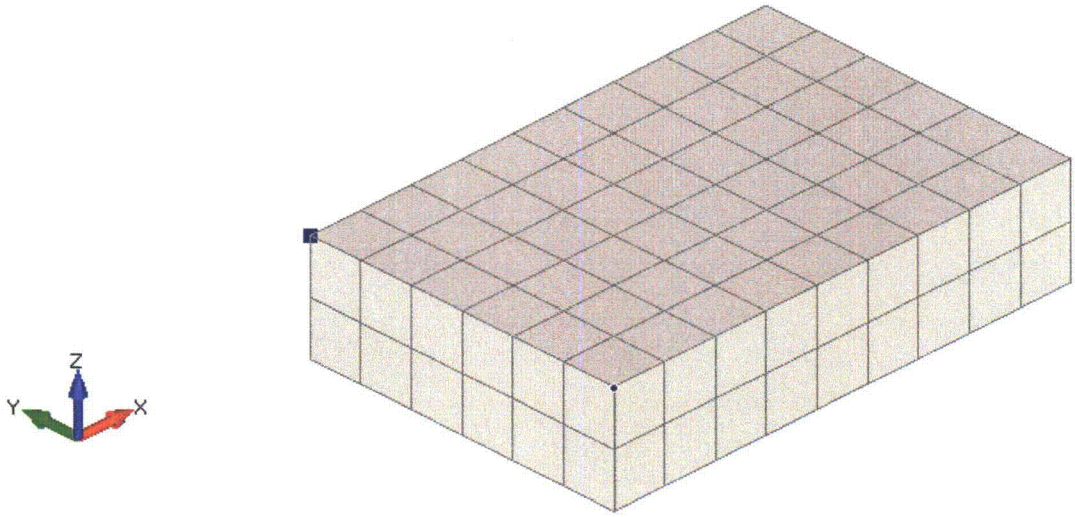

Figure 03.07.02-29.70: Isometric View of the Excavation Soil Elements

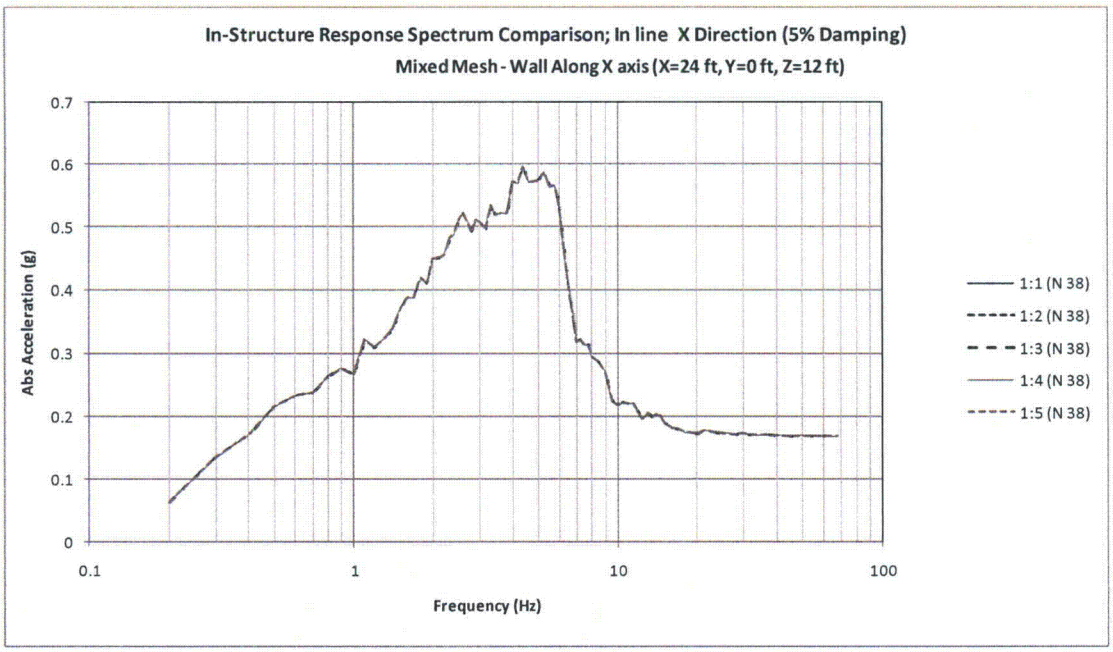

Figure 03.07.02-29.71: Comparison of In Structure Response Spectra for Mixed Mesh Models; Wall along X Axis; X Direction Analysis

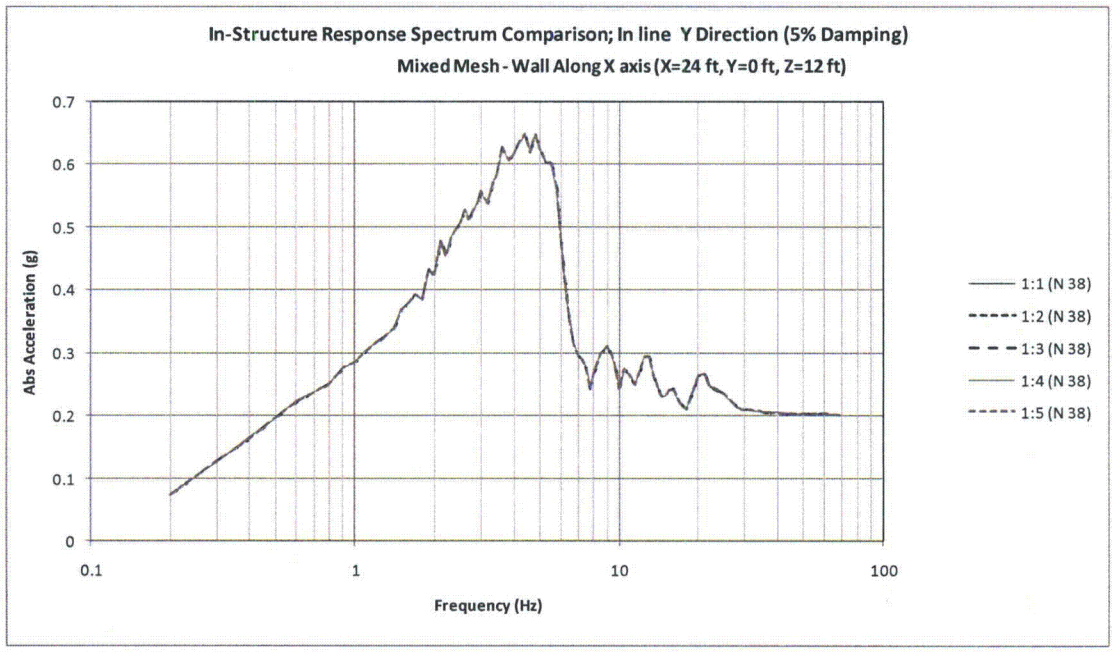

Figure 03.07.02-29.72: Comparison of In Structure Response Spectra for Mixed Mesh Models; Wall along X Axis; Y Direction Analysis

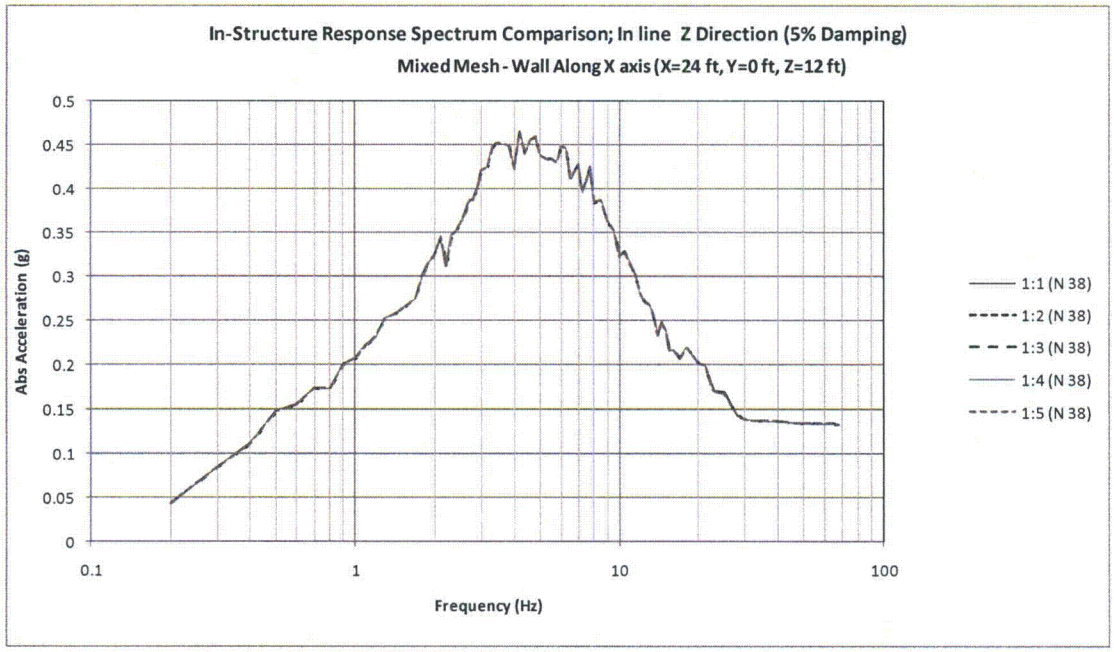

Figure 03.07.02-29.73: Comparison of In Structure Response Spectra for Mixed Mesh Models; Wall along X Axis; Z Direction Analysis

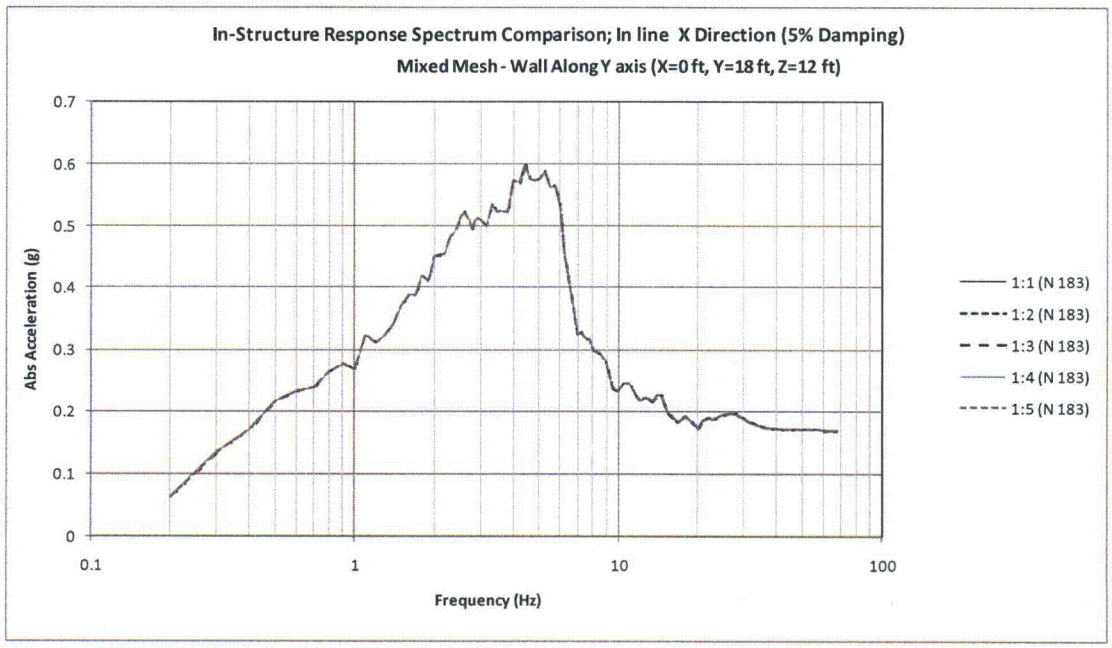

Figure 03.07.02-29.74: Comparison of In Structure Response Spectra for Mixed Mesh Models; Wall along Y Axis; X Direction Analysis

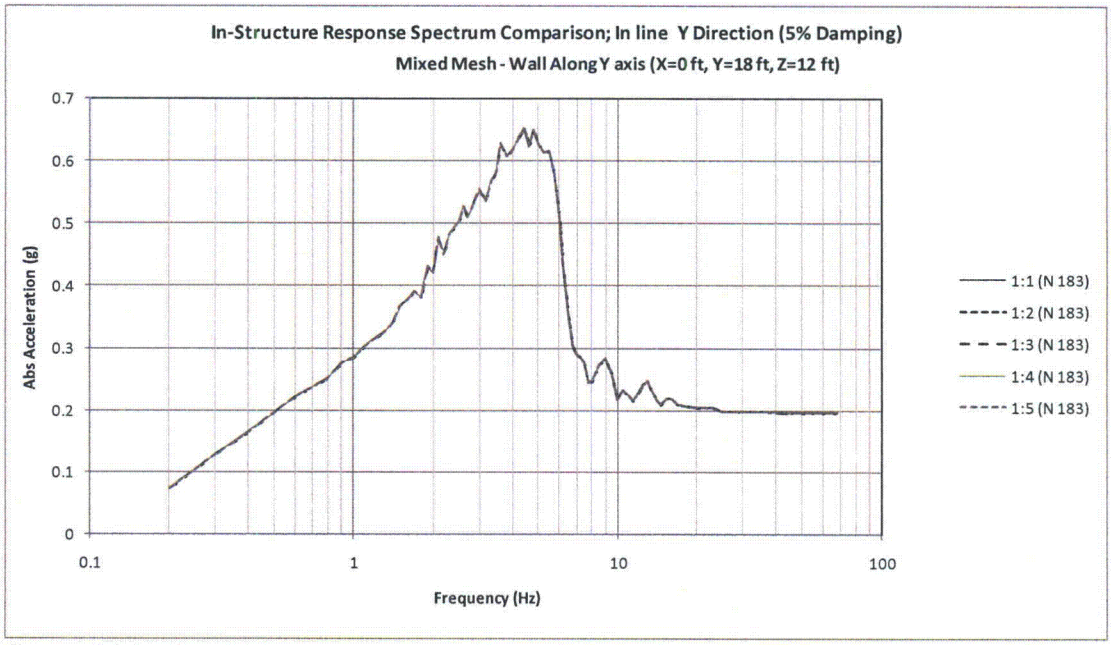

Figure 03.07.02-29.75: Comparison of In Structure Response Spectra for Mixed Mesh Models; Wall along Y Axis; Y Direction Analysis

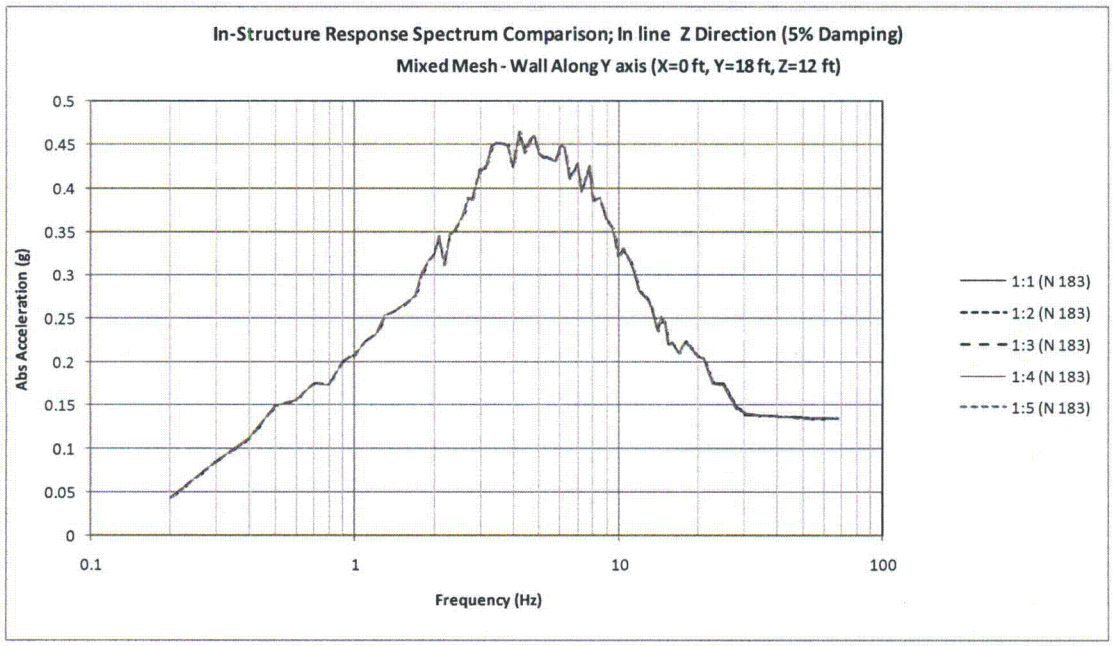

Figure 03.07.02-29.76: Comparison of In Structure Response Spectra for Mixed Mesh Models; Wall along Y Axis; Z Direction Analysis

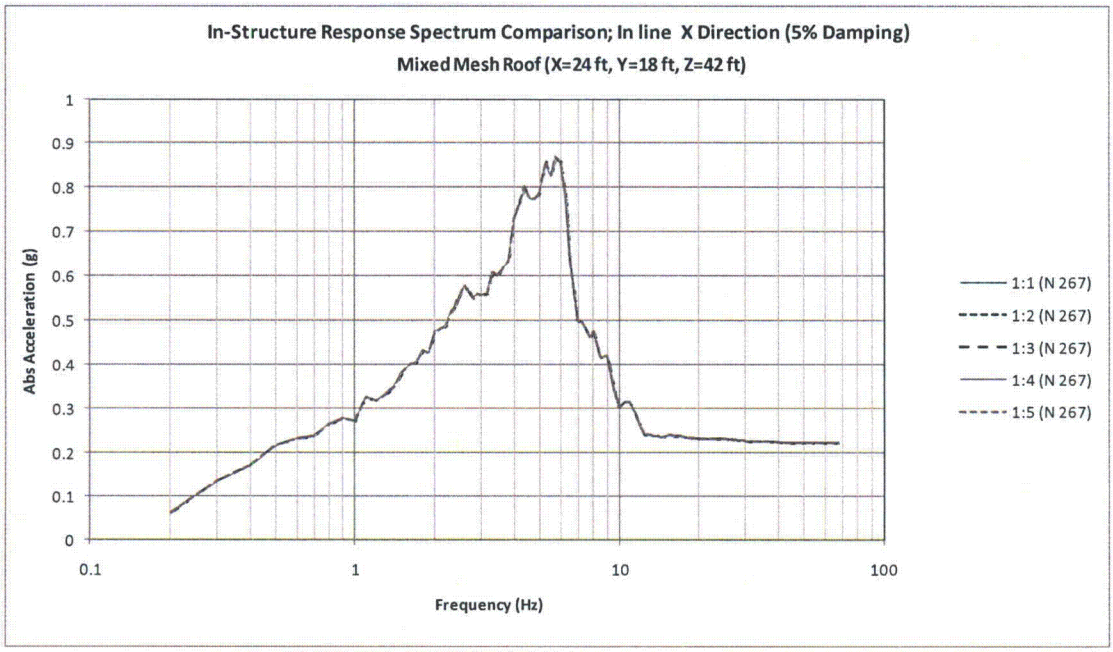

Figure 03.07.02-29.77: Comparison of In Structure Response Spectra for Mixed Mesh Models; Roof ; X Direction Analysis

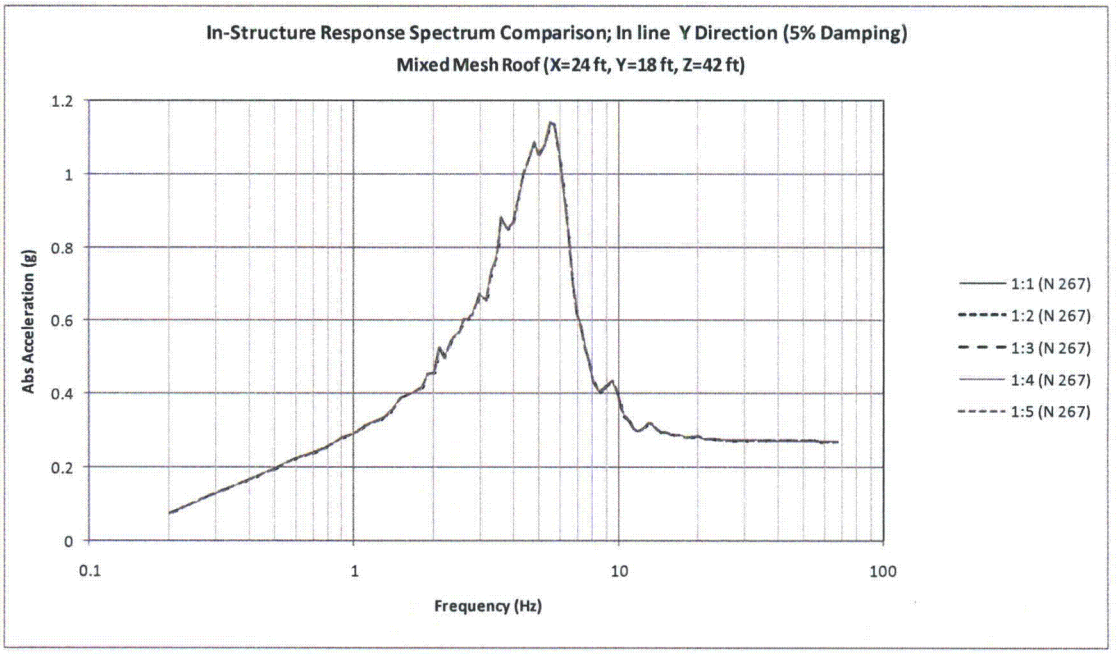

Figure 03.07.02-29.78: Comparison of In Structure Response Spectra for Mixed Mesh Models; Roof ; Y Direction Analysis

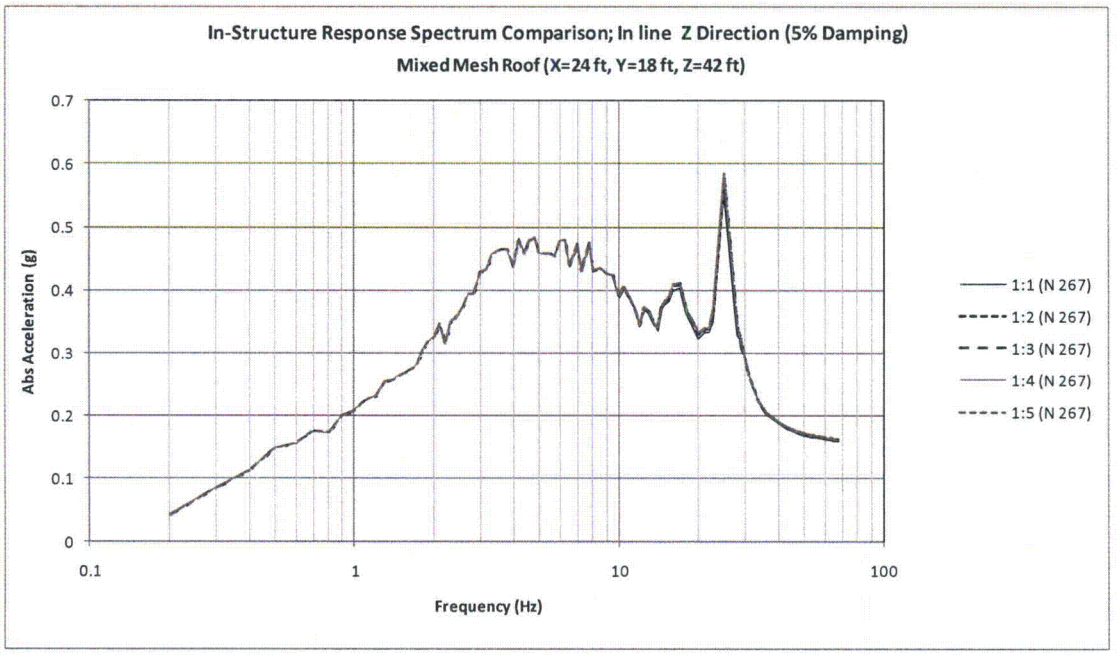

Figure 03.07.02-29.79: Comparison of In Structure Response Spectra for Mixed Mesh Models; Roof ; Z Direction Analysis

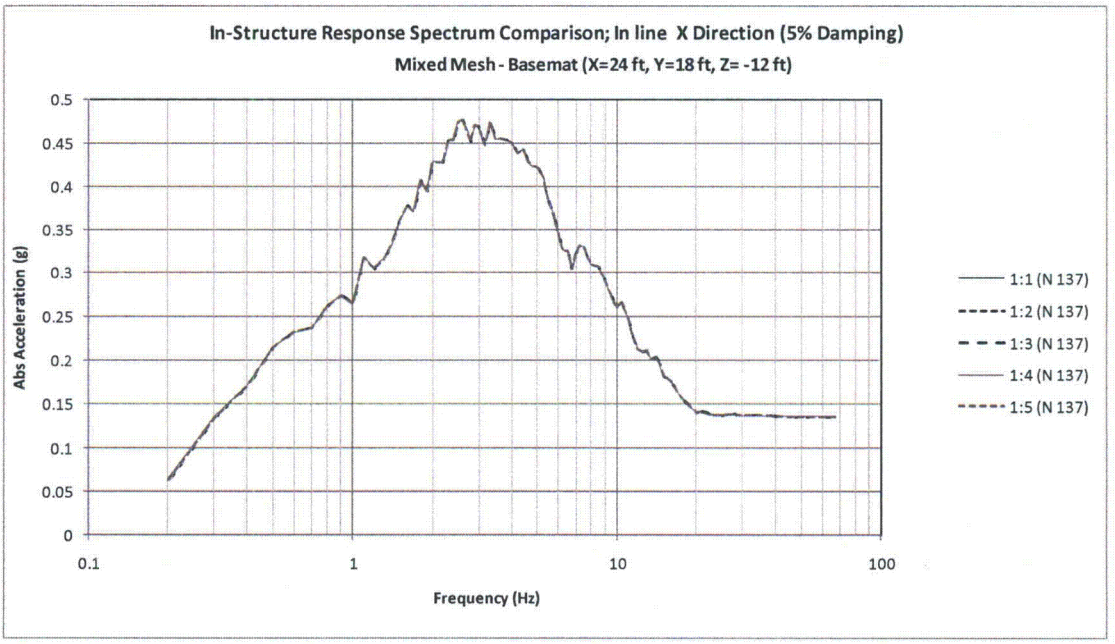

Figure 03.07.02-29.80: Comparison of In Structure Response Spectra for Mixed Mesh Models; Basemat ; X Direction Analysis

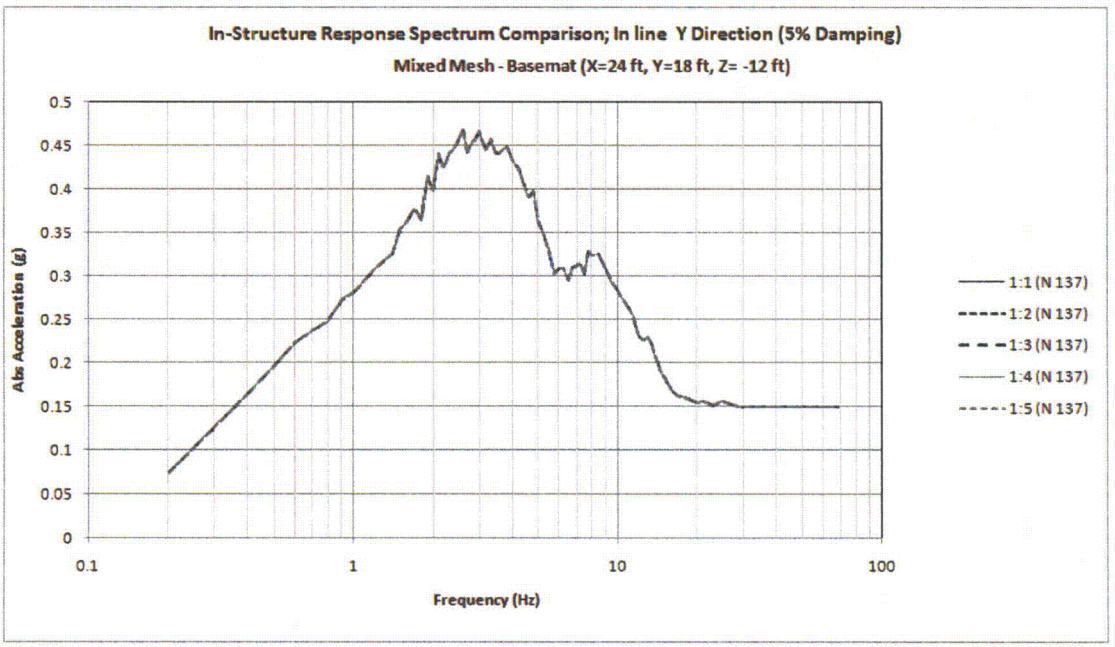

Figure 03.07.02-29.81: Comparison of In Structure Response Spectra for Mixed Mesh Models; Basemat ; Y Direction Analysis

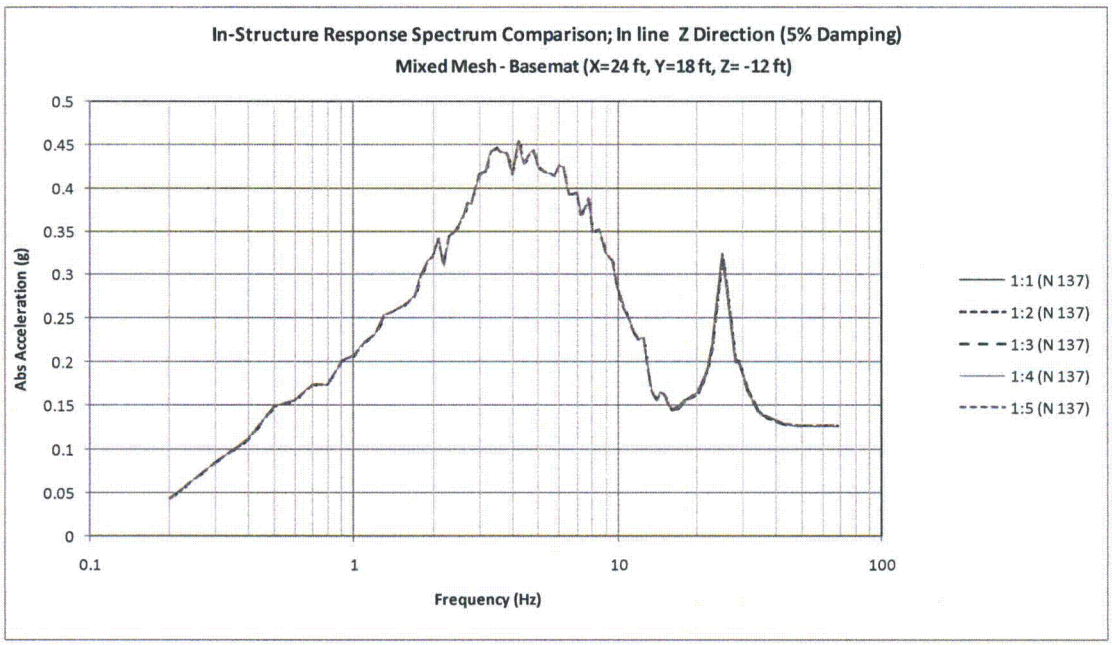

Figure 03.07.02-29.82: Comparison of In Structure Response Spectra for Mixed Mesh Models; Basemat ; Z Direction Analysis

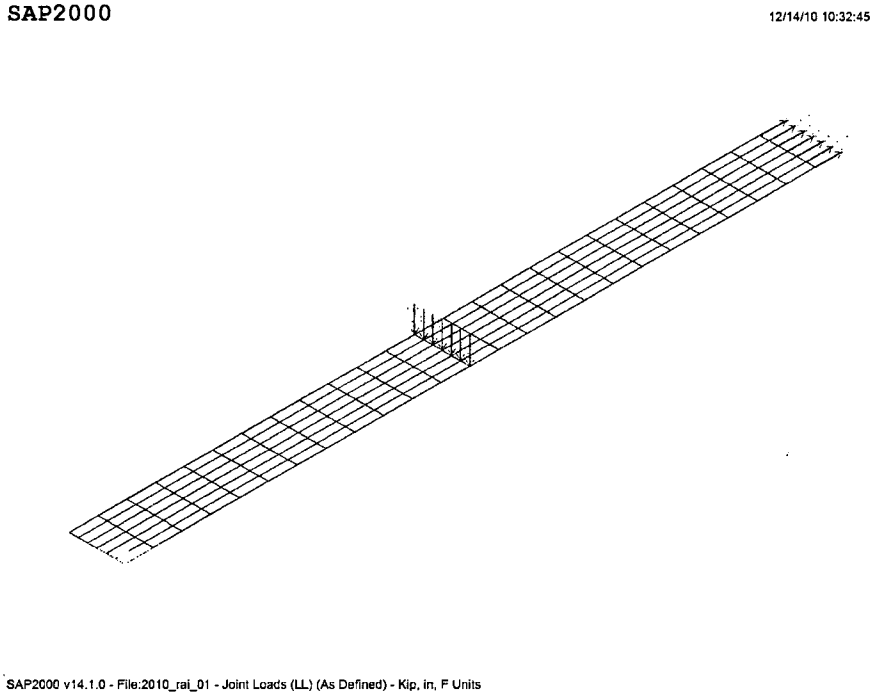

Figure 03.07.02-29.83: SAP2000 Finite Element Model for V&V of Cut Sections

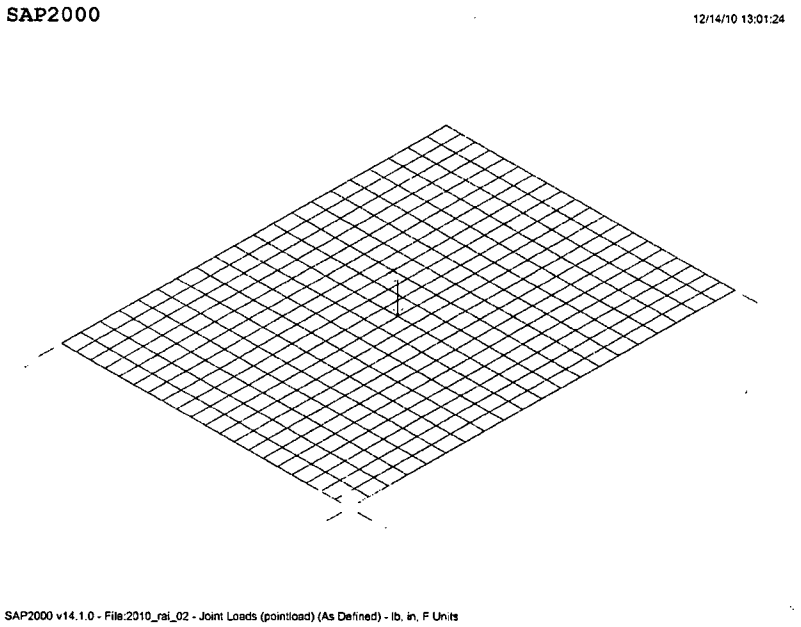

Figure 03.07.02-29.84: SAP2000 Finite Element Model for V&V of Thick Shell Element Out-of-plane Dynamic Responses

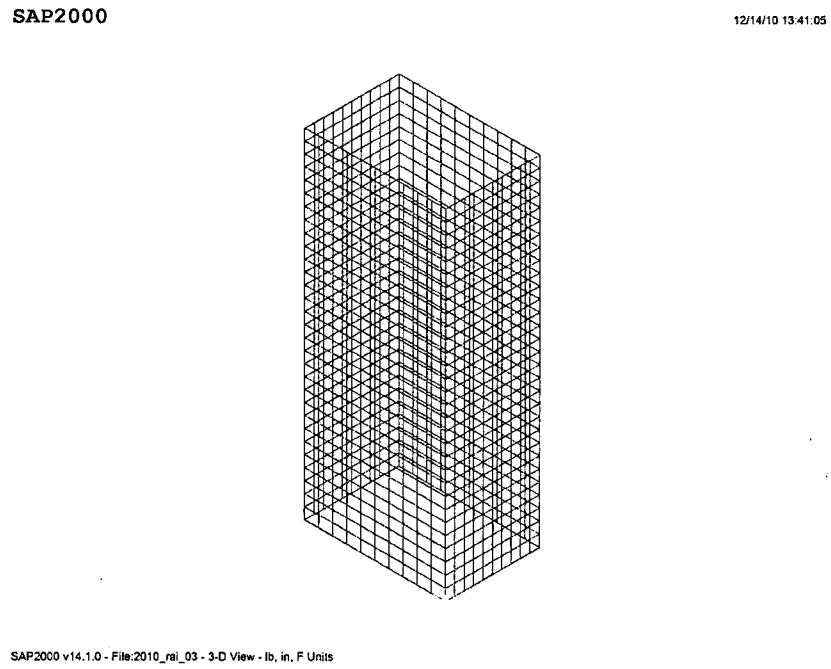

Figure 03.07.02-29.85: SAP2000 Finite Element Model for V&V of Time-history Modal Analysis of Fixed-base Structures using Shell Elements

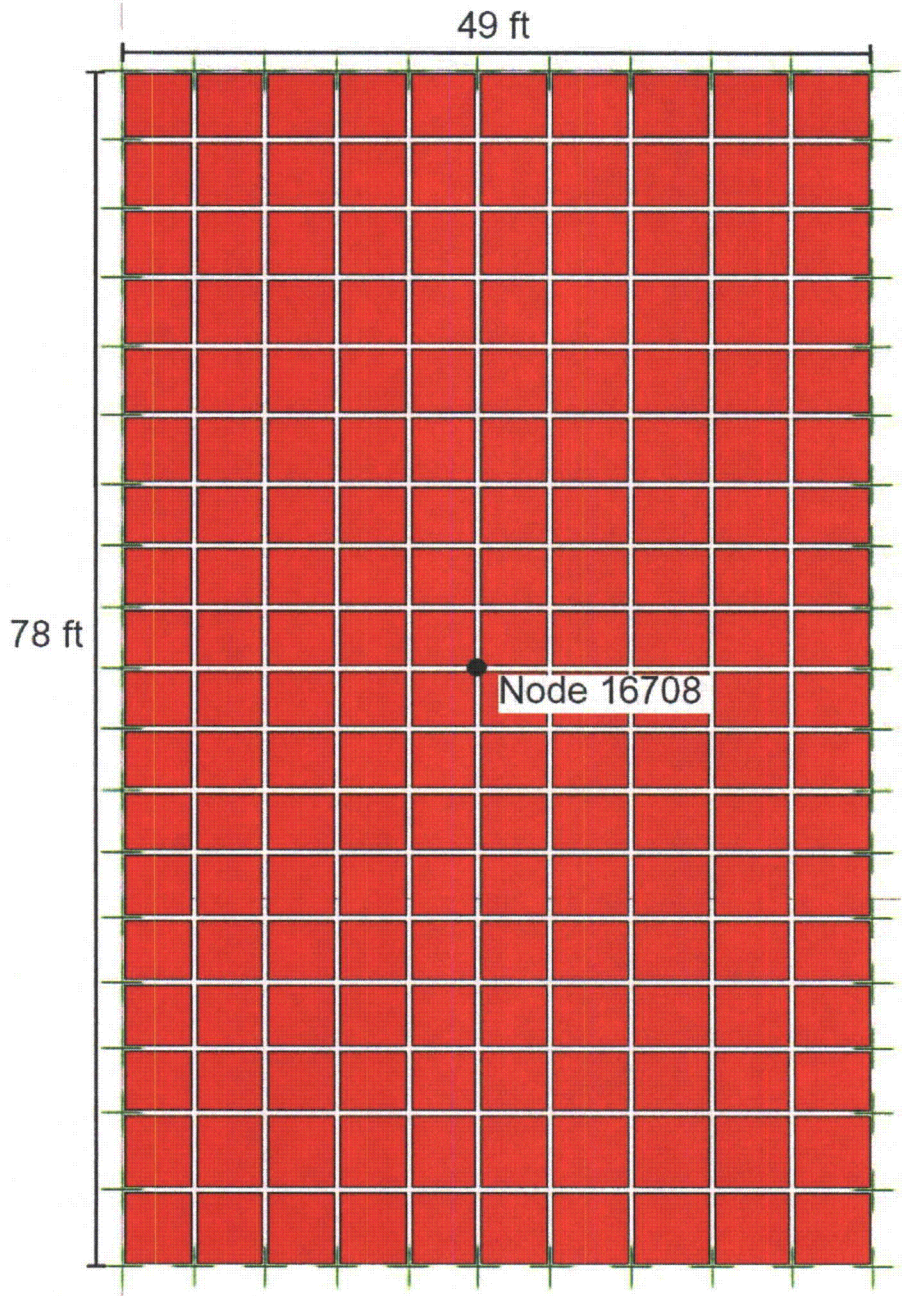

Figure 03.07.02-29.86: Finite Element Model of Slab Fixed on All Four Sides (Slab dimensions are similar to one bay of STP Pump House Roof)

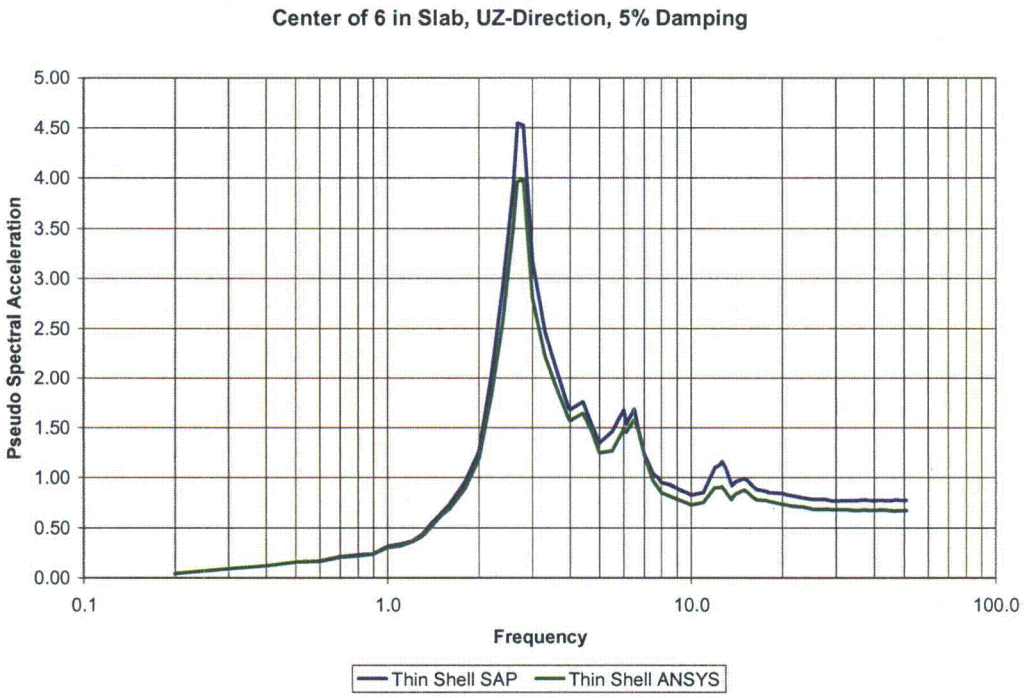

Figure 03.07.02-29.87: Spectra Comparison at Center of 6 Inch Slab (Thin Shell Elements) Using SAP2000 and ANSYS

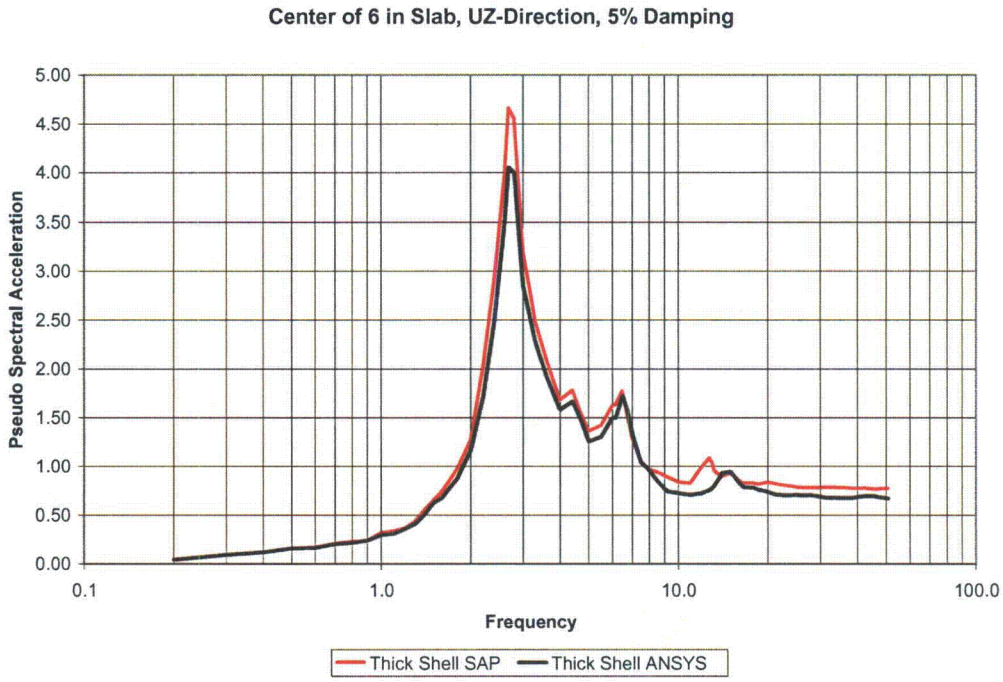

Figure 03.07.02-29.88: Spectra Comparison at Center of 6 Inch Slab (Thick Shell Elements) Using SAP2000 and ANSYS

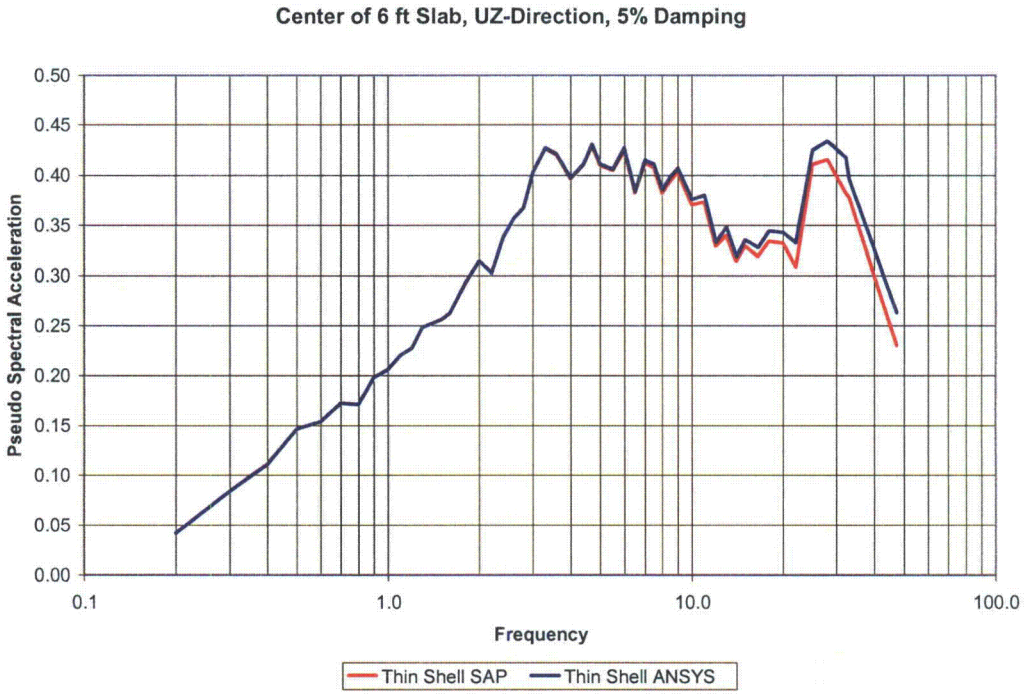

Figure 03.07.02-29.89: Spectra Comparison at Center of 6 Foot Slab (Thin Shell Elements) Using SAP2000 and ANSYS

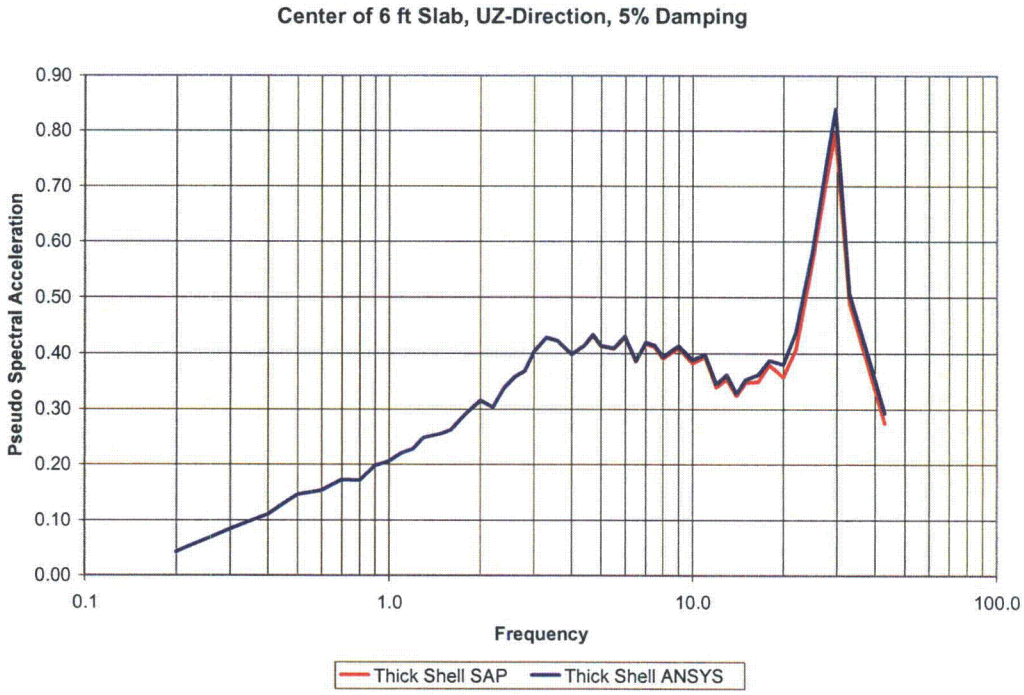

Figure 03.07.02-29.90: Spectra Comparison at Center of 6 Foot Slab (Thick Shell Elements) Using SAP2000 and ANSYS

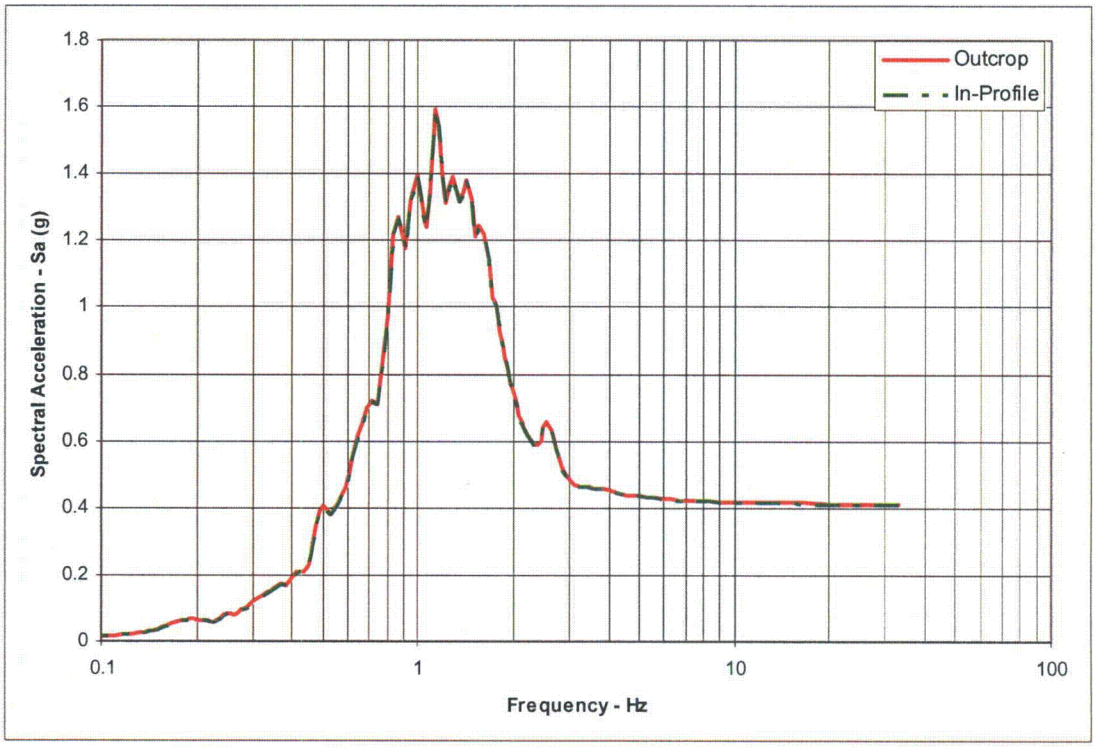

Figure 03.07.02-29.91: Comparison of 5% damped Spectra at 1 ft Below Ground Surface (SHAKE2000 116 Layer Validation Problem 3)

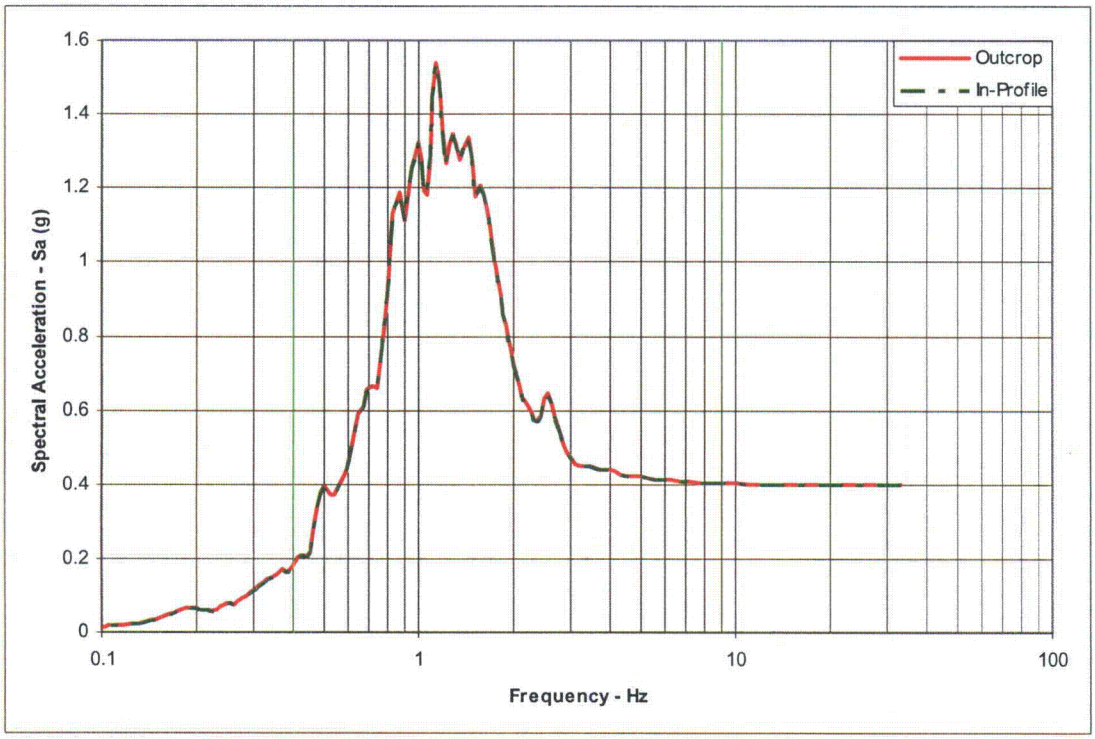

Figure 03.07.02-29.92: Comparison of 5% damped Spectra at 1 ft Below Ground Surface (SHAKE2000 116 Layer Validation Problem 4)

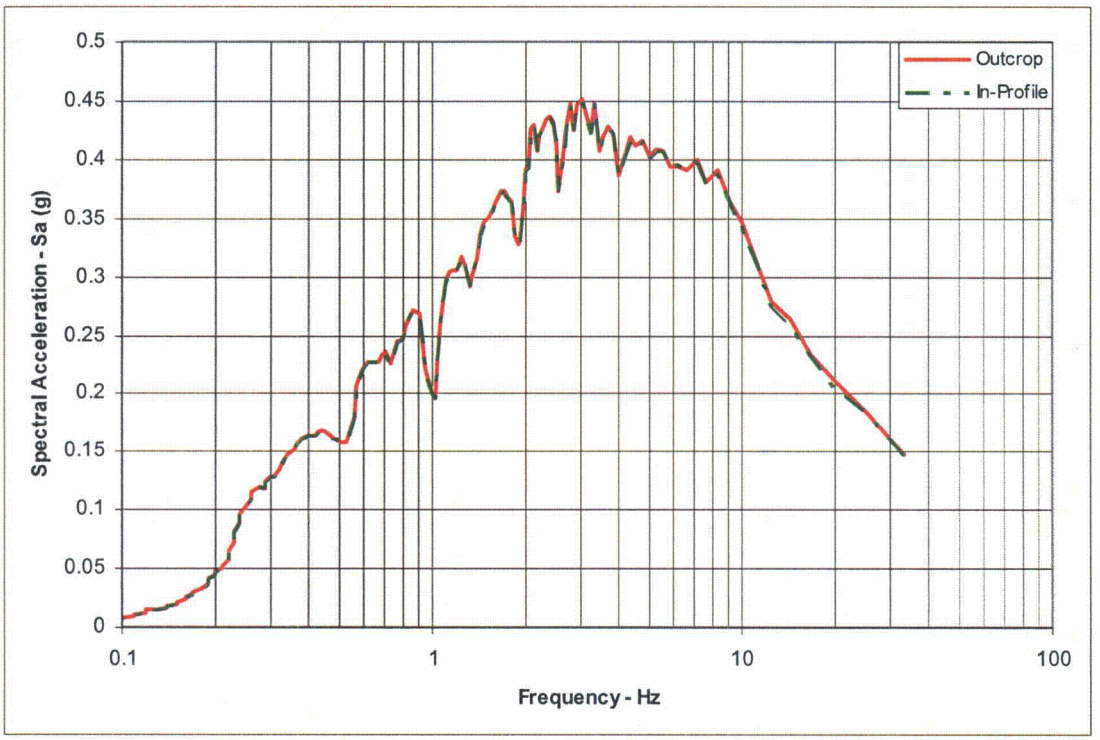

Figure 03.07.02-29.93: Comparison of 5% damped Spectra at 42 ft Below Ground Surface (SHAKE2000 116 Layer Validation Problem 5)

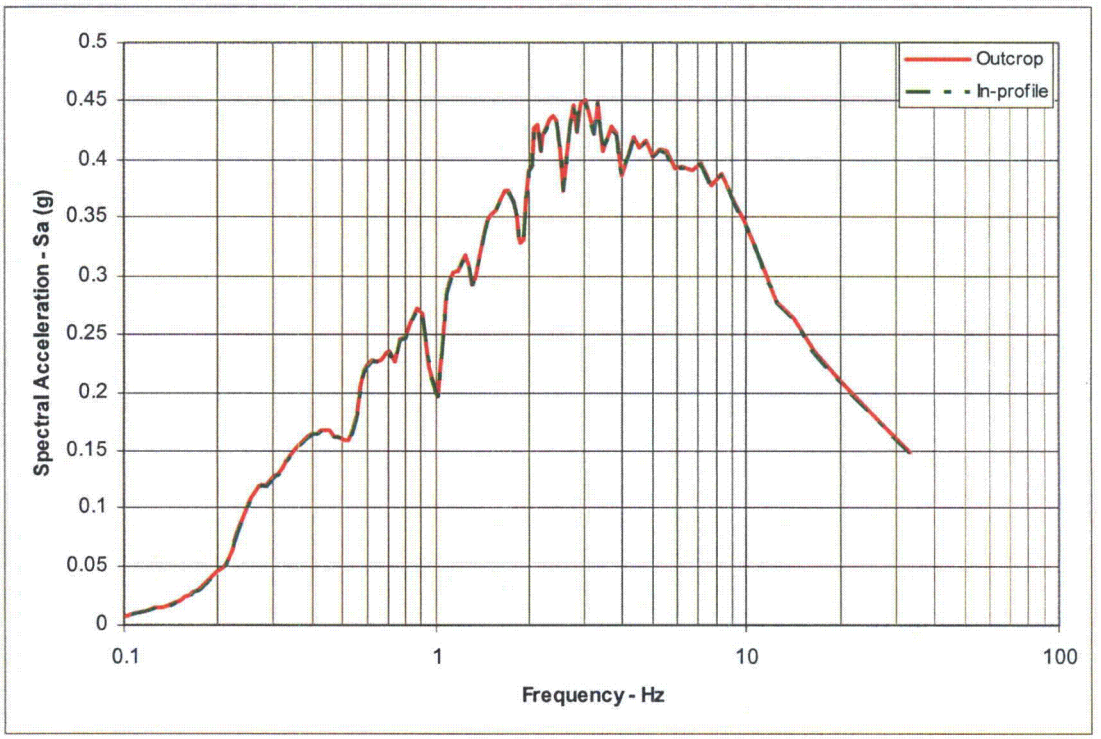

Figure 03.07.02-29.94: Comparison of 5% damped Spectra at 1 ft Below Ground Surface (SHAKE2000 116 Layer Validation Problem 6)

Enclosure 1
Revision to COLA Appendix 3C

3C.9 Free-Field Site Response Analysis (SHAKE2000 and P-SHAKE)

3C.9.1 Description

SHAKE2000 is used to perform the free-field site response analysis to generate the design- earthquake-induced strain-compatible free-field soil properties and site response motions required in the seismic SSI analysis. SHAKE2000 is a software application that integrates SHAKE, SHAKE91 and ShakEdit. SHAKE is a computer program for earthquake response analysis of horizontally layered sites developed at the University of California, Berkeley, by B. Schnabel, John Lysmer and H. B. Seed in 1972. SHAKE91 is a modified version of SHAKE for conducting equivalent linear seismic response analyses of horizontally layered soil deposits developed at the University of California, Davis, by I. M. Idriss and J. I. Sun. ShakEdit is a pre and postprocessor for SHAKE and SHAKE91 developed by Gustavo A. Ordonez.

P-SHAKE is a Bechtel proprietary modified version of SHAKE. P-SHAKE generates the same design earthquake-induced strain-compatible soil properties and site response motions as SHAKE does, and the input files of the two programs for the most part are compatible. However, P-SHAKE is built on a different program logic that allows the site response analysis to be performed with acceleration response spectrum as input instead of acceleration time histories used by SHAKE.

3C.9.2 Validation

SHAKE2000 was purchased from Gustavo A. Ordonez and validated by Sargent & Lundy~~developed by UC Berkeley~~. The program validation documentations is available at Sargent & Lundy~~are located at UC Berkeley~~.

P-SHAKE was developed by Bechtel. The program validation documents are located in Bechtel's Computation Service Library.

3C.9.3 Extent of Application

SHAKE2000 is used to generate free-field site response motions for use in seismic analysis of Category I structures, e.g., Reactor Building, Control Building and Ultimate Heat Sink.

P-SHAKE is used to provide site-specific earthquake-induced design ground motions and the associated strain-compatible soil properties for Category I structures, e.g., Reactor Building, Control Building, and Ultimate Heat Sink.

RAI 03.08.04-18, Revision 1, Supplement 2

QUESTION:

Follow-up to Question 03.08.04-2 (RAI 2964)

The applicant's response to Question 03.08.04-2 states that the Radwaste Building (RWB) will be designed in accordance with the requirements of RG 1.143, Revision 2. The applicant also discussed the design criteria for this building for seismic category II/I evaluation. In order for the staff to conclude that the Radwaste Building design meets the requirements of RG 1.143, and also meets the requirement in ABWR DCD Section 3.7.2.8, item (3), the FSAR needs to include sufficient design information for the building to demonstrate that the design meets the pertinent design criteria. Guidance provided in SRP Section 3.8.4 may be used for providing such information. Therefore, the applicant is requested to provide design information for the RWB in the FSAR that includes more detailed description of the structure; applicable codes, standards and specifications; loads and load combinations including live loads, seismic loads, thermal loads, flood loads, tornado loads, lateral soil pressure, etc.; design and analysis procedures; structural acceptance criteria; materials and quality control; design of critical sections, stability evaluation, etc.

SUPPLEMENTAL RESPONSE:

Revision 1 to this RAI response was submitted with STPNOC letter U7-C-STP-NRC-100124 on June 2, 2010. Supplement 1 to this RAI was submitted with STPNOC letter U7-C-STP-NRC-100193 dated August 19, 2010. This supplemental response provides the following based on discussions during the meetings with NRC on February 2nd and 3rd, 2011.

1. COLA mark-up for an additional load combination for the safe shutdown earthquake (SSE) loading used for seismic II/I evaluation and a figure illustrating how the loads are considered for stability evaluation.

2. Confirmation that Standard Review Plan (SRP) 3.3.2, Rev.2, July 1981, is the applicable SRP for tornado loading, as stated in Section 3H.3.4.1.

3. COLA mark-up to add the maximum static and dynamic bearing pressures and the bearing capacity under the basemat.

4. COLA reference confirming that the input motion used for seismic analysis includes the effect of the adjacent Reactor Building (RB).

Issue Response:

1. As stated in COLA Part 2, Tier 2, Section 3H.3, the design of the RWB is based on Regulatory Guide 1.143. The loads and load combinations are provided in COLA Part 2, Tier 2, Section 3H.3.4.3, including the load combinations for tornado and flood.

   Enclosure 1 of this response also includes a revision to COLA Part 2, Tier 2, Section 3H.3.5.3, to include extreme environmental load combinations for safe shutdown earthquake, to be used for the Seismic II/I evaluation, for both steel and concrete. A table that includes parameters such as seismic input motion, tornado, tornado missiles and flood that are used for design, II/I evaluations and stability evaluations of each structure is available for NRC review.

   The stability evaluations for II/I have been performed using the site specific earthquake and site specific soils and foundation materials. Enclosure 1 of this response includes revision to COLA Part 2, Tier 2 to reference the added Figure 3H.3-52 which illustrates the methodology used for the stability evaluation.

2. Calculation of tornado loading (Wt) is per NUREG-0800, SRP 3.3.2, Rev. 2. The tornado parameters (wind speed, depressurization, and missile spectrum) are per Regulatory Guide 1.143 for RW-IIa classification. The applicable revision of Regulatory Guide 1.76 is Revision 1, as stated in COLA Part 2, Tier 2, Section 3H.3.4.1.

3. COLA Part 2, Tier 2, Section 3H.3.4.2.1 provides the factors of safety against static and dynamic bearing capacity. Enclosure 1 of this response revises the COLA Part 2, Tier 2, Section 3H.3.4.2.1 to include the static and dynamic bearing pressures.

4. The effect of the adjacent RB has been considered on the input motion used for the Seismic II/I evaluation, as described in COLA Part 2, Tier 2, Section 3H.3.5.3.

RAI 03.08.04-18, Revision 1, Supplement 2
Enclosure 1

Mark-up for COLA Part 2, Tier 2, Section 3H.3

3H.3.4.2.1 Soil Parameters

- Poisson's ratio (above groundwater) 0.42
- Poisson's ratio (below groundwater) 0.47
- Unit Weight (moist) ..... 120 pcf
- Unit Weight (saturated) ..... 140 pcf
- Liquefaction potential ..... None
- Static Soil Bearing Pressure (plus weight of 2 ft of fill concrete) ..... 9.8 ksf
- Ultimate Static Soil Bearing Capacity ..... 91.1 ksf
- Static Soil Bearing Capacity Factor of Safety ..... ≥ 9.3
- Dynamic Soil Bearing Pressure ..... 11.0 ksf
- Ultimate Dynamic Soil Bearing Capacity ..... 71.4 ksf
- Dynamic Soil Bearing Capacity Factor of Safety ..... ≥ 6.5

3H.3.5.3 Seismic II/I Evaluation

The seismic II/I evaluation for the RWB is performed to ensure that the RWB will not collapse on the nearby Category I structures. The structure is conservatively designed to remain elastic for this evaluation. The earthquake input used at the foundation level is the envelope of 0.3g RG 1.60 response spectrum and the induced acceleration response spectrum due to site-specific SSE that is determined from an SSI analysis which accounts for the impact of the nearby Reactor Building (RB). In this SSI analysis, five interaction nodes at the depth corresponding to the bottom elevation of the RWB foundation are added to the three dimensional SSI model of the RB. These five interaction nodes correspond to the four corners and the center of the RWB foundation. The average response of these five interaction nodes is enveloped with the 0.3g RG 1.60 spectra to determine the SSE input at the foundation level.

For tornado parameters, including the missiles, the same parameters as those defined in DCD Tier 1 Table 5.0 are used. For flood, the extreme flood level of 40 ft (12.2 m) MSL with maximum hydrodynamic force of 44 psf is used, which is caused by the Main Coolant Reservoir dike breach.

The II/I stability evaluations for sliding and overturning are performed using the site-specific SSE and other site-specific parameters such as soil properties. Figure 3H.3-52 outlines the methodology followed for the seismic II/I stability evaluation of the RWB.

3H.3.5.3.1 Load Combinations

The following load combinations, in addition to the extreme environmental load combinations from Sections 3H.3.4.3.4 are used for Seismic II/I considerations.

3H.3.5.3.1.1 Notations

E_{SSE} = Safe Shutdown Earthquake load (as discussed in Section 3H.3.5.3 above)

Other loads are as defined in Section 3H.3.4.3.4.1.

3H.3.5.3.1.2 Structural Steel Load Combinations

$1.6S = D + L + F + H + R_o + T_o + E$

For the computation of global seismic loads, the live load is limited to the expected live load present during normal plant operation which is defined as 25% of the normal floor and roof live loads.

3H.3.5.3.1.3 Reinforced Concrete Load Combinations

$U = D + L + F + H + R_o + T_o + E$

For the computation of global seismic loads, the live load is limited to the expected live load present during normal plant operation which is defined as 25% of the normal floor and roof live loads.

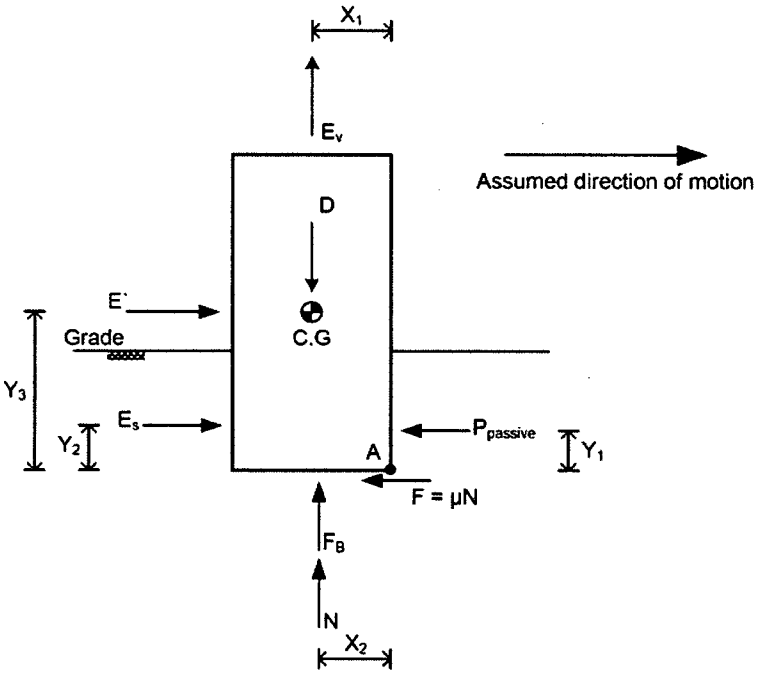

Factors of Safety against Sliding and Overturning about point A are calculated as follows:

$$SF_{sliding} = \frac{P_{passive} + F}{E_s + E`}$$

$$SF_{OT\_A} = \frac{(P_{passive})(Y_1) + (D)(X_1) - (F_B)(X_2)}{(E_s)(Y_2) + (E`)(Y_3) + (E_v)(X_1)}$$

Where:

$SF_{sliding}$ = Safety factor against sliding

SF_{OT_A} = Safety factor against overturning about "A"

D = Dead load

$P_{passive}$ = Total passive soil pressure

$F = \mu N$ = friction force and μ is the coefficient of friction

E_s = Static and dynamic soil pressure (active condition)

$E`$ = Self weight excitation in the horizontal direction

E_v = Self weight excitation in the vertical direction

F_B = Buoyancy force

N = Vertical reaction $= D - F_B - E_v$

Figure 3H.3-52: Formulations Used for Calculations of Factors of Stability Against Sliding and Overturning for Seismic II/I Considerations

RAI 03.08.04-30, Revision 1

QUESTION:

Follow-up to Question 03.08.04-23

In response to staff question requesting additional information (Letter U7-C-STP-NRC-100036, dated February 10, 2010) about how various steel and concrete elements of site-specific structures are designed, and the design results, the applicant provided some analysis and design information. The applicant also referred to the Supplement 2 response to Question 03.07.01-13 (Letter U7-C-STP-NRC-090230, dated 12/30/09) for pertinent design summary information. In order for the staff to conclude that the design of site-specific structures meet the requirements of GDC 2 by meeting the guidance provided in SRP 3.8.4 and 3.8.5, or otherwise, the applicant is requested to provide the following additional information:

1. The applicant states in the response that a three dimensional finite element analysis (FEA) is used for structural analysis and design of the UHS/RSW Pump House. FSAR Section 3H.6.6.1 states that analysis for the seismic loads was performed using equivalent static loads and the induced forces due to X, Y, and Z seismic excitations were combined using the SRSS method of combination. However, the applicant did not describe how the equivalent static loads due to seismic excitation were determined and applied to the static FEA model from the results of soil structure interaction (SSI) analysis used for determination of seismic response. Therefore, the applicant is requested to provide details of how seismic response analysis results from dynamic SSI analysis were transferred to the static FEA model, including how the effects of accidental torsion were included in the analysis and design of UHS/RSW Pump house. Please also update FSAR with the information, as appropriate.

2. The applicant stated in its response that the modulus of subgrade reaction for static loading was calculated as the average of the local values at nine locations under the foundation. The applicant is requested to provide these nine values, and explain why it is considered appropriate to use the average value. Please also explain how the foundation subgrade modulus was used for calculating nodal springs for the FEA model, and how the effect due to coupling of soil springs was considered in the analysis.

3. For seismic loading, the applicant has outlined a hand-calculated procedure that utilizes published formulas and charts to estimate the foundation spring constants. According to this procedure, the equivalent modulus and Poisson's ratio of a layered soil system are first estimated using the cumulative strain energy method. The resulting values are then used in the equations for computation of the spring constants for a rigid foundation of an arbitrary shape embedded in a uniform half-space. The shear moduli used for individual layers are strain compatible values, and include the mean, upper bound, and lower bound soil cases. The approximate procedure outlined above for developing the foundation spring constants does not take into account the pressure distribution under the base slab. Furthermore, this procedure does not account for the frequency dependence of these springs. As such, the applicant is requested to provide a

justification for not considering the effects of pressure distribution and system frequency in developing the foundation dynamic springs including describing the impact on the calculated results.

4. The applicant's response does not provide details as to how the soil springs calculated under static and seismic loadings are inputted to the 3-D static FEA model to calculate the design stresses. Therefore, the applicant is requested to describe in detail how the static and seismic soil springs are inputted into the FEA model, and how the results are obtained for stress evaluations. Specifically, the applicant is requested to explain if the two sets of springs were used in a single model, and how the two sets were combined to a single set of springs. Otherwise, if the two sets of springs were applied to separate FEA models, describe how the load combinations were performed. The applicant is also requested to provide sufficient detail to assist staff in understanding how static and seismic soil springs are used in the FEA model and results combined for stress evaluations.

5. In the FSAR mark-up of Sections 3H.6.6.3.1 and 3H.6.6.3.2 provided with the response, the applicant identifies the method used by the applicant for combining forces and moments. In this method, for each reinforcing zone, the maximum force or moment is coupled with the corresponding moment or force for design for the same load combination. It is not clear if this method of combining forces and moments for design will envelop the worst combination of forces and moments for all elements in a reinforcing zone. Therefore, the applicant is requested to describe the method of combining forces and moments used by the applicant with a typical example of a reinforcing zone, and demonstrate that this method of combination will yield the worst combination of forces and moments that should be considered for design.

6. The staff notes that in the FSAR mark-up of Section 3H.6.6.3.1 provided with the response, the reported values of soil springs for the RSW Pump House are significantly larger than those for the UHS basin. The applicant is requested to confirm these values, and explain the reason for the large difference.

7. The response did not include any information about the maximum static and dynamic bearing pressures under the foundations of UHS/RSW Pump House. The applicant is requested to provide the maximum static and dynamic bearing pressure under the foundations of UHS/RSW Pump House, compare these values with the maximum allowable static and dynamic bearing pressures, and include this information in the FSAR.

8. In its response to Question 03.07.01-19 (letter U7-C-STP-NRC-100129, dated June 7, 2010), the applicant provided analysis and design information for the seismic category I Diesel Generator Fuel Oil Storage Vault (DGFOSV) which was not previously included in the FSAR. The information included in the response does not describe how structural analysis and design of the structure was performed. Also, reference is made to FSAR Section 3H.6.4 for design loads. FSAR Section 3H.6.4 has been updated several times in various responses, and it is not clear where this information can be found. Therefore, the

applicant is requested to provide complete structural analysis and design information for the DGFOSV to ensure it meets acceptance criteria 1 through 7 of SRP 3.8.4 and 3.8.5. The staff needs this information to conclude that the DGFOSV is designed to withstand seismic loads and meet GDC 2. Include in the response an updated version of Appendix 3H where structural analysis and design information for all seismic category I structures can be found.

9. While reviewing this response, and other responses referenced in this response, the staff noted that the applicant has used different values of coefficient of friction for sliding stability evaluation; e.g., the value 0.3 was used for the RSW Pump House, 0.4 was used for UHS basin, 0.58 was used DGFOSV, and for the Reactor Building (RB) and the Control Building (CB), it was stated to be more than 0.47. It is not clear if these values are the required coefficient of friction, or the minimum coefficient of friction available. The applicant is requested to clearly specify the minimum coefficient of friction at various locations of the site, if they are different, and explain how these values were determined. Please also clarify this information in the FSAR.

10. The staff noted references to Diesel Generator Fuel Oil Tunnel (DGFOT) in several RAI responses. Please confirm that DGFOT is not a seismic category I structure, and if it is seismic category I, include the analysis and design information to show how the design of the DGFOT meets the acceptance criteria 1 through 7 in the SRP 3.8.4 and 3.8.5 in the FSAR.

REVISED RESPONSE:

The original response to Parts 8, 9 and 10 of this RAI was submitted with STPNOC letter U7-C-STP-NRC-110008, dated January 17, 2011 which provided the analysis and design results for the Diesel Generator Fuel Oil Storage Vaults (DGFOSV) and the Diesel Generator Fuel Oil Tunnels (DGFOT). The response to Parts 1 through 7 of this RAI is included in Supplement 1 to this RAI response, being submitted concurrently with this response.

This revision to the original response provides the following:

- The structural analysis and design results provided in Table 3H.6-11 of the original response are revised in this revised response due to a discrepancy found in the supporting calculation (See Enclosure 3).

- Enclosure 4 includes mark-ups for Section 3H.7 to provide additional clarification on the design of the DGFOT. It also includes a discussion on Section 3H.7.5.2.4 based on discussions during the meetings with NRC on February 2nd and 3rd, 2011.

- Table 3.2-1 is included in Enclosure 5. This table is revised to include the DGFOSV.

The revisions are indicated by revision bars in the margin.

In addition the following COLA mark-ups are provided based on discussions during the NRC audit performed during the week of October 18, 2010.

- Mark-up for Section 3.7.2.8 provides a summary of the seismic input motion used for seismic II/I evaluation of Non-Seismic Category I structures (see Enclosure 1).

- Mark-up for Section 3.8.6.1 clarifies that the minimum required coefficient of friction for waterproof membrane is determined based on sliding stability of the structure considering the site-specific SSE motion (Enclosure 2)

8. The following response is broken into sub-sections a through g to address the design of the Diesel Generator Fuel Oil Storage Vaults (DGFOSV).

   a) Soil-Structure Interaction Analyses:

   The structural analysis and design of the Diesel Generator Fuel Oil Storage Vault (DGFOSV) described in the response to RAI 03.07.01-19, Revision 2 (submitted with letter U7-C-STP-NRC-100129, dated June 7, 2010), has been revised.

   The revised soil-structure interaction (SSI) analyses for generation of in-structure response spectra considering both full and empty fuel oil tanks, and the two (2) new two-dimensional (2D) structure-soil-structure interaction (SSSI) analyses for obtaining seismic soil pressures were provided in the response to RAI 03.07.01-27, Supplement 1, Revision 1, submitted with NINA letter U7-C-NRC-NINA-110042, dated March 7, 2011.

   b) Equivalent Static Method Used for Design:

   The design of the DGFOSVs has been revised. In the revised design, the seismic loads are conservatively determined using the equivalent static method described below.

   The structural analysis and design of the Diesel Generator Fuel Oil Storage Vault (DGFOSV) was performed using a finite element analysis (FEA). The finite element model (FEM) for this FEA is shown in COLA Part 2, Tier 2 Figure 3H.6-140. The maximum nodal accelerations from the SSI analysis in the X, Y, and Z direction for the subgrade and above grade roofs were averaged and used as the accelerations in the X, Y, and Z directions for the entire structure to obtain the equivalent static seismic loads. The induced forces due to the X, Y, and Z seismic excitations were combined using the square-root-sum-of-squares (SRSS) method.

   In order to demonstrate that the above equivalent static method is conservative, the seismic in-plane shear forces, axial forces and in-plane moments for the shear walls of this structure from the equivalent static method and those from the SSI analyses were compared at a section cut just above the basemat (see Figure 03.08.04-30.1 for location of this section cut). Tables 03.08.04-30.1 and 03.08.04-30.2 provide the results of this comparison. As seen from these tables, the use of equivalent static method for determination of seismic loads yields seismic loads in excess of those from the SSI analyses. Thus, use of the equivalent static method is conservative.

The design of the DGFOSV meets Acceptance Criteria 1 through 7 of Standard Review Plans 3.8.4, Revision 2, and 3.8.5, Revision 2, as noted in the referenced sections of COLA Part 2, Tier 2 and the COLA mark-ups provided in Enclosure 3 of this response as described below:

1. Description of the Structures and Foundation: Refer to COLA Part 2, Tier 2, Section 3H.6.7 and Section 3H.6.7.3 provided in Enclosure 3.
2. Applicable Codes, Standards and Specifications: Refer to Section 3H.6.7.1 provided in Enclosure 3.
3. Loads and Load Combinations: Refer to Section 3H.6.7.1 provided in Enclosure 3.
4. Design and Analysis Procedures: Refer to Section 3H.6.7.2 provided in Enclosure 3.
5. Structural Acceptance Criteria: Refer to COLA Part 2, Tier 2, Section 3H.6.4.3.4.
6. Materials, Quality Control and Special Construction Techniques: Refer to Section 3H.6.7.1 provided in Enclosure 3 and COLA Part 2, Tier 2, Section 3H.5.6.
7. Testing and Inservice Surveillance Requirements: Testing and inservice surveillance requirements are not applicable to the DGFOSVs.

c) Design Loads and Load Combinations:

The loads and load combinations used for the design of DGFOSVs are in accordance with those described in COLA Part 2, Tier 2 Section 3H.6.4.3.

d) Foundation and Soil Springs

The foundation for the DGFOSV consists of a reinforced concrete mat and a lean concrete mud mat. The basemat deflections due to the flexibility of the basemat and supporting soil were accounted for through the use of foundation soil springs in the SAP2000 FEA models. Both the Winkler Method and the Pseudo-Coupled Method were used to model the foundation soil springs, and the results of the two analyses were enveloped for design purposes. Additional information on these two methods for modeling of the foundation soil springs is provided in the response to RAI 03.08.05-4, Supplement 1, submitted with STPNOC letter U7-C-STP-NRC-100248, dated November 17, 2010.

In addition, two different subgrade reactions (soil spring constants) are used, one for seismic loads and one for non-seismic loads. The following soil spring constants were used in the FEA models of the DGFOSVs:

Vertical springs (with static loads).....60 kips/ft/ft^2
Vertical springs (with seismic loads).....314 kips/ft/ft^2
North-south springs (with static and seismic loads).....229 kips/ft/ft^2
East-west springs (with static and seismic loads).....213 kips/ft/ft^2

e) Uplift

The SAP2000 finite element models were checked for uplift effects by reviewing the joint reaction at the basemat. It was determined that under seismic loading the DGFOSV experiences uplift. Using the 100%, 40%, 40% rule for combination of three seismic

excitations, non-linear analysis was run on each model with uniform Winkler soil springs and pseudo-coupled soil springs to determine an enveloping adjustment factor for forces and moments from the linear analysis for the foundation mat and the connecting walls. The non-linear analysis iterates multiple times removing soil springs that go into tension during each iteration until no soil springs are in tension. For the directional earthquake loading required for the nonlinear analysis, the DGFOSV critical loading, a safe shutdown earthquake (SSE) from the southwest in combination with static active and passive loads for SSE, is considered (See Figure 03.08.04-30.2 for a schematic view of the directional seismic load).

Comparing resultant foundation mat and wall reactions from the linear analysis with mat and wall reactions from the nonlinear analysis, there is a maximum reaction increase of approximately 67% for the foundation mat shear and axial forces, 17% increase for the foundation mat bending moments, and 6% increase for the connecting walls shear forces, axial forces, and bending moments (enveloping cases with Winkler and pseudo-coupled soil springs) in the nonlinear analysis. To account for this, the resulting forces and moments from the linear analyses were adjusted by applying an increase factor of 1.67 to all forces in the foundation mat, an increase factor of 1.17 to all moments in the foundation mat, and an increase factor 1.06 to all forces and moments in the connecting walls for the DGFOSV design.

f) Stability

Detailed stability evaluations were performed for sliding, overturning, and flotation as described in response to RAI 03.07.01-19, Revision 2 (letter U7-C-STP-NRC-100129, dated June 7, 2010). For sliding and overturning evaluations, the 100%, 40%, 40% rule was used for consideration of the X, Y, and Z seismic excitations. Since the orientation of the DGFOSVs in the horizontal plane can be along the East-West or North-South axes, the horizontal seismic values used in the stability calculation envelope the SSI accelerations in the X and Y directions. The stability safety factors considering the revised SSI analyses are provided in Table 3H.6-12 (see Enclosure 3).

g) Design Results:

The strength design criteria of ACI 349-97, as supplemented by RG 1.142, were used for the design of the reinforced concrete elements of the DGFOSV. Concrete with minimum compressive strength of 4.0 ksi (27.6 MPa) and reinforcing steel with yield strength of 60 ksi (414 MPa) are considered in the design.

Due to difference in soil spring constants for seismic and non-seismic loads, the FEA analyses for the non-seismic loads and equivalent static seismic loads were run on different FEA models and the results from these models were combined and adjusted per paragraph (e) above outside the SAP2000 model to obtain the combined total design forces and moments for the seismic load combinations.

The revised design forces and provided reinforcement for the DGFOSV walls and slabs are shown in Table 3H.6-11 included in Enclosure 3. Each face and each direction of each wall and slab has a corresponding longitudinal reinforcement zone figure. Each wall and slab also

has a corresponding transverse shear reinforcement zone figure where transverse shear reinforcement is required. The reinforcement zone figures (Figure 3H.6-142 through 3H.6-208 included in Enclosure 3) show the various zones used to define the provided reinforcement based on the finite element analysis results. Actual provided reinforcement, based on final rebar layout, may exceed the reported provided reinforcement and the zones with higher reinforcement may be extended beyond their reported zone boundaries.

The shell forces from every element for every load combination in the finite element analysis were evaluated to determine the provided reinforcement in each reinforcement zone. For each reinforcement zone, the following out-of-plane moment and axial force coupled with the corresponding load combination are reported in Table 3H.6-11 (see Enclosure 3):

- The maximum tension axial force with the corresponding moment acting simultaneously from the same load combination.
- The maximum compression axial force with the corresponding moment acting simultaneously from the same load combination.
- The maximum moment that has a corresponding axial tension acting simultaneously in the same load combination.
- The maximum moment that has a corresponding axial compression acting simultaneously in the same load combination.

For each reinforcement zone, the following in-plane and transverse shears with the corresponding load combination are reported in Table 3H.6-11 (see Enclosure 3):

- The in-plane shear is the maximum average in-plane shear along a plane that crosses the longitudinal reinforcement zone.
- The transverse shear is the maximum average transverse shear along a plane in that transverse reinforcement zone.

The provided longitudinal reinforcing for each face and each direction is determined based on the out-of-plane moments, axial forces, and in-plane shears occurring simultaneously for every load combination.

The provided transverse shear reinforcing (as required) is determined based on the transverse shears and axial forces perpendicular to the shear plane occurring simultaneously for every load combination.

The DGFOSV below grade roof was designed with composite steel beams and concrete slabs for vertical loading. The composite beams span in the SAP2000 model Y-direction with the concrete slab designed as spanning one-way between the composite beams. The below grade roof slab acts as a diaphragm to transfer lateral loads. The provided reinforcing for the below grade roof slab is reported in Table 3H.6-11 (see Enclosure 3).

A Reviewers Guide for Section 3H will be made available upon completion of the changes affecting this section.

9. Sliding Stability Evaluations

Ultimate Heat Sink (UHS)/Reactor Service Water (RSW) Pump House:

The sliding stability of the UHS/RSW Pump House against sliding, overturning and flotation was re-evaluated considering the latest SSI analyses described in the response to RAI 03.07.02-24, Supplement 2, submitted with STPNOC letter U7-C-STP-NRC-100268, dated December 14, 2010 considering both full and empty basin conditions. The UHS/RSW Pump House considering a full basin condition was found to be stable against sliding without utilizing any passive pressure. The UHS/RSW Pump House considering an empty basin condition was found to be stable against sliding by engaging some passive pressure. The at-rest coefficients of friction considered for these stability evaluations were 0.3 for RSW Pump House and 0.4 for UHS Basin. The available at-rest (static) coefficient of friction based on tangent of the soil friction angle (phi) is 0.70.

DGFOSV:

The DGFOSV sliding stability evaluation was based on mobilization of passive pressure using a sliding coefficient of friction of 0.39, which is equal to two-thirds of the minimum available at-rest (static) coefficient of friction of 0.58. The available at-rest (static) coefficient of friction of 0.58 is based on tangent of the soil friction angle (φ).

Control Building:

The Control building stability evaluation is based on mobilization of passive pressure using a sliding coefficient of friction of 0.47, which is equal to two-thirds of the minimum available at-rest (static) coefficient of friction of 0.70. The available at-rest (static) coefficient of friction of 0.70 is based on tangent of the soil friction angle (φ).

Reactor Building:

Please see the response to part 4 of RAI 03.08.04-28, Revision 1, submitted with NINA letter U7-C-NINA-NRC-110042, dated March 7, 2011.

10. The layout of the Diesel Generator Fuel Oil Tunnels (DGFOTs) is as shown in COLA Part 2, Tier 2 Figure 3H.6-221 provided in response to Part 1(a) of RAI 03.07.01-27, Supplement 1, Revision 1, submitted with NINA letter U7-C-NINA-NRC-110042 dated March 7, 2011. There are three (3) reinforced concrete DGFOTs approximately 50 ft, 200 ft, and 220 ft long for each unit. Each DGFOT is connected at one end to the Reactor Building (RB) and at the other end to a Diesel Generator Fuel Oil Storage Vault (DGFOSV). There is a seismic gap between each of the DGFOT and the adjoining RB and DGFOSV. For magnitude of the required and provided seismic gaps at interface of DGFOTs and the adjoining RB and

DGFOSVs, see the Supplement 1, Revision 1 response to RAI 03.08.04-31 submitted with NINA letter U7-C-NINA-NRC-110008, dated January 31, 2011.

Each DGFOT has two access regions which extend above grade; one access region is located where the tunnel interfaces with the DGFOSV and another where the tunnel interfaces with the RB. The top of the DGFOT is located at grade. Any fuel leak from the fuel oil lines or water infiltration within the tunnels will be collected in a sump and removed by pumps. The access regions provide access to the below grade portions of the DGFOTs during maintenance and inspection. The overall above grade dimensions of the access regions are approximately 7.5 ft wide by 7.5 ft long and 15 ft high.

For details of the soil-structure interaction (SSI) analysis for generation of in-structure response spectra and structure-soil-structure (SSSI) analysis for determination of seismic soil pressures, see the Supplement 2, Revision 1 response to RAI 03.07.01-27 submitted with NINA letter U7-C-NINA-NRC-110042, dated March 7, 2011.

The DGFOTs are Seismic Category I structures. The structural analysis and design of the DGFOT is performed using a three-dimensional (3D) SAP 2000 finite element analysis (FEA) with shell elements representing the walls, slabs and mat. The foundation soil is represented by vertical and horizontal springs. The FEA finite element model (FEM) is shown in Figure 3H.7-1 (see Enclosure 4).

The DGFOT No. 1B, which is the shortest tunnel, running approximately 50 ft between the RB and DGFOSV No. 1B, has a wall thickness of 2'-0" on both sides. The interior below grade dimensions of this tunnel are approximately 7 ft high by 3.5 ft wide. The other two longer DGFOTs (approximately 200 ft and 220 ft long) have a wall thickness of 2'-0" on one side and 2'-6" on the other side to allow for placement of embedded conduits. The interior below grade dimensions of these tunnels are approximately 7 ft high by 3 ft wide. DGFOT No. 1B, with a wall thickness of 2'-0" on both sides and shorter tunnel length for resisting torsion effects, is selected as the critical tunnel for the FEA.

The Safe Shutdown Earthquake (SSE) design forces (E') are conservatively determined using equivalent static seismic loads. The mass of the structure, equipment weights, and seismic live loads are excited in the X, Y, and Z directions using the enveloping maximum nodal accelerations in the X, Y, and Z directions from the soil-structure interaction (SSI) analysis. A comparison between the maximum accelerations from the SSI analysis and the design accelerations for the DGFOT shows the design accelerations envelope the SSI analysis accelerations. The comparison is provided in Table 03.08.04-30.3. The resulting element forces and moments due to X, Y, and Z excitations are combined using the SRSS method.

Figures 3H.7-5 through 3H.7-8 (see Enclosure 4) show a comparison of the SSI soil pressures, the SSSI soil pressures, the ASCE 4-98 soil pressures and the total enveloping soil pressure used in design on the walls of the DGFOT.

The codes and standards used for the design of the DGFOT are as outlined in Section 3H.7.4.1 provided in the COLA mark-ups in Enclosure 4 of this response. The loads and load combinations are as noted in Section 3H.7 provided in the COLA mark-ups in

Enclosure 4 of this response.

Additionally, the axial strain on the DGFOT due to SSE wave propagation is determined based on the equations and commentary outlined in Section 3.5.2.1 of ASCE 4-98. The maximum curvature is computed based on Equation 3.5-3 in Section 3.5.2.1.3 of ASCE 4-98. The forces at bends due to SSE wave propagation are determined based on Section 3.5.2.2 of ASCE 4-98. The forces at tunnel bends are included as additional loads in the SAP2000 models.

Multiple SAP2000 FEA models were created to represent different conditions and load combinations for the DGFOTs. Additional information on the SAP2000 models is documented in Section 3H.7.5.1 (see Enclosure 4). The following is a breakdown of the different FEA models:

1. Normal (Operating Condition, Heavy Load Condition, and Flood Load Condition):

   The purpose of these models is to consider the effects of operating load conditions (i.e. dead loads, minimum live loads, etc.), the heavy load condition (when heavy vehicles and cargo are moved across the top of the tunnel), and the flood load condition (the extreme flood loads due to a MCR breach).

2. SSE (SSE loads without SSE Wave Propagation):

   The purpose of these models is to consider the effects of SSE loads without the effects of the SSE wave propagation, which are considered in a separate model. The dead loads, live loads, soil loads, and accidental eccentricity loads are applied to the static (non-seismic) model. The SSE loads are combined using the SRSS method in the dynamic (seismic) model.

3. SSE (SSE loads with SSE Wave Propagation per ASCE 4-98):

   The purpose of these models is to consider the effects of SSE loads with the effects of the SSE wave propagation and additional forces and moments due to bends in the tunnel per ASCE 4-98. The dead loads, live loads, soil loads, accidental eccentricity loads, SSE wave propagation loads and additional forces and moments due to bends in the tunnel are applied to the static (non-seismic) model. The SSE loads are combined using the SRSS method in the dynamic (seismic) model.

4. Tornado Missile:

   The purpose of these models is to consider the effects of tornado missiles. The full tornado load combinations, outlined in Section 3H.7.4.3.4.2 (see Enclosure 4) are applied to the model considering a vertical tornado missile. The results of this SAP2000 model are combined with those from a manual calculation which considers the full tornado load combination and a horizontal tornado missile.

5. Effect of Uplift:

   The purpose of this model is to consider the effects of uplift on the basemat during a seismic event. All loads are simultaneously applied to a single static model.

The models described above are developed to determine the reinforcement required for their specific loading conditions. The results are post-processed as described in Section 3H.7.5.3.1 (see Enclosure 4).

The required reinforcement (longitudinal, in-plane shear and transverse) reported in Table 3H.7-1 (see Enclosure 4) is based on the envelop of the required reinforcement determined from all the SAP2000 FEA analyses and the required reinforcement determined via the manual calculation for the full tornado load combination.

The stability of the DGFOT is evaluated for the various load combinations listed in Section 3H.7.4.5 (see Enclosure 4). The DGFOT factors of safety against sliding, overturning and flotation are provided in Table 3H.7-2 (see Enclosure 4). These factors of safety meet the requirements of Standard Review Plan (SRP) 3.8.5. For sliding and overturning evaluations, the 100%, 40%, 40% rule was used for consideration of the X, Y, and Z seismic excitations.

More detailed and specific description of loads, load combinations and results of analysis and design of the DGFOT is provided in the COLA mark-up shown in Enclosure 4.

COLA will be revised as shown in Enclosures 1 through 5 as a result of this response.

		In-plane Shear Force (kip)	In-plane Moment (kip-ft)	Axial Force (kip)
Long Direction (Two Walls)	SAP2000 section cut seismic design forces:	6847	74581	
	Enveloped SSI peak section cut forces:	6451	53060	
	Ratio SAP2000/SSI section cut forces:	1.06	1.41	
Short Direction (Two Walls)	SAP2000 section cut seismic design forces:	5277	32140	
	Enveloped SSI peak section cut forces:	4162	25651	
	Ratio SAP2000/SSI section cut forces:	1.27	1.25	N/A
Total Building	SAP2000 section cut forces due to Z-direction seismic load:	N/A	N/A	2559
	Enveloped SSI peak section cut forces:	N/A	N/A	2488
	Ratio SAP2000/SSI section cut forces:	N/A	N/A	1.03

Table 03.08.04-30.1: SAP2000 (Uniform Springs Model) vs SSI Model Section Cut Seismic Force and Moment Comparison for DGFOSV

		In-plane Shear Force (kip)	In-plane Moment (kip-ft)	Axial Force (kip)
Long Direction (Two Walls)	SAP2000 section cut seismic design forces:	6808	71838	
	Enveloped SSI peak section cut forces:	6451	53060	
	Ratio SAP2000/SSI section cut forces:	1.06	1.35	
Short Direction (Two Walls)	SAP2000 section cut seismic design forces:	5239	33571	
	Enveloped SSI peak section cut forces:	4162	25651	
	Ratio SAP2000/SSI section cut forces:	1.26	1.31	N/A
Total Building	SAP2000 section cut forces due to Z-direction seismic load:	N/A	N/A	2559
	Enveloped SSI peak section cut forces:	N/A	N/A	2488
	Ratio SAP2000/SSI section cut forces:	N/A	N/A	1.03

Table 03.08.04-30.2: SAP2000 (Coupled Springs Model) vs SSI Model Section Cut Seismic Force and Moment Comparison for DGFOSV

Table 03.08.04-30.3: Comparison of SSI Accelerations vs. Design Accelerations for DGFOT

	Horizontal (X & Y)		Vertical (Z)	
	From SSI Analysis (g)	Used in Design (g)	From SSI Analysis (g)	Used in Design (g)
Tunnel (0.0 <= Z <= 9.0)	0.3591	0.45	0.3078	0.37
Access Regions (9.0 < Z <= 23.17)	0.7324	0.85	0.3286	0.40

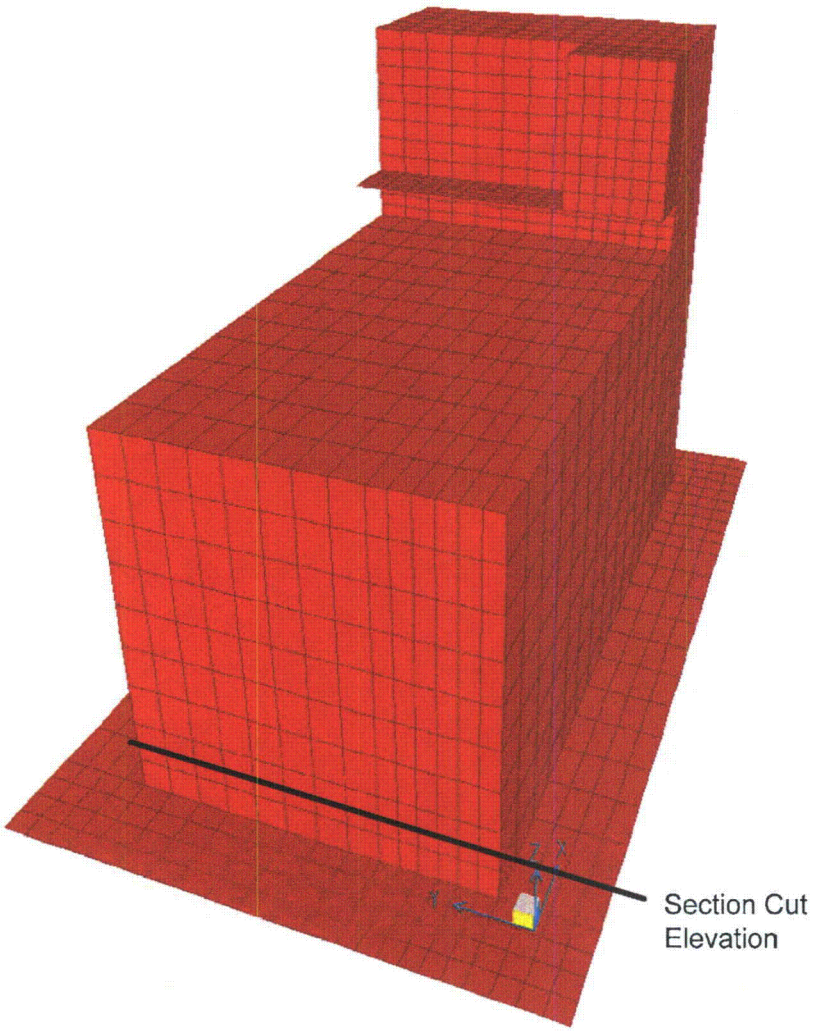

Note:

The first row of elements at the bottom of the DGFOSV walls are 3' link elements that model the distance from the center of the 6' basemat to the bottom of the walls. Therefore, the section cuts are taken at the second row of elements from the bottom of the walls.

Figure 03.08.04-30.1: Location of section cut in SAP2000 design model

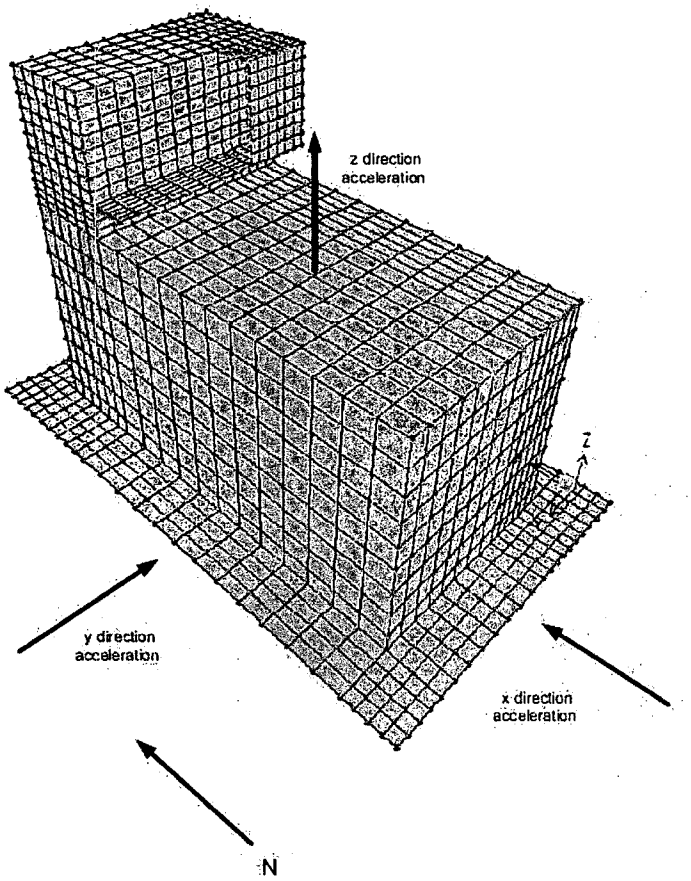

Figure 03.08.04-30.2: Schematic view of the Directional Seismic Load

Enclosure 1
Revision to COLA Section 3.7

3.7.2.8 Interaction of Non-Seismic Category I Structures, Systems and Components with Seismic Category I Structures, Systems and Components

The Category I structures and their physical proximity to nearby non-Category I structures are shown in Figure 3.7-40. None of the non-Category I structures proposed as part of STP Units 3 and 4 is intended to meet Criterion (2) of DCD Section 3.7.2.8. Rather, for each non-Category I structure, either: (1) it is determined that the collapse of the non-Category I structure will not cause the non-Category I structure to strike a Category I structure; or (2) the non-Category I structure will be analyzed and designed to prevent its failure under SSE conditions in a manner such that the margin of safety of the structure is equivalent to that of Seismic Category I structures. Non-Category I structures that can interact with Seismic Category I structures include the Turbine Building (TB), Radwaste Building (RWB), Service Building (SB), Control Building Annex (CBA) and the stack on the Reactor Building roof. Table 3H.6-14 provides sliding and overturning factors of safety under site-specific SSE for TB, RWB, SB, and CBA.

The seismic input motions for the design of the five non-seismic category I structures noted above are described in the following:

- TB: 0.3g Regulatory Guide 1.60 spectra.
- RWB: as described in Section 3H.3.5.3 and shown in Figures 3.7-40 through 3.7-42.
- SB: 0.3g Regulatory Guide 1.60 spectra.
- CBA: as described in Section 3.7.3.16 and shown in Figures 3.7-38 and 3.7-39.

Stack on the Reactor Building roof: seismic loading at its location, resulting from the SSE analysis of the Reactor Building.